Recent advancements toward generalized sampling strategies for multifidelity Uncertainty Quantification

SAND2019-3110PE

Gianluca Geraci[1], Alex A. Gorodetsky[2], Michael S. Eldred[1]
and John D. Jakeman[1]

[1]Sandia National Laboratories, Albuquerque
[2]Department of Aerospace Engineering, University of Michigan

Uncertainty quantification for nonlinear problems and applications in porous media
NORCE Norwegian Research Centre
March 27th 2019

Plan of the talk

- Sandia National Laboratories
- Uncertainty Quantification
- Multifidelity sampling
- Leveraging Active Directions for Multifidelity UQ
- Conclusions

Sandia National Laboratories

Sandia National Laboratories

Origin

Exceptional service in the national interest

- July 1945: Los Alamos creates Z Division
- Nonnuclear component engineering
- November 1, 1949: Sandia Laboratory established

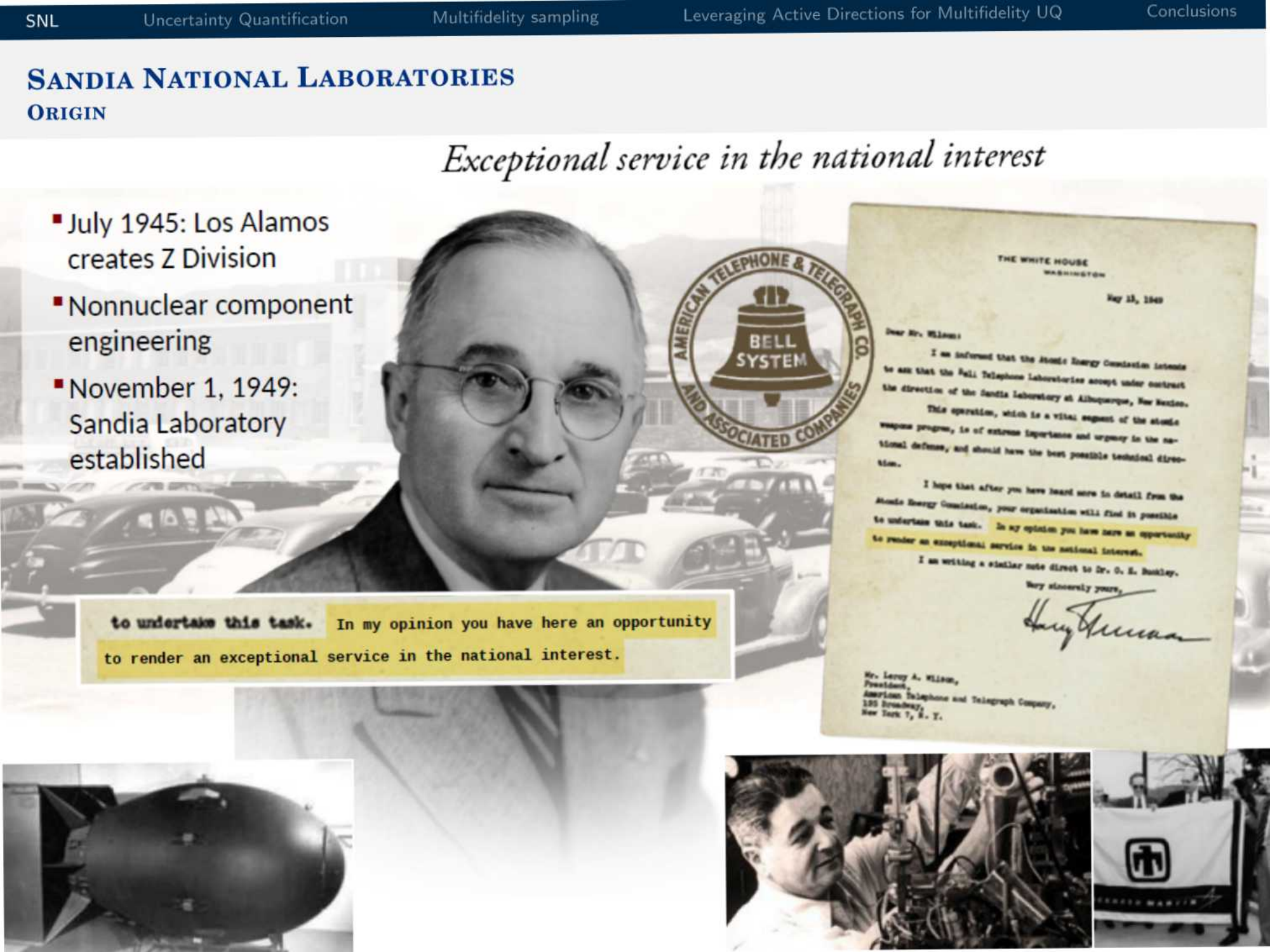

SANDIA NATIONAL LABORATORIES

MAIN ROLE AND AREAS OF INTEREST

SANDIA HAS FIVE MAJOR PROGRAM PORTFOLIOS

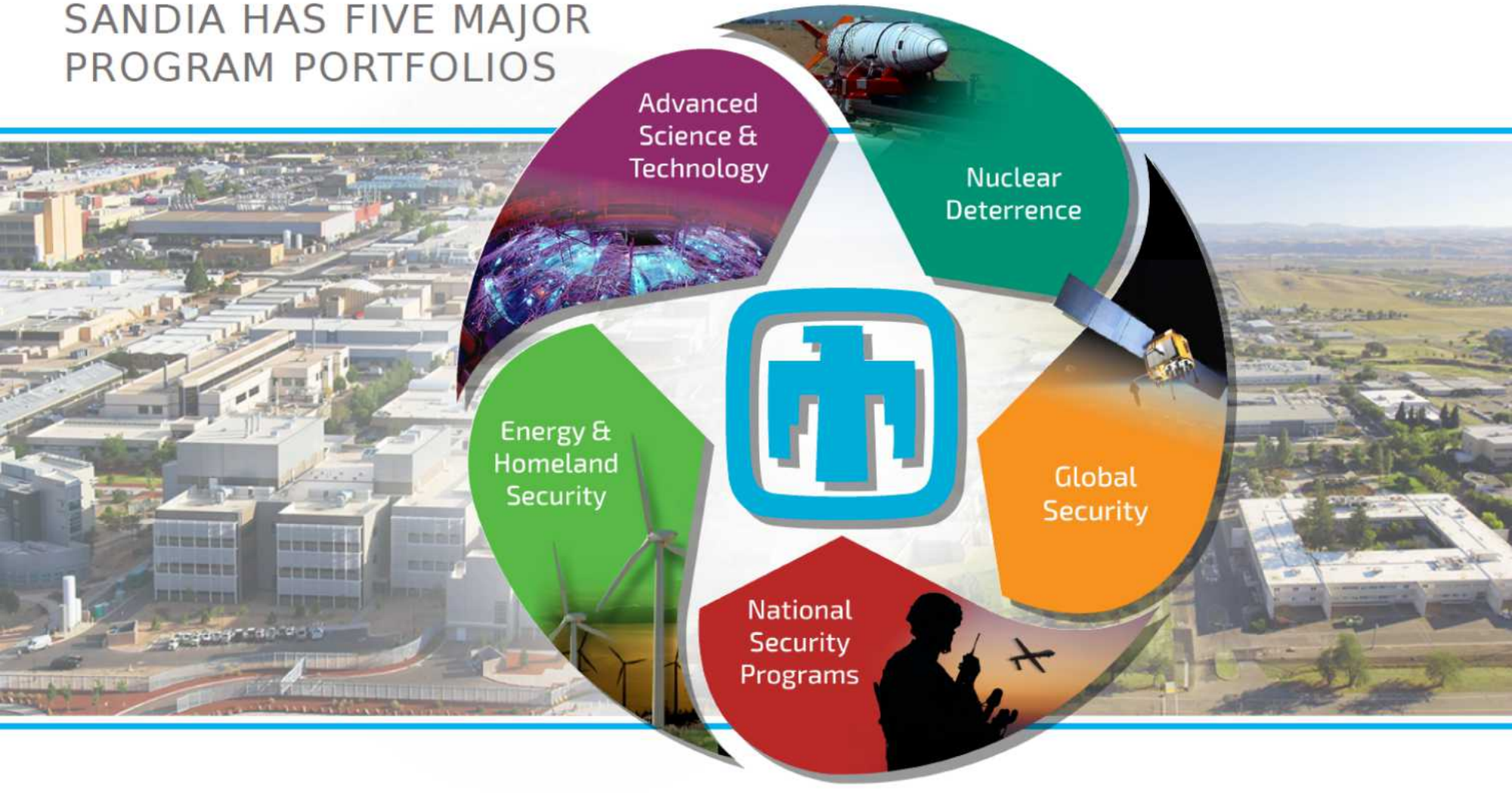

SANDIA NATIONAL LABORATORIES
ADVANCED SCIENCE & TECHNOLOGY

Computing & Information Sciences

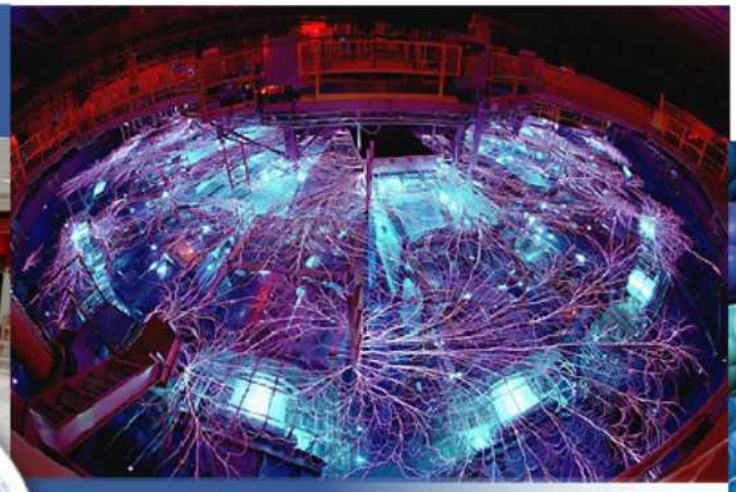

Radiation Effects & High Energy Density Science

Materials Sciences

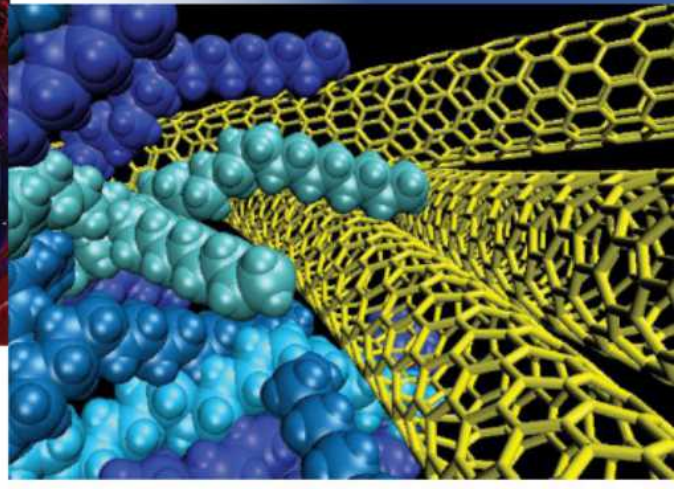

Engineering Sciences

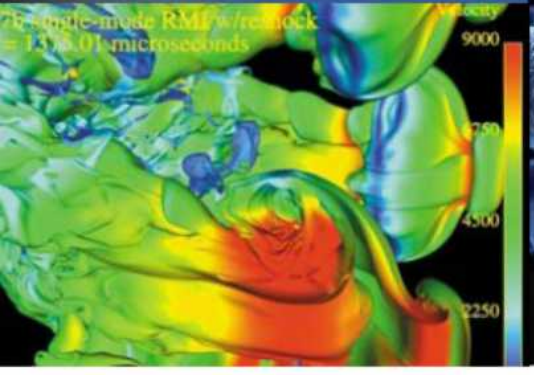

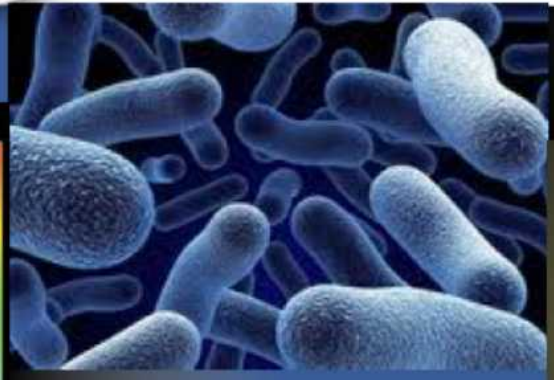

Bioscience

Nanodevices & Microsystems

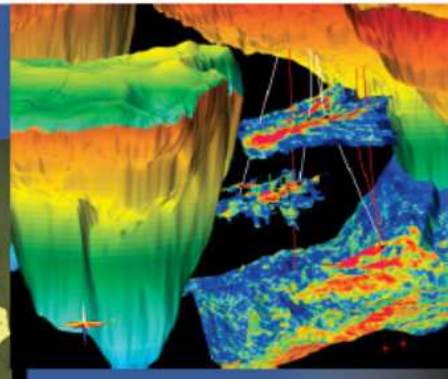

Geoscience

Sandia National Laboratories

Algorithms R&D: From Core Solvers to Modeling and Simulation Applications

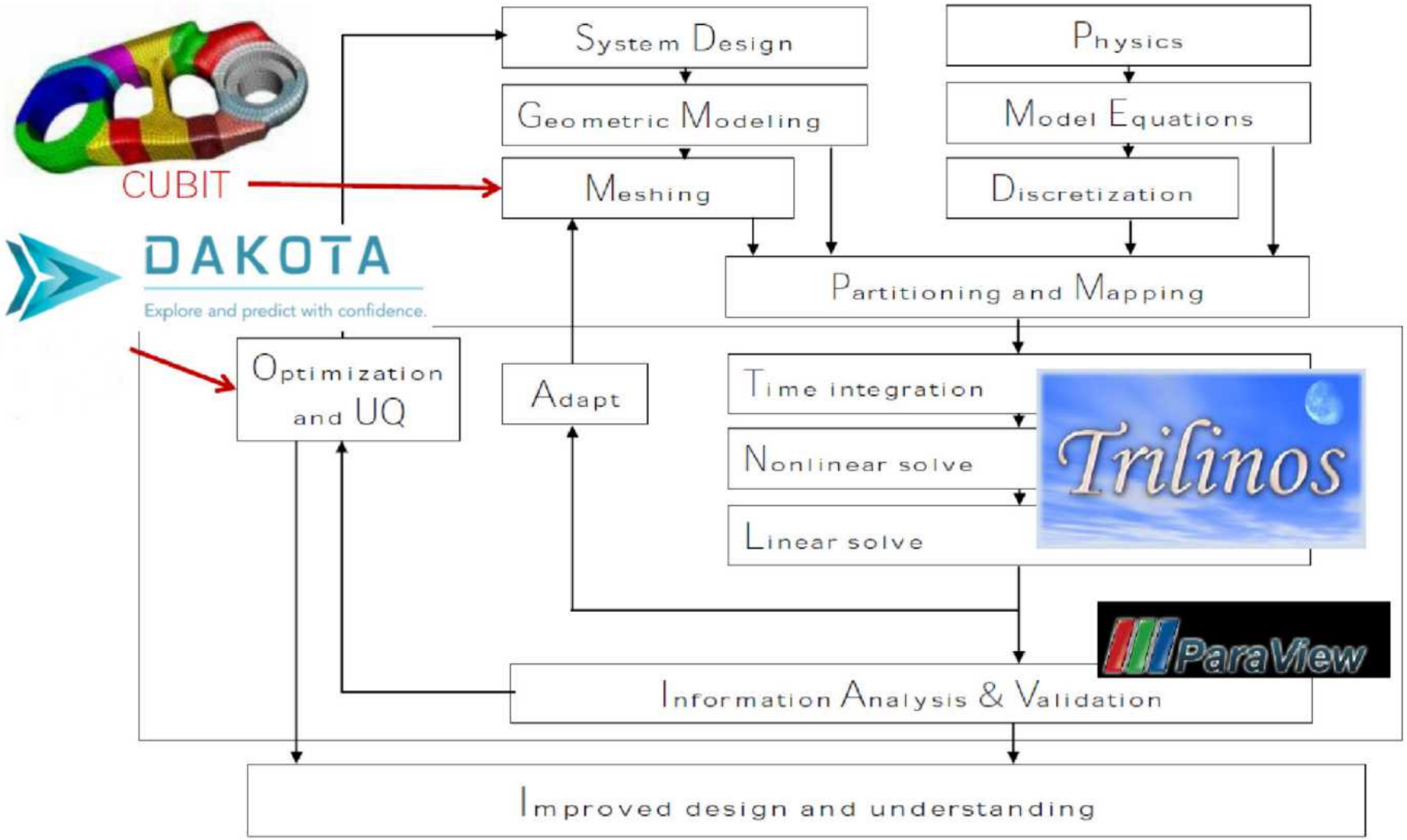

FIGURE: Courtesy of Brian Adams

Sandia National Laboratories
DAKOTA – Explore and Design with confidence

Algorithms for **design exploration** and **simulation credibility**

- Suite of iterative mathematical and statistical methods that interface to computational models
- Makes sophisticated parametric exploration of simulations practical for a computational design-analyze-test cycle

Features

- **Sensitivity:** Which are the crucial factors/parameters?
- **Uncertainty:** How safe, reliable, or robust is my system?
- **Optimization:** What is the best performing design or control?
- **Calibration/Parameter Estimation:** What models and parameters best match data?

Credible Prediction

- **Verification:** Is the model implemented correctly, converging as expected?
- **Validation:** How does the model compare to experimental data, including uncertainties?

DAKOTA

Explore and predict with confidence.

https://dakota.sandia.gov/

Uncertainty Quantification

Uncertainty Quantification
DoE and DoD deployment activities

Stewardship (NNSA ASC)
Safety in abnormal environments

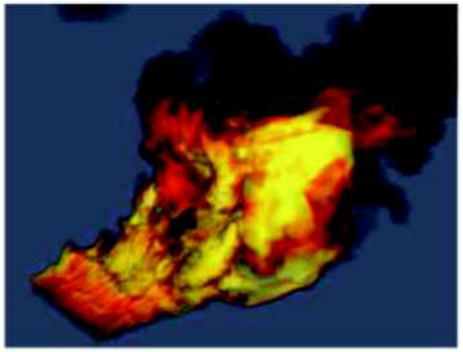

Energy (ASCR, EERE, NE)
Wind turbines, nuclear reactors

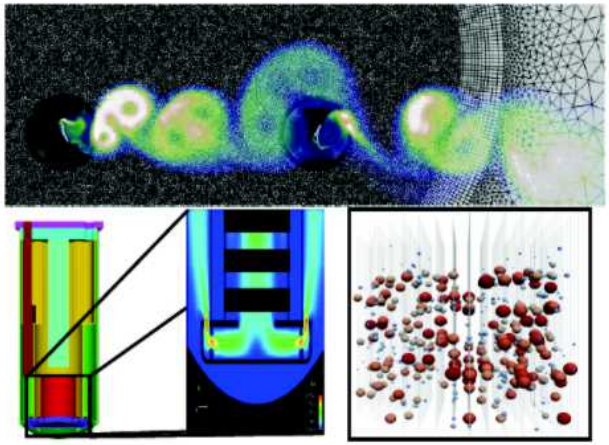

Climate (SciDAC, CSSEF, ACME)
Ice sheets, CISM, CESM, ISSM, CSDMS

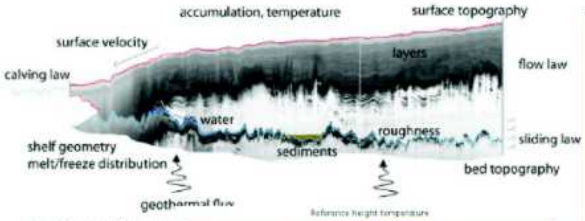

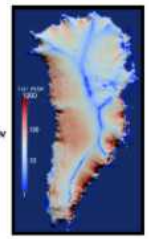

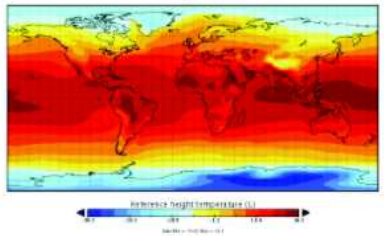

Addtnl. Office of Science:
(SciDAC, EFRC)
Comp. Matls: waste forms / hazardous matls (WastePD, CHWM)
MHD: Tokamak disruption (TDS)

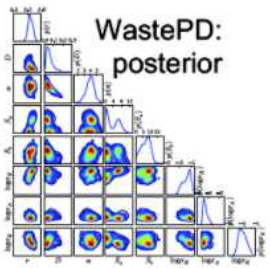

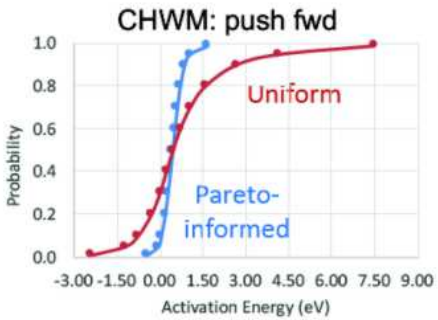

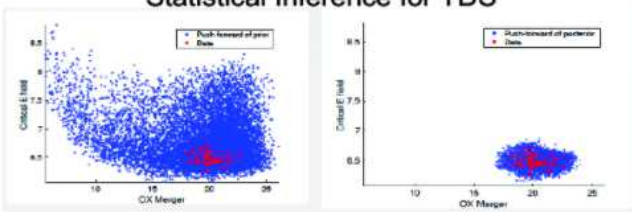

FIGURE: Courtesy of Mike Eldred

High-fidelity state-of-the-art modeling and simulations with HPC

- **Severe** simulations **budget constraints**
- **Significant dimensionality** driven by model complexity

Uncertainty Quantification

Rich set of modeling choices – Discretization Vs Fidelity

Multi-fidelity: several accuracy levels available

- Physical models (Laminar/Turbulent, Reacting/non-reacting, viscous/inviscid...)
- Numerical methods (high/low order, Euler/RANS/LES, *etc*...)
- Numerical discretization (fine/coarse mesh...)
- Quality of statistics (long/short time history for turbulent flow...)

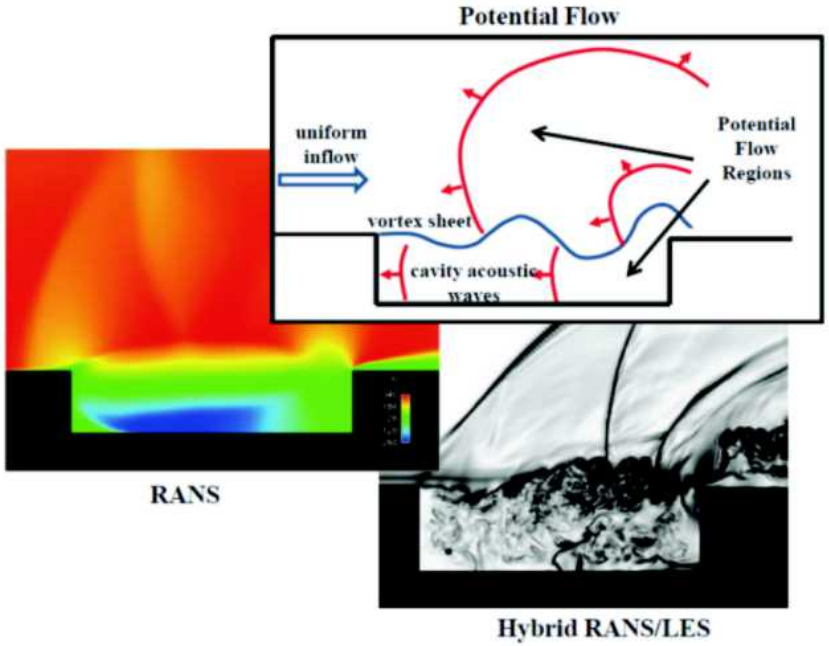

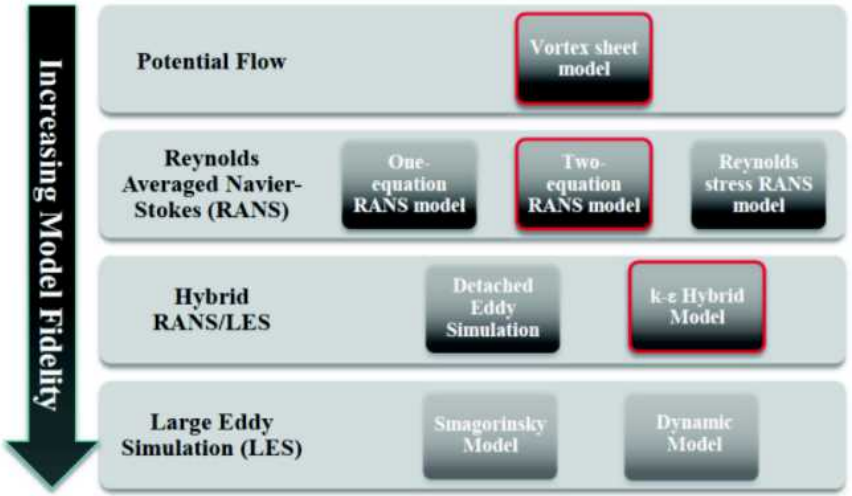

Relationships amongst models can be difficult to anticipate

- A simple **hierarchical sequence** can correspond to strict modeling choices (*e.g.* discretization levels)
- More often, for some QoI, we can have **peer models**

(Multifidelity/Multilevel) Sampling-based approaches

Uncertainty Quantification

Forward Propagation – Why Sampling Methods?

UQ context at a glance:

- High-dimensionality, non-linearity and possibly non-smooth responses
- Rich physics and several discretization levels/models available

Natural candidate:

- **Sampling**-based (MC-like) approaches because they are **non-intrusive**, **robust** and **flexible**...
- **Drawback:** Slow convergence $\mathcal{O}(N^{-1/2}) \rightarrow$ many realizations to build reliable statistics

Goal of the talk: **Reducing the computational cost** of obtaining MC reliable statistics

Pivotal idea:

- Simplified (**low-fidelity**) models are **inaccurate** but **cheap**
  - **low-variance** estimates
- **High-fidelity** models are **costly**, but **accurate**
  - **low-bias** estimates

Monte Carlo

Monte Carlo
Generalities

Let consider a random variable Q, we want to compute **its expected value** $\mathbb{E}[Q]$ (or some high-order moment):

$$\hat{Q}_N^{\mathrm{MC}} = \frac{1}{N} \sum_{i=1}^{N} Q^{(i)}$$

Monte Carlo
Generalities

Let consider a random variable Q, we want to compute **its expected value** $\mathbb{E}[Q]$ (or some high-order moment):

$$\hat{Q}_N^{\mathrm{MC}} = \frac{1}{N}\sum_{i=1}^{N} Q^{(i)}$$

Let's use MC to compute the value $\pi \propto \dfrac{\#\mathrm{Hit}}{N}$

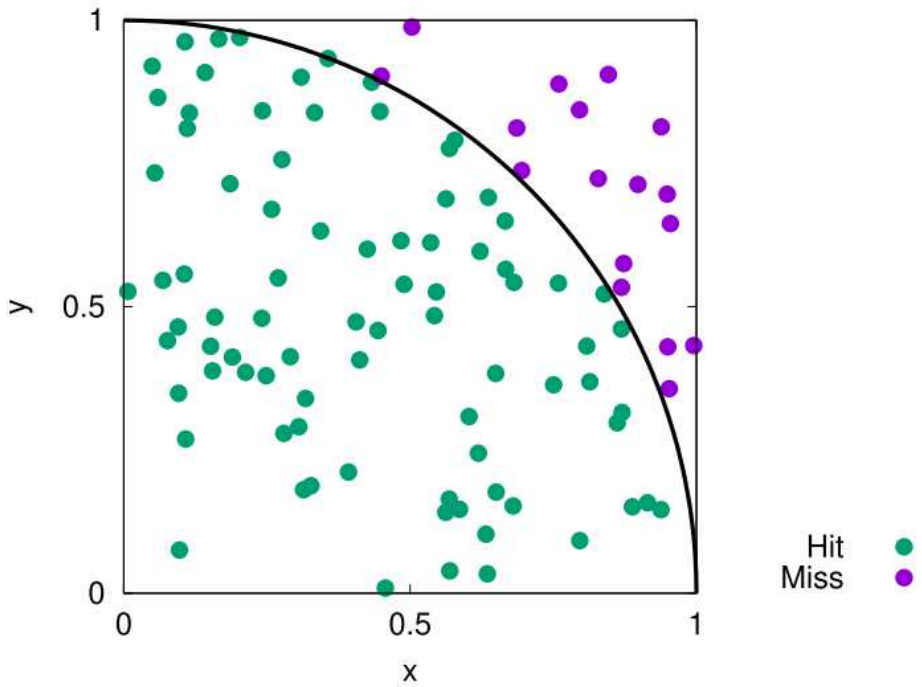

Monte Carlo
Generalities

Let consider a random variable Q, we want to compute its **expected value** $\mathbb{E}[Q]$ (or some high-order moment):

$$\hat{Q}_N^{\mathrm{MC}} = \frac{1}{N} \sum_{i=1}^{N} Q^{(i)}$$

Let's use MC to compute the value $\pi \propto \dfrac{\#\mathrm{Hit}}{N}$

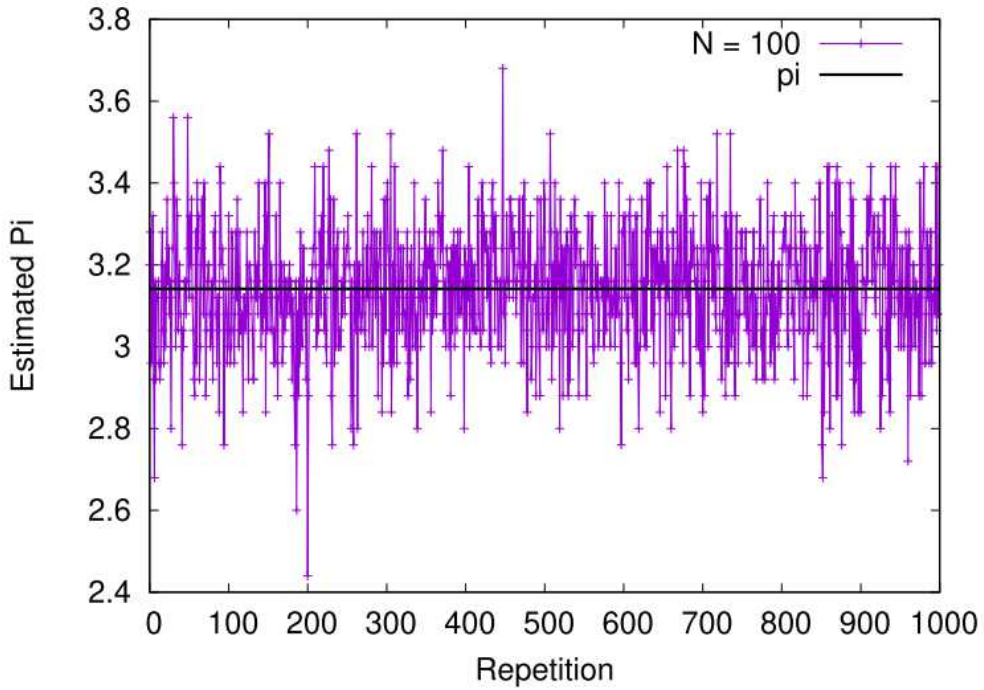

Monte Carlo
Generalities

Let consider a random variable Q, we want to compute its **expected value** $\mathbb{E}[Q]$ (or some high-order moment):

$$\hat{Q}_N^{\mathrm{MC}} = \frac{1}{N} \sum_{i=1}^{N} Q^{(i)}$$

Let's use MC to compute the value $\pi \propto \dfrac{\#\mathrm{Hit}}{N}$

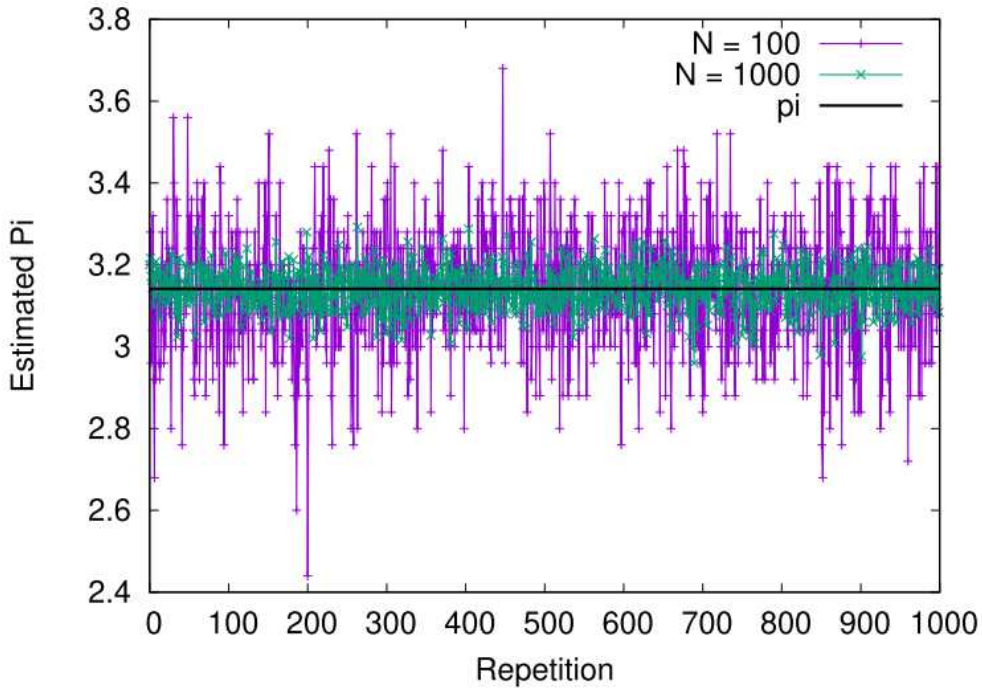

Monte Carlo

Introducing the notion of fidelity

Numerical problems **cannot be resolved with infinite accuracy**: a discretization/numerical error is often introduced

$$\hat{Q}^{MC}_{M,N} \overset{\text{def}}{=} \frac{1}{N}\sum_{i=1}^{N} Q^{(i)}_M$$

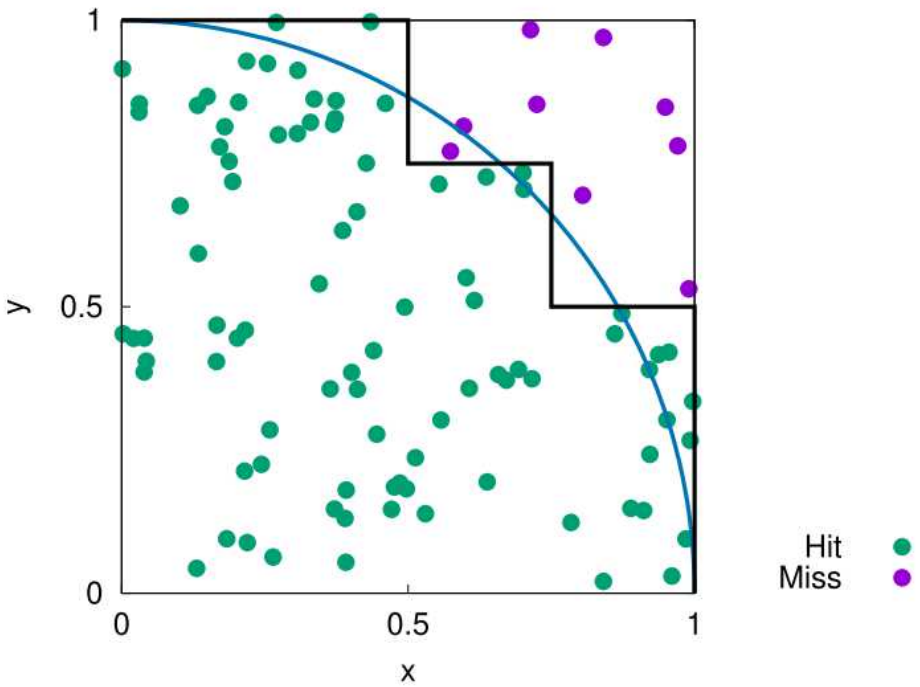

Monte Carlo

Introducing the notion of fidelity

Numerical problems **cannot be resolved with infinite accuracy**: a discretization/numerical error is often introduced

$$\hat{Q}^{MC}_{M,N} \overset{\text{def}}{=} \frac{1}{N}\sum_{i=1}^{N} Q^{(i)}_M$$

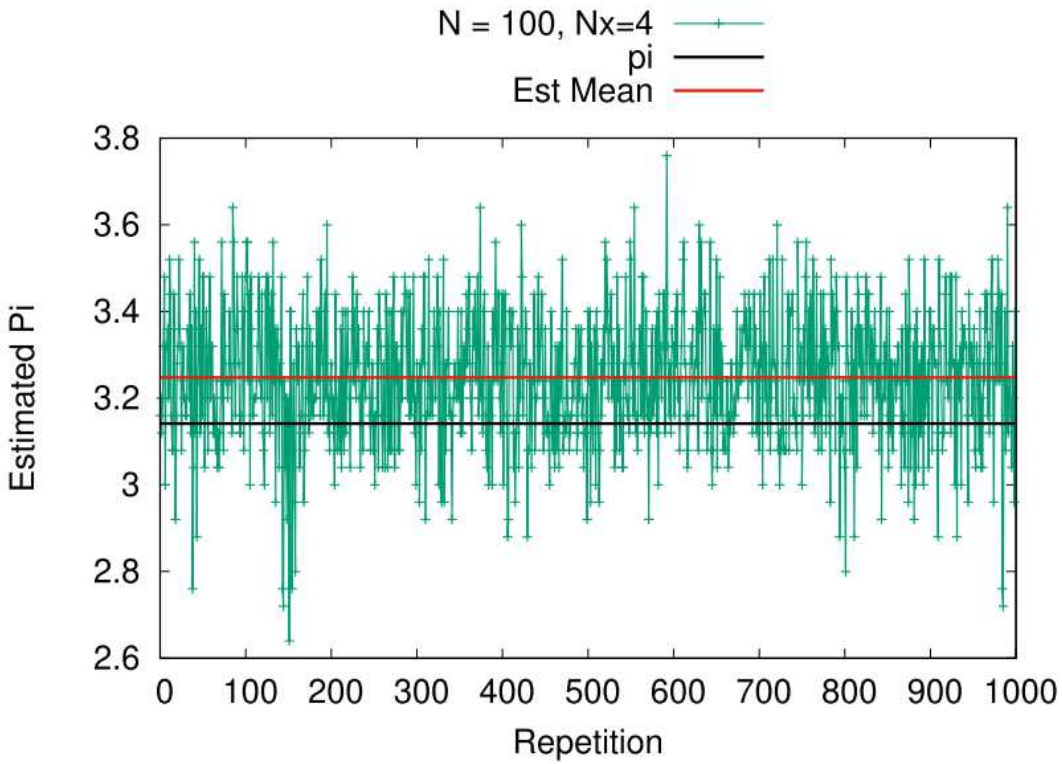

Monte Carlo

Introducing the notion of fidelity

Numerical problems **cannot be resolved with infinite accuracy**: a discretization/numerical error is often introduced

$$\hat{Q}^{MC}_{M,N} \overset{\text{def}}{=} \frac{1}{N}\sum_{i=1}^{N} Q^{(i)}_{M}$$

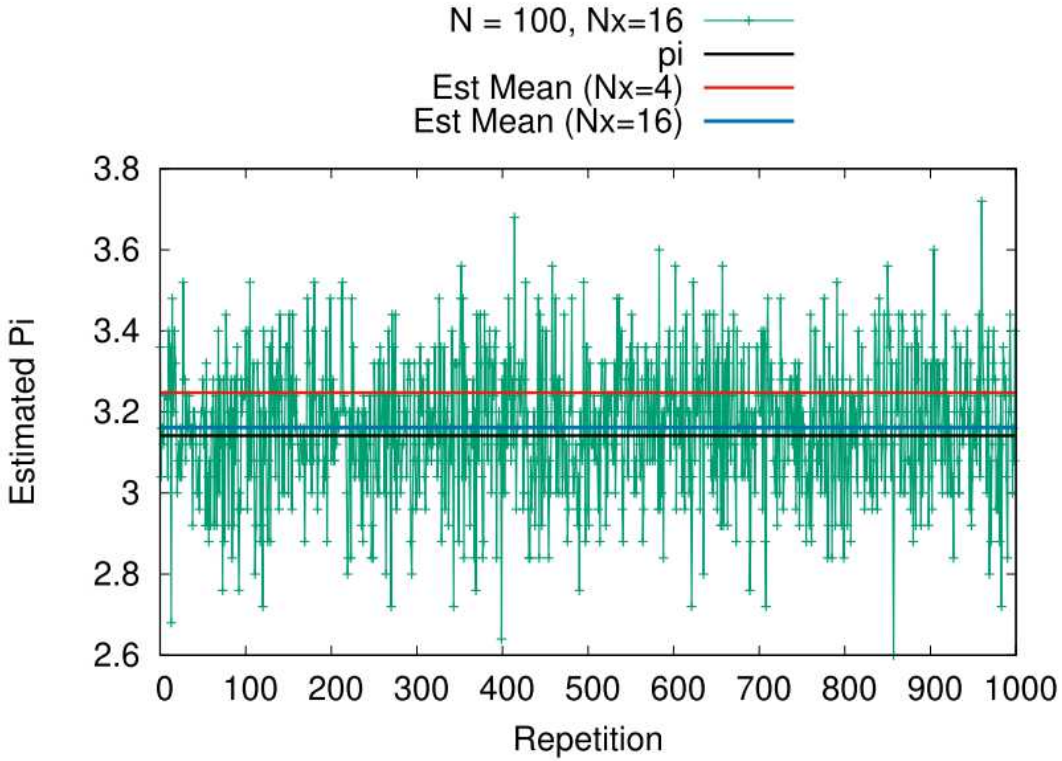

Monte Carlo
Overall estimator error

Two sources of error in the **Mean Square Error**:

$$\mathbb{E}\left[(\hat{Q}^{MC}_{M,N} - \mathbb{E}[Q])^2\right] = \mathbb{V}\mathbf{ar}\left[\hat{\mathbf{Q}}^{\mathbf{MC}}_{\mathbf{M},\mathbf{N}}\right] + (\mathbb{E}[\mathbf{Q_M} - \mathbf{Q}])^{\mathbf{2}}$$

- **Sampling error:** replacing the expected value by a (finite) sample average, *i.e.*

$$\mathbb{V}ar\left[\hat{Q}^{MC}_{M,N}\right] = \frac{\mathbb{V}ar[Q]}{N}$$

From the CLT, for $N \to \infty$

$$\left(\hat{Q}^{MC}_{M,N} - \mathbb{E}[Q]\right) \sim \sqrt{\frac{\mathbb{V}ar[Q]}{N}}\mathcal{N}(0,1)$$

- **Model fidelity (e.g. discretization):** finite accuracy

Monte Carlo
Overall estimator error

Two sources of error in the **Mean Square Error**:

$$\mathbb{E}\left[(\hat{Q}^{MC}_{M,N} - \mathbb{E}[Q])^2\right] = \mathbb{V}\mathbf{ar}\left[\hat{\mathbf{Q}}^{\mathbf{MC}}_{\mathbf{M},\mathbf{N}}\right] + (\mathbb{E}[\mathbf{Q_M} - \mathbf{Q}])^{\mathbf{2}}$$

- **Sampling error:** replacing the expected value by a (finite) sample average, *i.e.*

$$\mathbb{V}ar\left[\hat{Q}^{MC}_{M,N}\right] = \frac{\mathbb{V}ar[Q]}{N}$$

From the CLT, for $N \to \infty$

$$\left(\hat{Q}^{MC}_{M,N} - \mathbb{E}[Q]\right) \sim \sqrt{\frac{\mathbb{V}ar[Q]}{N}}\mathcal{N}(0,1)$$

- **Model fidelity (e.g. discretization):** finite accuracy

Accurate estimation $\Rightarrow$ **Large number** of **samples** evaluated for the **high fidelity** model

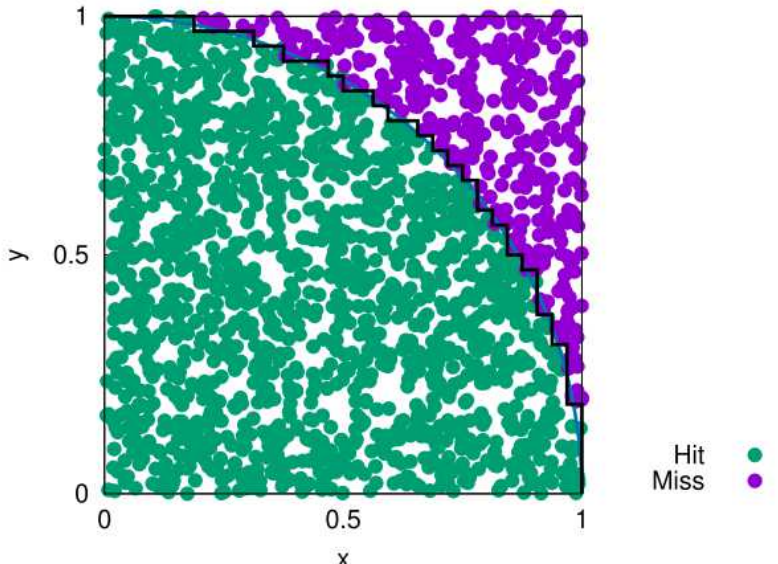

Accelerating Monte Carlo

Bringing multiple fidelity models into the picture

Pivotal idea:

- **High-fidelity** models are **costly**, but **accurate**
  - **low-bias** estimates
- Simplified (**low-fidelity**) models are **inaccurate** but **cheap**
  - **low-variance** estimates

Single Fidelity

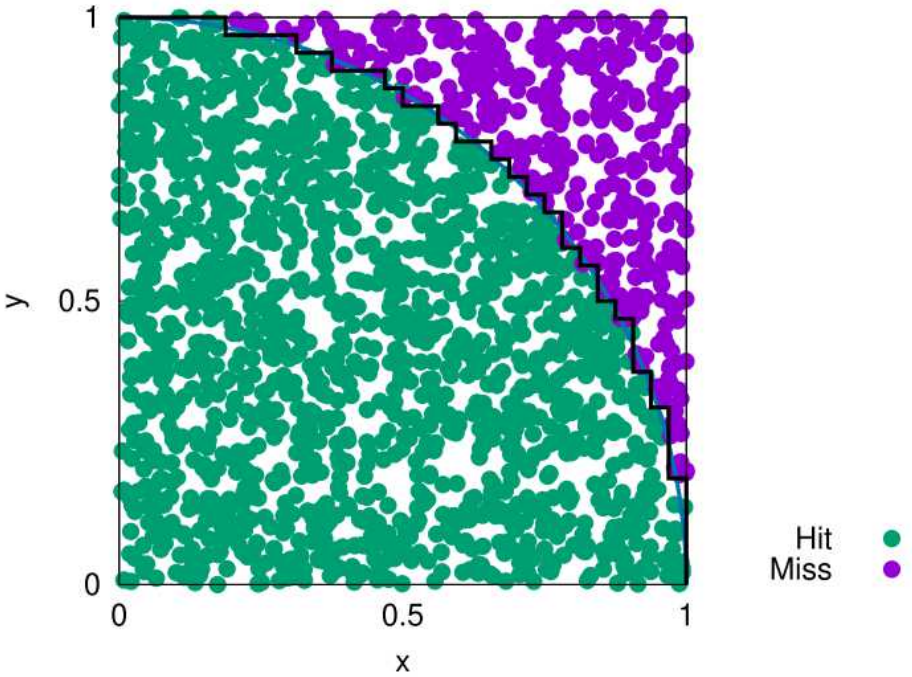

Multi Fidelity

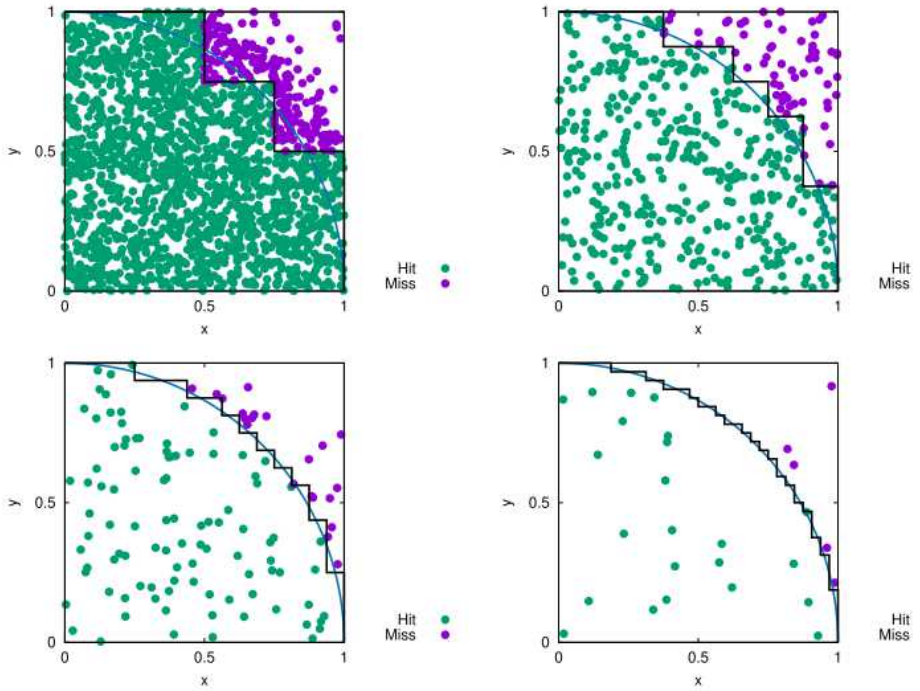

Control variate
Pivotal role

A **Control Variate** MC estimator (function G with $\mathbb{E}[G]$ **known**)

$$\hat{Q}_N^{CV} = \hat{Q}_N^{MC} - \beta\left(\hat{G}_N^{MC} - \mathbb{E}[G]\right)$$

Properties:

- Unbiased, *i.e.* $\mathbb{E}\left[\hat{Q}_N^{CV}\right] = \mathbb{E}\left[\hat{Q}_N^{MC}\right]$
- $\underset{\beta}{\operatorname{argmin}}\, \mathbb{V}ar\left[\hat{Q}_N^{CV}\right] \rightarrow \beta = -\rho\dfrac{\mathbb{V}ar^{1/2}(Q)}{\mathbb{V}ar^{1/2}(G)}$
- Pearson's $\rho = \dfrac{\mathrm{Cov}(Q,G)}{\mathbb{V}ar^{1/2}(Q)\,\mathbb{V}ar^{1/2}(G)}$ where $|\rho| < 1$

$$\boxed{\mathbb{V}ar\left[\hat{Q}_N^{CV}\right] = \mathbb{V}ar\left[\hat{Q}_N^{MC}\right]\left(1-\rho^2\right)}$$

Control variate
Pivotal role

A **Control Variate** MC estimator (function G with $\mathbb{E}[G]$ **known**)

$$\hat{Q}_N^{CV} = \hat{Q}_N^{MC} - \beta\left(\hat{G}_N^{MC} - \mathbb{E}[G]\right)$$

Properties:

- Unbiased, *i.e.* $\mathbb{E}\left[\hat{Q}_N^{CV}\right] = \mathbb{E}\left[\hat{Q}_N^{MC}\right]$
- $\underset{\beta}{\operatorname{argmin}}\, \mathbb{V}ar\left[\hat{Q}_N^{CV}\right] \rightarrow \beta = -\rho\dfrac{\mathbb{V}ar^{1/2}(Q)}{\mathbb{V}ar^{1/2}(G)}$
- Pearson's $\rho = \dfrac{\mathrm{Cov}(Q,G)}{\mathbb{V}ar^{1/2}(Q)\,\mathbb{V}ar^{1/2}(G)}$ where $|\rho| < 1$

$$\boxed{\mathbb{V}ar\left[\hat{Q}_N^{CV}\right] = \mathbb{V}ar\left[\hat{Q}_N^{MC}\right]\left(1-\rho^2\right)}$$

Q: How does the **control variate** approach enter in the picture?
A: By means of the (geometrical) MLMC and multifidelity strategy

0. Single resolution level
   - Cheap lower fidelity (**Multifidelity**)
1. Applying it recursively
   - Spatial discretization (**Multilevel**)
2. Applying it recursively across resolutions/model forms
   - Spatial discretization and cheap lower fidelity (**Multilevel-Multifidelity**)

Multifidelity Monte Carlo

MULTIFIDELITY

PRACTICAL IMPLICATIONS OF UNKNOWN LOW-FIDELITY STATISTICS

Let's modify the high-fidelity QoI, Q_M^{HF}, to decrease its variance

$$\hat{Q}_{M,N}^{\mathrm{HF},CV} = \hat{Q}_{M,N}^{\mathrm{HF}} + \alpha \left(\hat{Q}_{M,N}^{\mathrm{LF}} - \mathbb{E}\left[Q_M^{\mathrm{LF}} \right] \right).$$

MULTIFIDELITY

PRACTICAL IMPLICATIONS OF UNKNOWN LOW-FIDELITY STATISTICS

Let's modify the high-fidelity QoI, Q_M^{HF}, to decrease its variance

$$\hat{Q}_{M,N}^{\mathrm{HF},CV} = \hat{Q}_{M,N}^{\mathrm{HF}} + \alpha \left(\hat{Q}_{M,N}^{\mathrm{LF}} - \mathbb{E}\left[Q_M^{\mathrm{LF}} \right] \right).$$

In practical situations

- the term $\mathbb{E}\left[Q_M^{\mathrm{LF}} \right]$ is unknown (low fidelity $\neq$ analytic function)
- we use an additional and independent set $\Delta^{\mathrm{LF}} = (\mathbf{r} - 1)N^{\mathrm{HF}}$

$$\mathbb{E}\left[Q_M^{\mathrm{LF}} \right] \simeq \frac{1}{\mathbf{r}N^{\mathrm{HF}}} \sum_{i=1}^{\mathbf{r}N^{\mathrm{HF}}} Q_M^{\mathrm{LF},(i)}.$$

Finally the variance is

$$\boxed{\mathbb{V}ar\left[\hat{Q}_{M,N}^{\mathrm{HF},CV} \right] = \mathbb{V}ar\left[\hat{Q}_M^{\mathrm{HF}} \right] \left(1 - \frac{\mathbf{r} - \mathbf{1}}{\mathbf{r}} \rho_{HL}^2 \right)}$$

[1] Pasupathy, R., Taaffe, M., Schmeiser, B. W. & Wang, W., Control-variate estimation using estimated control means. *IIE Transactions*, **44**(5), 381–385, 2012

[2] Ng, L.W.T. & Willcox, K. Multifidelity Approaches for Optimization Under Uncertainty. *Int. J. Numer. Meth. Engng* 100, no. 10, pp. 746772, 2014.

[3] Peherstorfer, B., Willcox, K. & Gunzburger, M., Optimal Model Management for Multifidelity Monte Carlo Estimation. *SIAM J. Sci. Comput.* 38(5), A3163A3194.

Multifidelity

Minimization of the computational cost (Optimal solution)

The solution of the optimization problem is obtained as

$$r^\star = \sqrt{\frac{w\rho^2}{1-\rho^2}}$$

$$N^{\mathrm{HF},\star} = \frac{\mathbb{V}ar\left[Q_M^{\mathrm{HF}}\right]}{\varepsilon^2/2}\left(1 - \frac{r^\star - 1}{r^\star}\rho^2\right)$$

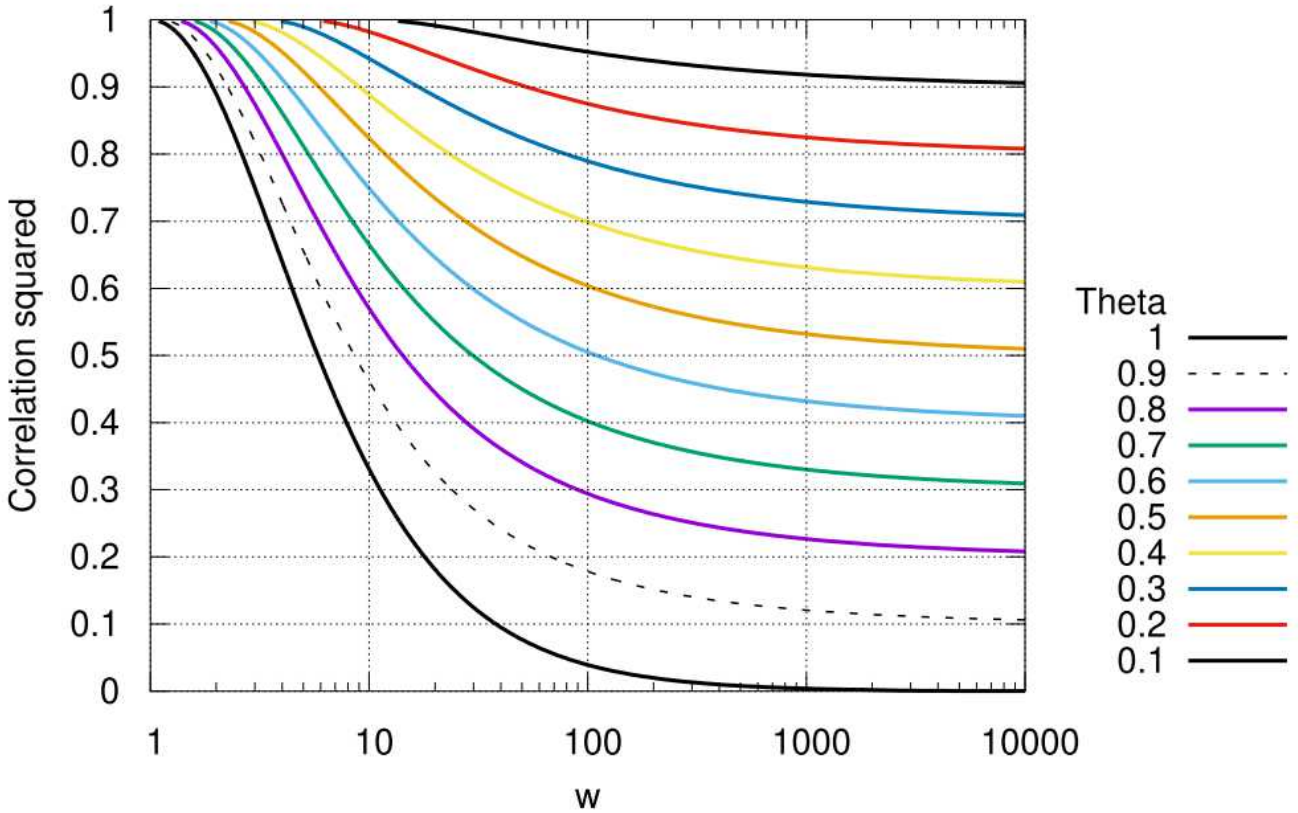

Multilevel Monte Carlo

GEOMETRICAL MLMC

ACCELERATING THE MONTE CARLO METHOD WITH MULTILEVEL STRATEGIES

Multilevel MC: Sampling from **several** approximations Q_M of Q (Multigrid...)

Ingredients:

- $\{M_\ell : \ell = 0, \dots, L\}$ with $M_0 < M_1 < \cdots < M_L \overset{\text{def}}{=} M$
- Estimation of $\mathbb{E}[Q_M]$ by means of **correction** w.r.t. the next lower level

$$Y_\ell \overset{\text{def}}{=} \begin{cases} Q_{M_\ell} - Q_{M_{\ell-1}} & \ell > 0 \\ Q_0 & \ell = 0 \end{cases} \xrightarrow{\textit{linearity}} \mathbb{E}[Q_M] = \mathbb{E}\left[Q_{M_0}\right] + \sum_{\ell=1}^{L} \mathbb{E}\left[Q_{M_\ell} - Q_{M_{\ell-1}}\right] = \sum_{\ell=0}^{L} \mathbb{E}[\mathbf{Y}_\ell]$$

- Multilevel Monte Carlo estimator

$$\hat{Q}_M^{\text{ML}} \overset{\text{def}}{=} \sum_{\ell=0}^{L} \hat{\mathbf{Y}}_{\ell,\mathbf{N}_\ell}^{\text{MC}} = \sum_{\ell=0}^{L} \frac{1}{N_\ell} \sum_{i=1}^{N_\ell} \left(\mathbf{Q}_{\mathbf{M}_\ell}^{(\mathbf{i})} - \mathbf{Q}_{\mathbf{M}_{\ell-1}}^{(\mathbf{i})} \right)$$

- The Mean Square Error is

$$\mathbb{E}\left[(\hat{Q}_M^{ML} - \mathbb{E}[Q])^2\right] = \sum_{\ell=0}^{\mathbf{L}} \mathbf{N}_\ell^{-1} \mathbb{V}\mathbf{ar}[\mathbf{Y}_\ell] + \left(\mathbb{E}[\mathbf{Q}_\mathbf{M} - \mathbf{Q}]\right)^2$$

Note If $Q_M \to Q$ (in a mean square sense), then $\mathbb{V}\mathbf{ar}[\mathbf{Y}_\ell] \xrightarrow{\ell \to \infty} 0$

GEOMETRICAL MLMC

DESIGNING A MLMC SIMULATION: COST ESTIMATION

Let us consider the **numerical cost** of the estimator

$$\mathcal{C}(\hat{Q}_M^{ML}) = \sum_{\ell=0}^{L} N_\ell \mathcal{C}_\ell$$

Determining the **ideal number of samples** per level (i.e. minimum cost at fixed variance)

$$\left.\begin{aligned} \mathcal{C}(\hat{Q}_M^{ML}) &= \sum_{\ell=0}^{L} N_\ell \mathcal{C}_\ell \\ \sum_{\ell=0}^{L} N_\ell^{-1} \mathbb{V}ar\left[Y_\ell\right] &= \varepsilon^2/2 \end{aligned}\right\} \xrightarrow{\textit{Lagrange multiplier}} \boxed{N_\ell = \frac{2}{\varepsilon^2}\left[\sum_{k=0}^{L}\left(\mathbb{V}ar\left[Y_k\right]\mathcal{C}_k\right)^{1/2}\right]\sqrt{\frac{\mathbb{V}ar\left[Y_\ell\right]}{\mathcal{C}_\ell}}}$$

$$\boxed{\mathbb{V}ar\left[\hat{Q}_M^{ML}\right] = \sum_{\ell=\mathbf{0}}^{\mathbf{L}} N_\ell^{-1}\mathbb{V}ar\left(Y_\ell\right).}$$

MLMC has been originally introduced for problems for which it is possible to control the highest resolution to achieve a desired MSE

[1] Giles, M.B., Multilevel Monte Carlo path simulation. *Oper. Res.* **56**, 607-617, 2008.

[2] Haji-Ali, A., Nobile, F., Tempone, R. Multi Index Monte Carlo: When Sparsity Meets Sampling, *Numerische Mathematik*, Vol. 132, Pages 767806, 2016.

Multilevel-Multifidelity Monte Carlo

Multilevel-Multifidelity approach

Combination of discretization and model form

- OUTER SHELL – **Multi-level**

$$\mathbb{E}\left[Q_M^{\mathrm{HF}}\right] = \sum_{l=0}^{L_{\mathrm{HF}}} \mathbb{E}\left[Y_\ell^{\mathrm{HF}}\right] = \sum_{l=0}^{L_{\mathrm{HF}}} \hat{Y}_\ell^{\mathrm{HF}}$$

- INNER BLOCK – **Multi-fidelity** (*i.e.* control variate on each level)

$$Y_\ell^{\mathrm{HF},\star} = \hat{Y}_\ell^{\mathrm{HF}} + \alpha_\ell \left(\hat{\mathbf{Y}}_\ell^{\mathrm{LF}} - \mathbb{E}\left[\mathbf{Y}_\ell^{\mathrm{LF}}\right]\right)$$

Final properties of the estimator

$$\boxed{\hat{Q}_M^{MLMF} = \sum_{l=0}^{L_{\mathrm{HF}}} \left[\hat{Y}_\ell^{\mathrm{HF}} + \alpha_\ell \left(\hat{\mathbf{Y}}_\ell^{\mathrm{LF}} - \mathbb{E}\left[\mathbf{Y}_\ell^{\mathrm{LF}}\right]\right)\right]}$$

and

$$\boxed{\mathbb{V}ar\left[\hat{Q}_M^{MLMF}\right] = \sum_{l=0}^{L_{\mathrm{HF}}} \left(\frac{1}{N_\ell^{\mathrm{HF}}} \mathbb{V}ar\left[Y_\ell^{\mathrm{HF}}\right] \left(1 - \frac{\mathbf{r}_\ell}{\mathbf{1} + \mathbf{r}_\ell} \rho_\ell^{\mathbf{2}}\right)\right)}$$

MULTILEVEL-MULTIFIDELITY

OPTIMAL ALLOCATION ACROSS DISCRETIZATION AND MODEL FORMS

- Target accuracy for the estimator: ε
- Cost per level is now $\mathcal{C}_\ell^{\text{eq}} = \mathcal{C}_\ell^{\text{HF}} + \mathcal{C}_\ell^{\text{LF}}\,(1 + r_\ell)$
- the (constrained) optimization problem is

$$\underset{N_\ell^{\text{HF}}, r_\ell, \lambda}{\text{argmin}}\ (\mathcal{L}), \quad \text{where} \quad \mathcal{L} = \sum_{\ell=0}^{L_{\text{HF}}} N_\ell^{\text{HF}} \mathcal{C}_\ell^{\text{eq}} + \lambda \left(\sum_{\ell=0}^{L_{\text{HF}}} \frac{1}{N_\ell^{\text{HF}}} \mathbb{V}ar\left[Y_\ell^{\text{HF}} \right] \Lambda_\ell(r_\ell) - \varepsilon^2/2 \right)$$

- $\Lambda_\ell(r_\ell) = 1 - \rho_\ell^2 \dfrac{r_\ell - 1}{r_\ell}$

After the first iteration the algorithm can adjust the number of samples on the HF or LF side depending on the correlation properties discovered on flight

After the minimization ($N_\ell^{\text{LF}} = N_\ell^{\text{HF}} + \Delta_\ell^{\text{LF}} = N_\ell^{\text{HF}} r_\ell$)

$$\begin{cases} r_\ell^\star = -1 + \sqrt{\dfrac{\rho_\ell^2}{1 - \rho_\ell^2} w_\ell}, \quad \text{where} \quad w_\ell = \mathcal{C}_\ell^{\text{HF}} / \mathcal{C}_\ell^{\text{LF}} \\ N_\ell^{\text{HF},\star} = \dfrac{2}{\varepsilon^2} \left[\displaystyle\sum_{k=0}^{L_{\text{HF}}} \left(\frac{\mathbb{V}ar\left[Y_\ell^{\text{HF}} \right] \mathcal{C}_\ell^{\text{HF}}}{\mathbf{1 - \rho_\ell^2}} \right)^{1/2} \Lambda_\ell \right] \sqrt{\left(\mathbf{1 - \rho_\ell^2} \right) \dfrac{\mathbb{V}ar\left[Y_\ell^{\text{HF}} \right]}{\mathcal{C}_\ell^{\text{HF}}}} \end{cases}$$

[1] G. Geraci, M.S. Eldred & G. Iaccarino, A multifidelity control variate approach for the multilevel Monte Carlo technique. *Center for Turbulence Research, Annual Research Briefs 2015*, pp. 169–181.

[2] G. Geraci, M.S. Eldred & G. Iaccarino, A multifidelity multilevel Monte Carlo method for uncertainty propagation in aerospace applications *19th AIAA Non-Deterministic Approaches Conference, AIAA SciTech Forum, (AIAA 2017-1951)*

Heat equation – Parabolic 1D

HEAT EQUATION

VERIFICATION TEST CASE (WE KNOW THE EXACT SOLUTION)

Heat-equation in presence of uncertain thermal diffusivity and initial condition:

$$\begin{cases} \dfrac{\partial u(x,\boldsymbol{\xi},t)}{\partial t} - \alpha(\boldsymbol{\xi})\dfrac{\partial^2 u(x,\boldsymbol{\xi},t)}{\partial x^2} = 0, \quad \alpha > 0,\ x \in [0,L] = \Omega \subset \mathbb{R} \\ u(x,\boldsymbol{\xi},0) = u_0(x,\boldsymbol{\xi}), \quad t \in [0,t_F] \quad \text{and} \quad \boldsymbol{\xi} \in \Xi \subset \mathbb{R}^d \\ u(x,\boldsymbol{\xi},t)|_{\partial\Omega} = 0 \\ u_0(x,\boldsymbol{\xi}) = \mathcal{G}(\boldsymbol{\xi})\mathcal{F}_1(\mathbf{x}) + \mathcal{I}(\boldsymbol{\xi})\mathcal{F}_2(\mathbf{x}) \end{cases}$$

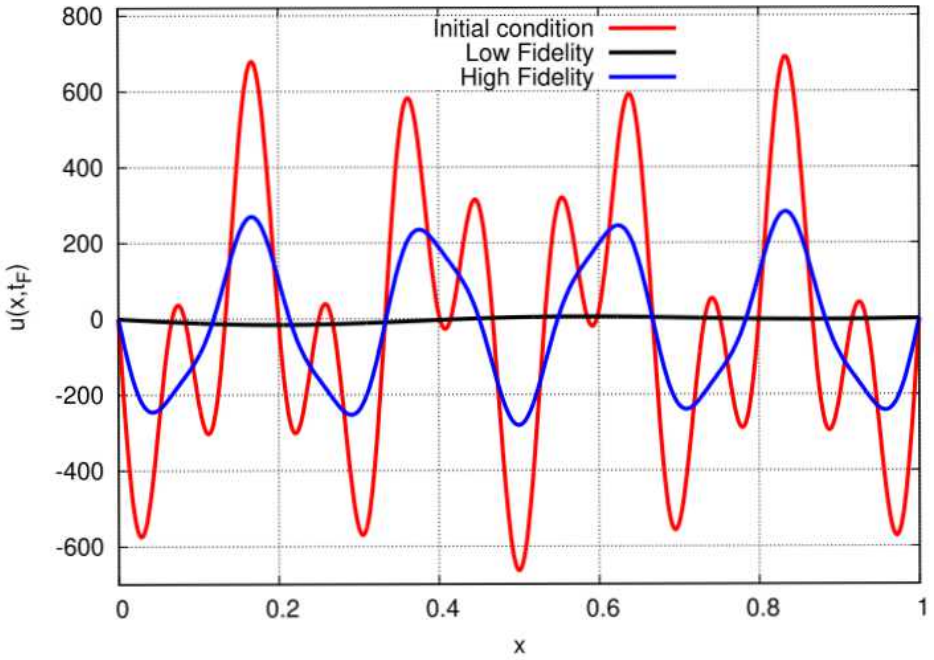

- **Low-fidelity:** $\bar{n}_{\text{low}} = \{1,2,3\} \rightarrow \mathbb{E}\left[Q_{\text{low}}\right] = 33.15$
- **High-fidelity:** $\bar{n}_{\text{high}} = \bar{n}_{\text{low}} \cup \{9,21\} \rightarrow \mathbb{E}\left[Q_{\text{high}}\right] = 41.98$
- Discrepancy $\mathbb{E}\left[Q_{\text{high}}\right] - \mathbb{E}\left[Q_{\text{low}}\right] = 8.83$ (21%)

NUMERICAL RESULTS

DESIGNING A CHALLENGING TEST CASE – MC ON $N_x = 1000$

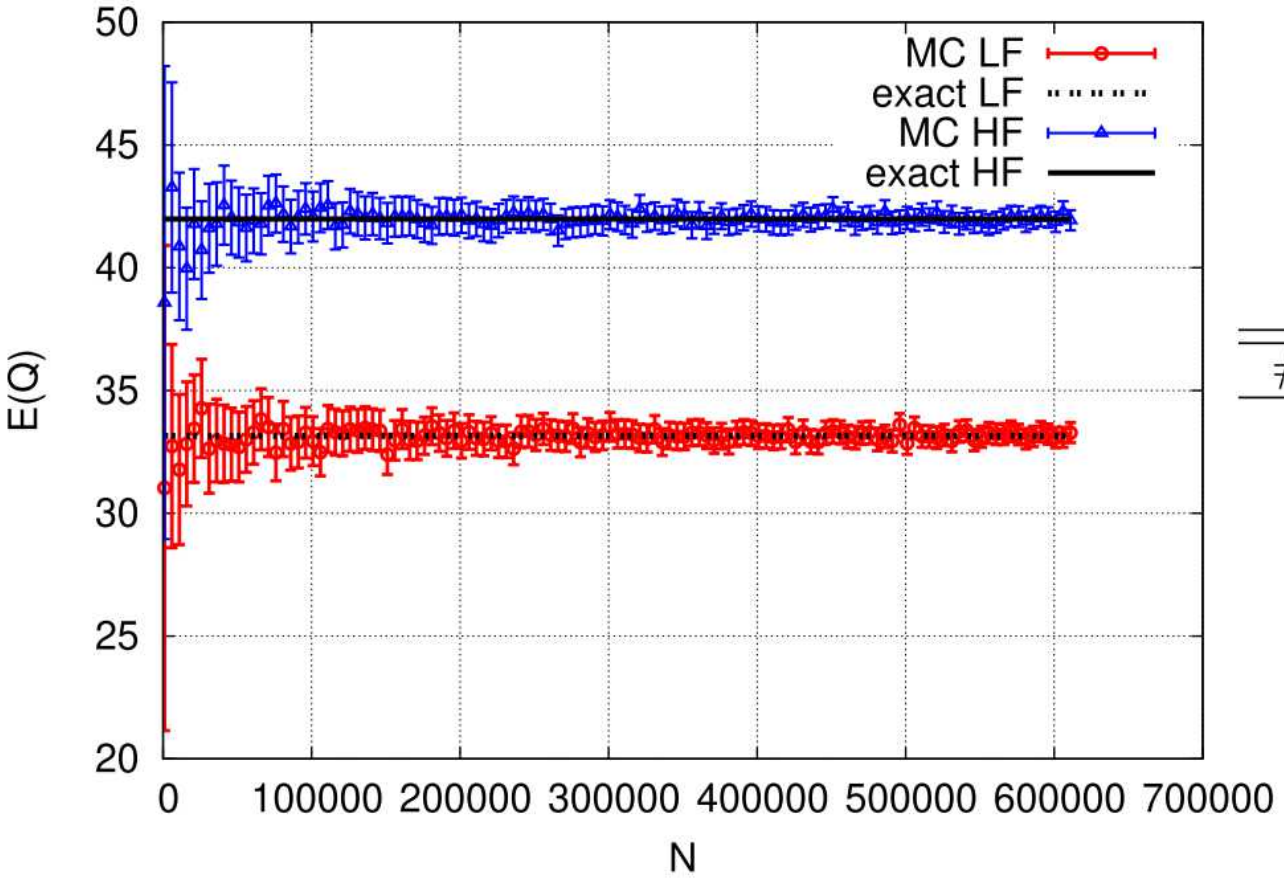

	LF	HF	
# modes	3	21	
	N_x		$\mathbf{w}_\ell$
$\ell = 0$	5	30	42
$\ell = 1$	15	60	28
$\ell = 2$	30	100	23
$\ell = 3$	60	200	23

The LF cannot increase the overall accuracy because it is heavily biased...

Numerical results

Multi-level Multi-fidelity (comparison with MLMC and MC)

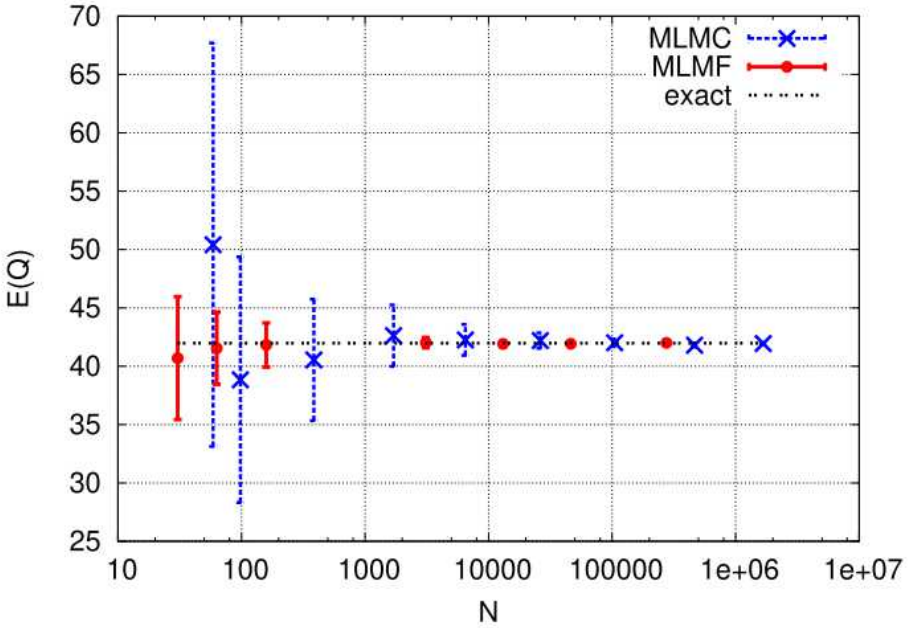

Expected Value

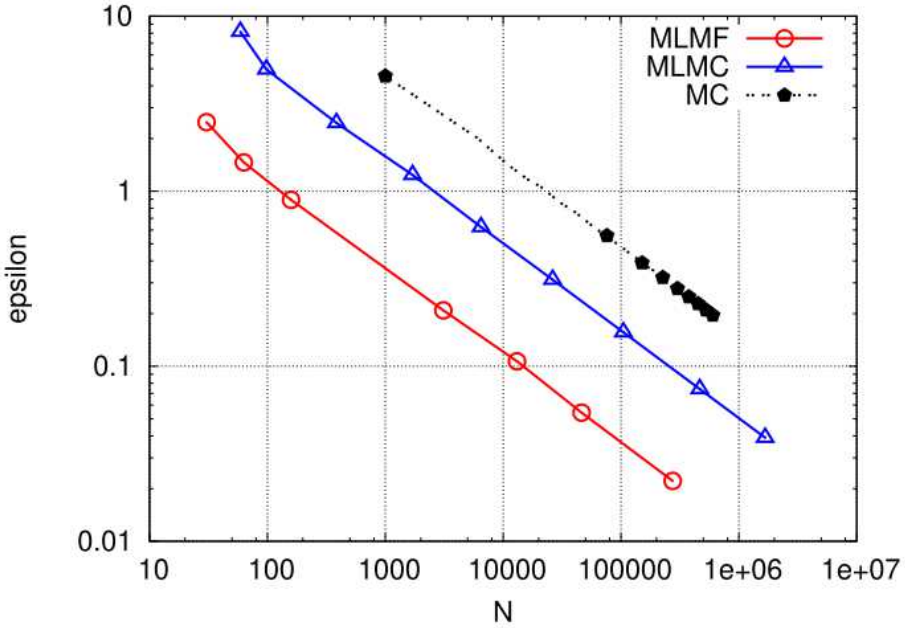

Accuracy ε

Non-linear elastic waves propagation – Hyperbolic CLAWs 1D

Elastic waves propagation in a composite material

28 uncertain variables

- Rod constituted by **50 layers**, two alternated materials (A and B) with constitutive laws

$$\begin{cases} \sigma_A = K_1^A \epsilon + K_2^A \epsilon^2, & K_1^A = 1 \quad \text{and} \quad K_2^A = \xi_j \quad \xi_j \sim \mathcal{U}(0.01, 0.02) \\ \sigma_B = K_1^B \epsilon + K_2^B \epsilon^2, & K_1^A = 1.5 \quad \text{and} \quad K_2^A = 0.8 \end{cases}$$

- Uncertain **initial static** $(u(x, t = 0) = 0)$ **pre-loading** state:

$$\sigma(x) = \begin{cases} \xi_3 \exp\left(-\dfrac{(x - 0.35)(x - 0.25)}{2 \times 0.002}\right) & \text{if} \quad 0 < x < 1/2 \quad \xi_3 \sim \mathcal{U}(0.5, 2) \\ \xi_2 \exp\left(-\dfrac{(x - 0.65)(x - 0.75)}{2 \times 0.002}\right) & \text{if} \quad 1/2 < x < 1 \quad \xi_2 \sim \mathcal{U}(0.5, 6.5) \end{cases}$$

- Spatially varying **uncertain density**: $\rho(x) = \xi_1 + 0.5 \sin(2\pi x), \xi_1 \sim \mathcal{U}(1.5, 2)$
- **Clamped rod** as B.C.

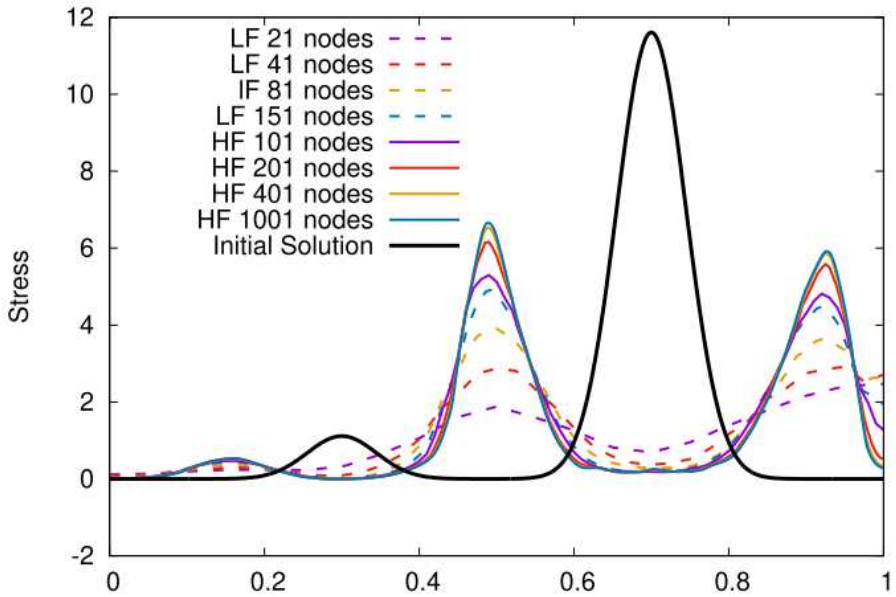

	N_x	N_t	Δ_t
Low-fidelity (GODUNOV)	21	50	3.6×10^{-3}
	41	100	1.8×10^{-3}
	81	150	1.2×10^{-3}
	151	288	6.25×10^{-4}
High-fidelity (MUSCL–van Leer)	101	200	9×10^{-4}
	201	400	4.5×10^{-4}
	401	900	2×10^{-4}
	1001	2000	9×10^{-5}

Table: Low- and high- fidelity simulations

Elastic waves propagation in a composite material

28 uncertain variables

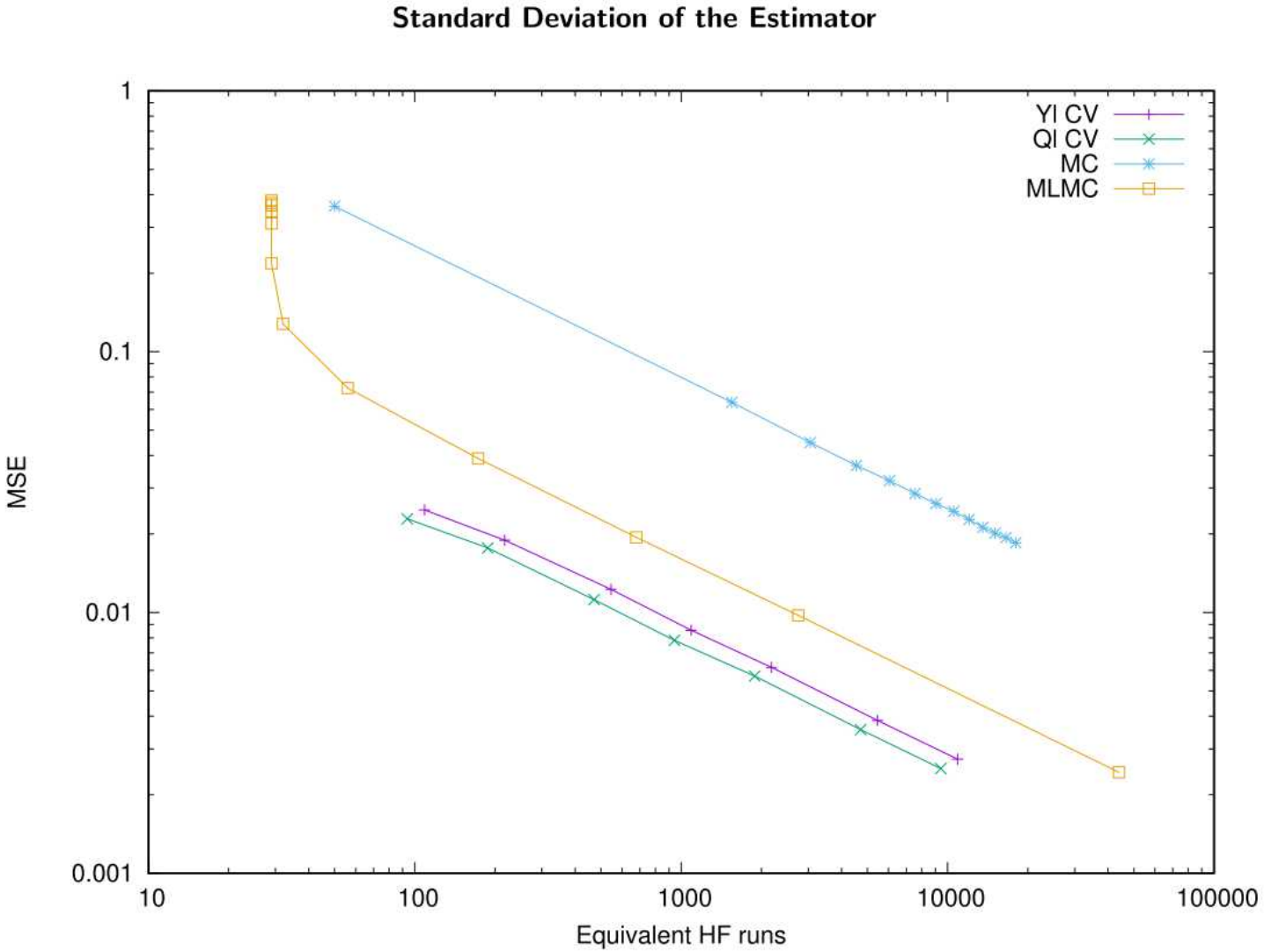

Elastic waves propagation in a composite material

28 uncertain variables – Average of 50 realizations

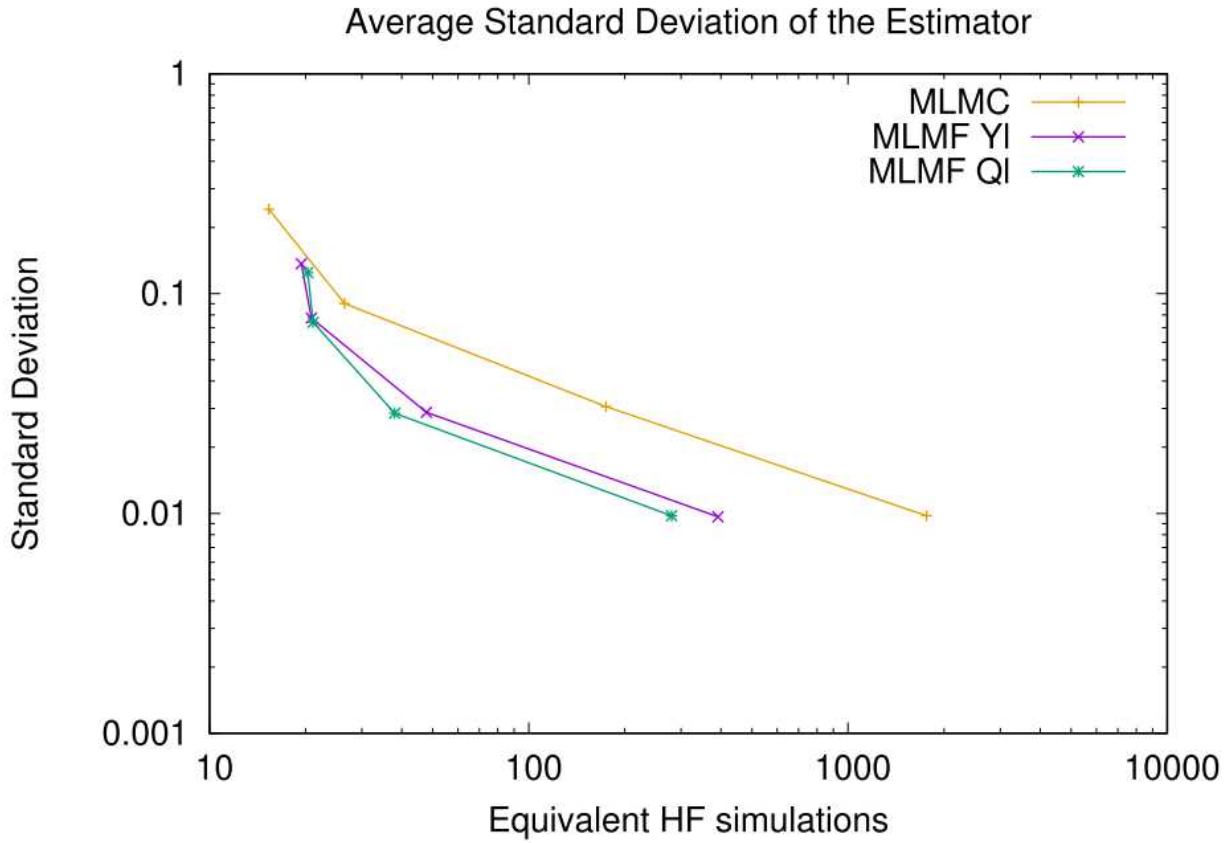

Level	MLMC	MLMF-YI				MLMF-QI			
	N_ℓ	N_ℓ^{HF}	N_ℓ^{LF}	r_ℓ	ρ_ℓ^2	N_ℓ^{HF}	N_ℓ^{LF}	r_ℓ	ρ_ℓ^2
0	80029	5960	243178	40	0.97	4682	192090	40	0.97
1	6282	2434	12487	4	0.49	1049	13781	12	0.83
2	1271	262	3877	14	0.82	151	3657	23	0.92
3	212	47	966	19	0.84	34	754	21	0.86

Elastic waves propagation in a composite material

28 uncertain variables – Average of 50 realizations

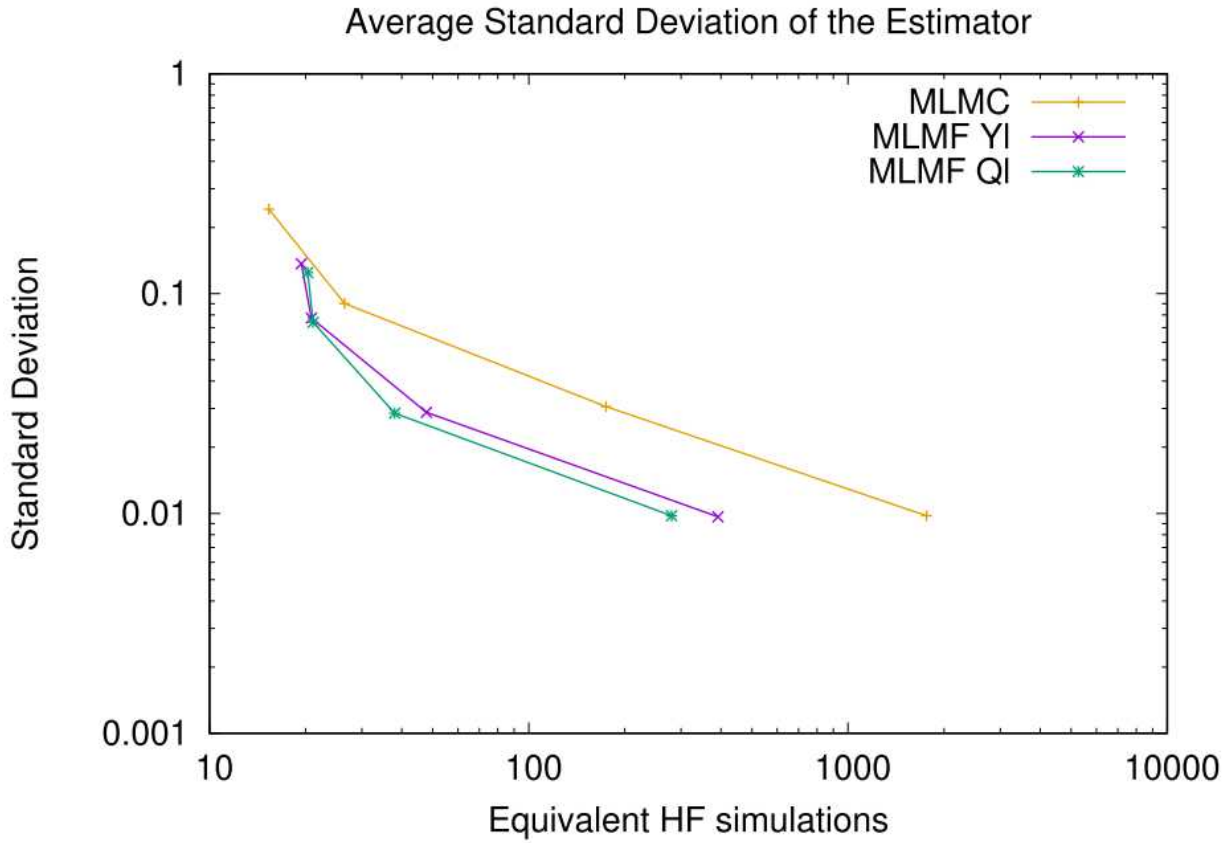

Level	MLMC	MLMF-YI				MLMF-QI			
	N_ℓ	N_ℓ^{HF}	N_ℓ^{LF}	r_ℓ	ρ_ℓ^2	N_ℓ^{HF}	N_ℓ^{LF}	r_ℓ	ρ_ℓ^2
0	80029	5960	243178	40	0.97	4682	192090	40	0.97
1	6282	2434	12487	4	0.49	1049	13781	12	0.83
2	1271	262	3877	14	0.82	151	3657	23	0.92
3	212	47	966	19	0.84	34	754	21	0.86

Elastic waves propagation in a composite material

28 uncertain variables – Average of 50 realizations

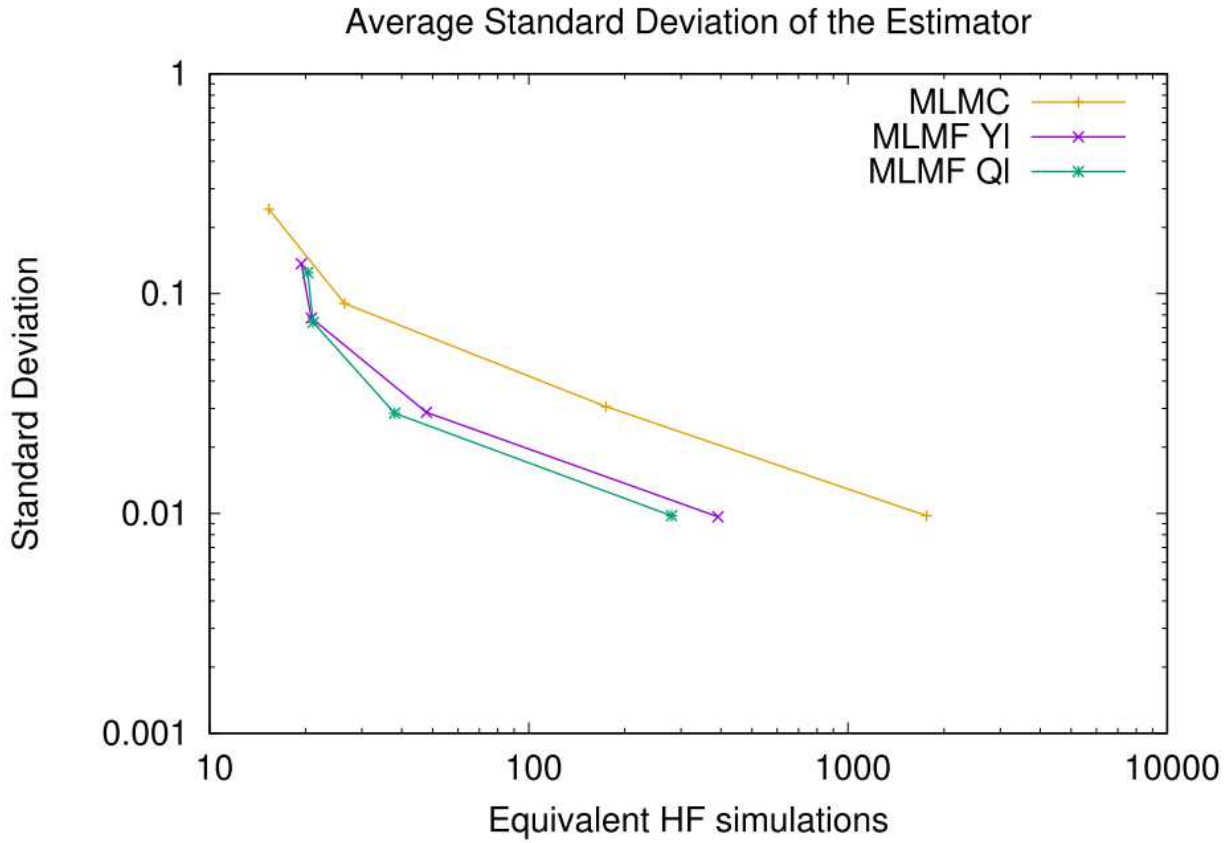

Level	MLMC	MLMF-YI				MLMF-QI			
	N_ℓ	N_ℓ^{HF}	N_ℓ^{LF}	r_ℓ	ρ_ℓ^2	N_ℓ^{HF}	N_ℓ^{LF}	r_ℓ	ρ_ℓ^2
0	80029	5960	243178	40	0.97	4682	192090	40	0.97
1	6282	2434	12487	4	0.49	1049	13781	12	0.83
2	1271	262	3877	14	0.82	151	3657	23	0.92
3	212	47	966	19	0.84	34	754	21	0.86

Approximate Control Variate

Optimal Control Variate

M low-fidelity models with known expected value

Let's consider M **low-fidelity models with known mean**. The Optimal Control Variate (OCV) is generated by adding M unbiased terms to the MC estimator

$$\hat{Q}^{\mathrm{CV}} = \hat{Q} + \sum_{i=1}^{M} \alpha_i \left(\hat{Q}_i - \mu_i \right)$$

- $\hat{Q}_i$ MC estimator for the ith low-fidelity model
- μ_i known expected value for the ith low-fidelity model
- $\underline{\alpha} = [\alpha_i, \ldots, \alpha_M]^{\mathrm{T}}$ set of weights (to be determined)

Let's define

- The covariance matrix among all the low-fidelity models: $\mathbf{C} \in \mathbb{R}^{M \times M}$
- The vector of covariances between the high-fidelity Q and each low-fidelity Q_i: $\mathbf{c} \in \mathbb{R}^{M}$
- $\bar{\mathbf{c}} = \mathbf{c} / \mathbb{V}ar\left[Q\right] = \left[\rho_1 \mathbb{V}ar\left[Q_1\right], \ldots, \rho_M \mathbb{V}ar\left[Q_M\right]\right]^{\mathrm{T}}$, where ρ_i is the correlation coefficient (Q, Q_i)

The optimal weights are obtained as $\underline{\alpha}^{\star} = -\mathbf{C}^{-1}\mathbf{c}$ and the variance of the OCV estimator

$$\begin{aligned} \mathbb{V}ar\left[\hat{Q}^{\mathrm{CV}}\right] &= \mathbb{V}ar\left[\hat{Q}\right] \gamma^{\mathrm{CV}}(\underline{\alpha}^{\star}) = \mathbb{V}ar\left[\hat{Q}\right] (1 - R^2_{OCV}) \\ &= \mathbb{V}ar\left[\hat{Q}\right] \left(1 - \bar{\mathbf{c}}^{\mathrm{T}} \mathbf{C}^{-1} \bar{\mathbf{c}}\right), \quad 0 \leq R^2_{OCV} \leq 1. \end{aligned}$$

For a single low-fidelity model: $R^2_{OCV-1} = \rho_1^2$

Approximate Control Variate

M low-fidelity models with unknown expected value

For complex engineering models the **expected values of the M low-fidelity models are unknown** *a priori*

- Let's define the set of sample used for the high-fidelity model: $\mathbf{z}$
- Let's consider N_i ordered evaluations for Q_i: $\mathbf{z_i}$ (we assume $N_i = \lfloor r_i N \rfloor$)
- Let's partition $\mathbf{z_i}$ in two ordered subsets $\mathbf{z_i^1} \bigcup \mathbf{z_i^2} = \mathbf{z_i}$ (note that in general $\mathbf{z}_i^1 \bigcap \mathbf{z}_i^2 \neq \emptyset$)

The **generic Approximate Control Variate** is defined as

$$\tilde{Q}\left(\underline{\alpha}, \underline{\mathbf{z}}\right) = \hat{Q}(\mathbf{z}) + \sum_{i=1}^{M} \alpha_i \left(\hat{Q}_i(\mathbf{z_i^1}) - \hat{\mu}_i(\mathbf{z_i^2})\right) = \hat{Q}(\mathbf{z}) + \sum_{i=1}^{M} \alpha_i \Delta_i(\mathbf{z_i}) = \hat{Q} + \underline{\alpha}^{\mathrm{T}} \underline{\Delta},$$

The **optimal weights** and **variance** can be obtained as

$$\underline{\alpha}^{\mathrm{ACV}} = -\mathbb{C}ov\left[\underline{\Delta}, \underline{\Delta}\right]^{-1} \mathbb{C}ov\left[\underline{\Delta}, \hat{Q}\right]$$

$$\begin{aligned}\mathbb{V}ar\left[\tilde{Q}\left(\underline{\alpha}^{ACV}\right)\right] &= \mathbb{V}ar\left[\hat{Q}\right]\left(1 - \mathbb{C}ov\left[\underline{\Delta}, \hat{Q}\right]^{\mathrm{T}} \frac{\mathbb{C}ov\left[\underline{\Delta}, \underline{\Delta}\right]^{-1}}{\mathbb{V}ar\left[\hat{Q}\right]} \mathbb{C}ov\left[\underline{\Delta}, \hat{Q}\right]\right) \\ &= \mathbb{V}ar\left[\hat{Q}\right]\left(1 - R^2_{\mathrm{ACV}}\right).\end{aligned}$$

For a single low-fidelity model: $R^2_{ACV-1} = \frac{r_1 - 1}{r_1}\rho_1^2$ (this result does not depend on the partitioning of $\mathbf{z_1}$)

Multilevel Monte Carlo

A recursive partitioning with independent estimators (Given a prescribed bias)

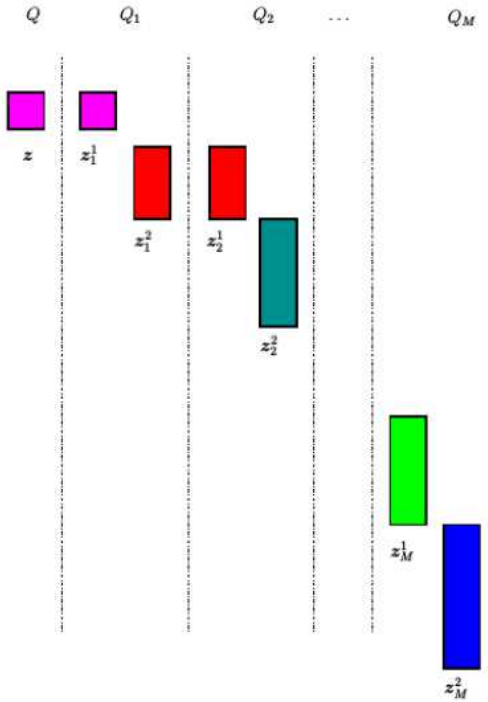

MLMC can be obtained from ACV with

- $\mathbf{z_i^1} = \mathbf{z}$
- $\mathbf{z_i^2} = \mathbf{z_{i+1}^1}$ for $i = 1, \ldots, M-1$
- $\alpha_\mathbf{i} = -\mathbf{1}$ for all i

$$\hat{Q}^{\text{MLMC}}(\mathbf{z}) = \hat{Q} + \sum_{i=1}^{M} (-1) \left(\hat{Q}_i(\mathbf{z_i^1}) - \hat{\mu}_i(\mathbf{z_i^2}) \right)$$

$$\mathbb{V}ar\left[\hat{Q}^{\text{MLMC}}\right] = \mathbb{V}ar\left[\hat{Q}\right]\left(1 - R^2_{\text{MLMC}}\right)$$

$$R^2_{\text{MLMC}} = -\sum_{i=1}^{M} \frac{\bar{r}_i + \bar{r}_{i-1}}{\bar{r}_i \bar{r}_{i-1}} \tau_i^2 + 2 \sum_{i=1}^{M-1} \frac{\rho_{i,i+1} \tau_i \tau_{i+1}}{\bar{r}_i} - 2\rho_1 \tau_1, \quad \tau_i = \sqrt{\mathbb{V}ar\left[Q_i\right] / \mathbb{V}ar\left[Q\right]}$$

where

- $\mathbf{z}_i^1$ and $\mathbf{z}_i^2$ is $\bar{r}_{i-1}N$ and $\bar{r}_i N$ and $\bar{r}_0 = 1$, it holds that $r_i = \bar{r}_i + \bar{r}_{i-1}$

Given the recursive nature of MLMC, we can show that $R^2_{\text{MLMC}} < \rho_1^2$

Multifidelity Monte Carlo

An approximated control variate with a recursive partitioning

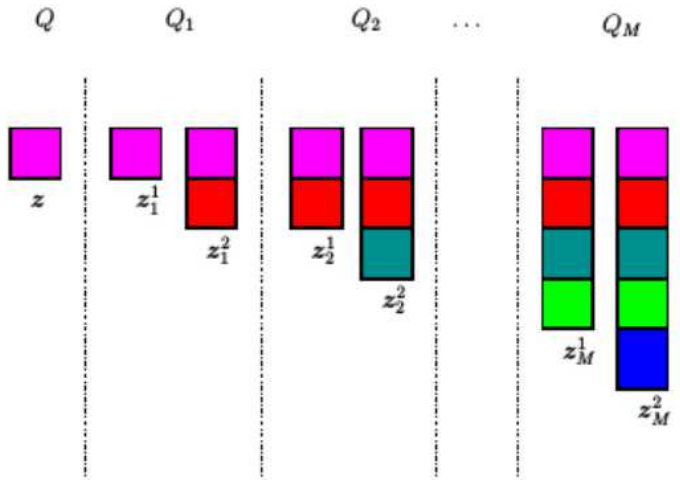

MFMC can be obtained from ACV with

- $\mathbf{z}_i^1 = \mathbf{z}_{i-1}$ and $\mathbf{z}_i^2 = \mathbf{z}_i$ for $i = 2, \dots, M$
- $\mathbf{z}_1^1 = \mathbf{z}$ and $\mathbf{z}_1^2 = \mathbf{z}_1$

$$\alpha_i^{\text{MFMC}} = -\frac{\mathbb{C}ov\left[Q, Q_i\right]}{\mathbb{V}ar\left[Q_i\right]}, \quad \text{for} \quad i = 1, \dots, M,$$

and the variance of the estimator is

$$\mathbb{V}ar\left[\underline{\alpha}^{\text{MFMC}}\right] = \mathbb{V}ar\left[\hat{Q}\right]\left(1 - R^2_{\text{MFMC}}\right)$$

$$R^2_{\text{MFMC}} = \sum_{i=1}^{M} \frac{r_i - r_{i-1}}{r_i r_{i-1}} \rho_i^2 = \rho_1^2 \left(\frac{r_1 - 1}{r_1} + \sum_{i=2}^{M} \frac{r_i - r_{i-1}}{r_i r_{i-1}} \frac{\rho_i^2}{\rho_1^2} \right).$$

Given the recursive nature of MFMC, we can show that $R^2_{\text{MFMC}} < \rho_1^2$

Examples of Convergent Estimators

Is it possible to overcome the limitation of the recursive sampling schemes?

We proposed two sampling strategies that overcome the limitation of the recursive schemes

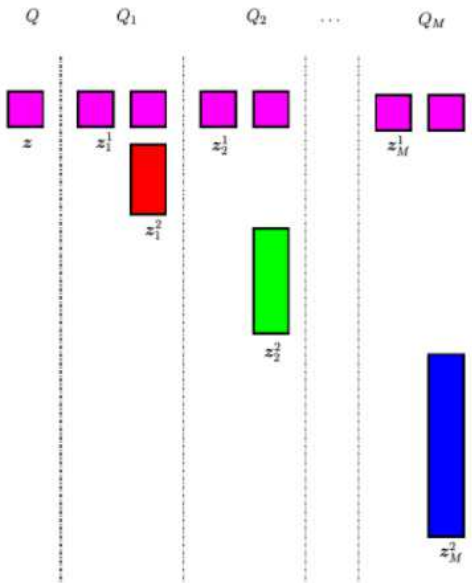

(a) ACV-IS sampling strategy.

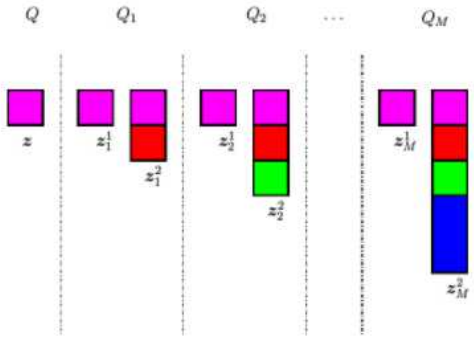

(b) ACV-MF sampling strategy.

As an example, let's consider the **ACV-MF estimator**

$$R^2_{\text{ACV}-\text{MF}} = \left[\text{diag}\left(\mathbf{F}^{(\text{MF})}\right) \circ \bar{\mathbf{c}}\right]^{\text{T}} \left[\mathbf{C} \circ \text{diag}\left(\mathbf{F}^{(\text{MF})}\right)\right]^{-1} \left[\text{diag}\left(\mathbf{F}^{(\text{MF})}\right) \circ \bar{\mathbf{c}}\right].$$

The matrix $\mathbf{F}^{(\text{MF})} \in \mathbb{R}^{M\times M}$ encodes the particular sampling strategy and is defined as

$$\mathbf{F}^{(\text{MF})}_{ij} = \begin{cases} \frac{\min(r_i,r_j)-1}{\min(r_i,r_j)} & \text{if } i \neq j \\ \frac{r_i-1}{r_i} & \text{otherwise} \end{cases}, \quad \text{for } \mathbf{r_i} \to \infty, \quad \mathbf{F}^{(\text{MF})} \to \mathbf{1_M} \text{ and } \mathbf{R^2_{\text{ACV}-\text{MF}}} \to \mathbf{R^2_{\text{OCV}}}$$

A PARAMETRIC MODEL PROBLEM

WHAT HAPPENS FOR A LIMITED NUMBER OF LOW-FIDELITY SIMULATIONS?

We designed a parametric test problem to explore different cost and correlation scenarios ($x, y \sim \mathcal{U}(-1, 1)$)

$$Q = A\left(\cos\theta\, x^5 + \sin\theta\, y^5\right)$$
$$Q_1 = A_1\left(\cos\theta_1\, x^3 + \sin\theta_1\, y^3\right)$$
$$Q_2 = A_2\left(\cos\theta_2\, x + \sin\theta_2\, y\right)$$

We use the following definitions

- $A = \sqrt{11}$, $A_1 = \sqrt{7}$, and $A_2 = \sqrt{3}$ (give unitary variance for each model)
- $\theta = \pi/2$ and $\theta_2 = \pi/6$ and θ_1 varies uniformly in the bounds $\theta_2 < \theta_1 < \theta$
- We consider a fixed cost ratio between models, *i.e.* a relative cost of 1 for Q, $1/w$ for Q_1 and $1/w^2$ for Q_2

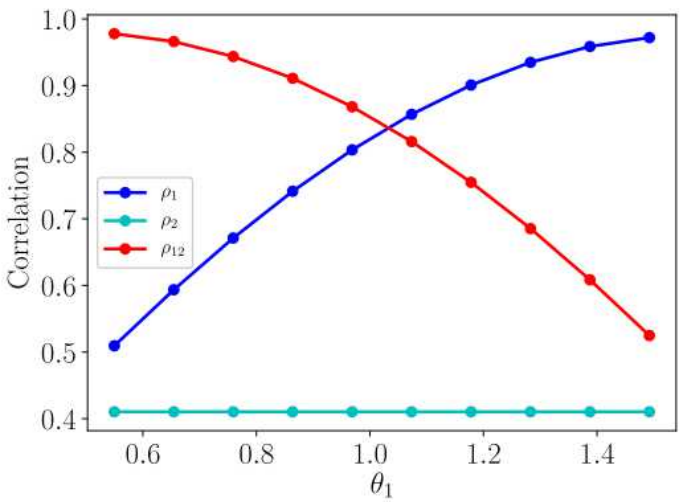

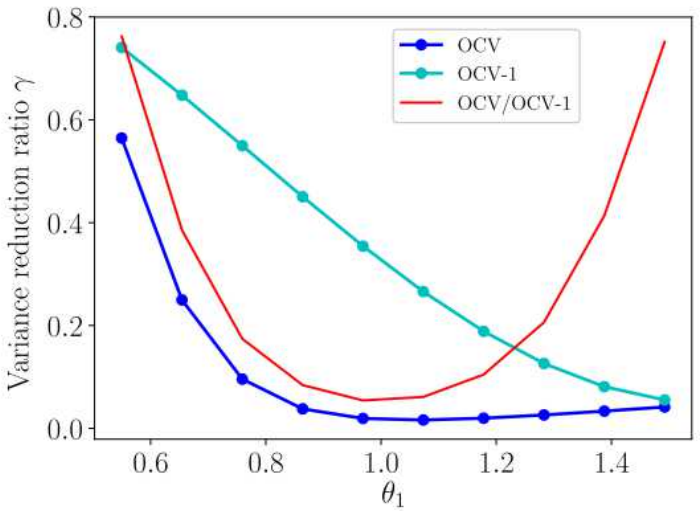

A PARAMETRIC MODEL PROBLEM

COMPARISON OF DIFFERENT ESTIMATORS

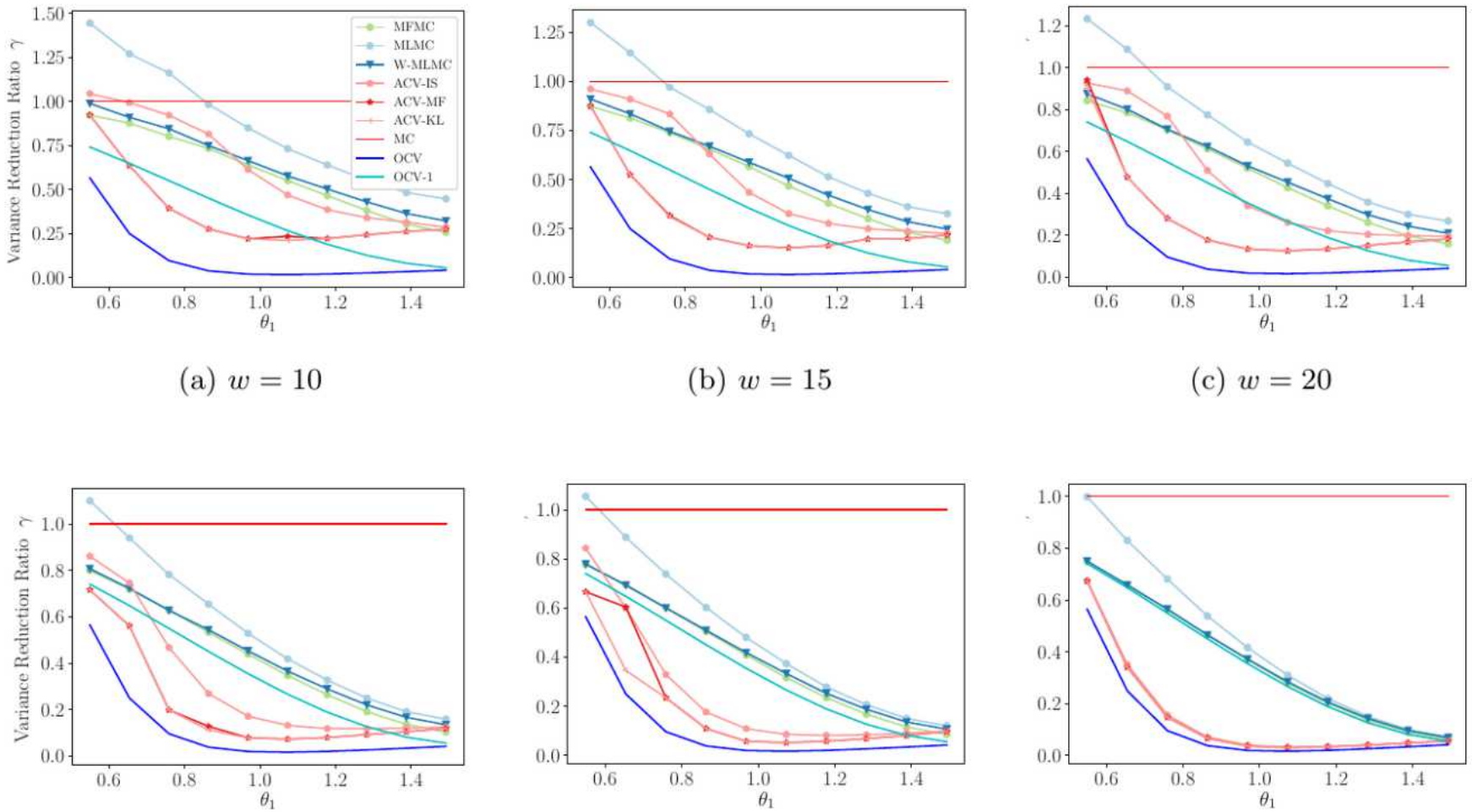

(a) $w = 10$ (b) $w = 15$ (c) $w = 20$

(d) $w = 50$ (e) $w = 100$ (f) $w = 1000$

FIGURE: Variance reduction for cost ratios of $[1, 1/w, 1/w^2]$ for Q, Q_1, and Q_2

Aero-thermo-structural analysis – A more realistic engineering example

Aero-thermo-structural analysis of a jet engine nozzle

Problem inspired by the Northrop Grumman UCAS X-47B

(a) X47B UCAS (b) Nozzle close-up

FIGURE: Northrop Grumman X-47B UCAS and close up of its nozzle[1].

Operative conditions

- Reconnaissance mission for an high-subsonic aircraft
- Most critical condition is the top-of-climb (Required thrust is $21,500$ N) @ $40,000$ ft and Mach 0.51

Nozzle structure Two layers separated by an air gap

- Inner thermal layer: ceramic matrix composite
- Outer load layer: composite sandwich material (titanium honeycomb between two layers of graphite-bismaleimide Gr/BMI)

Uncertain parameters 40 uncertain parameters – mix of uniform and log-normal variables

- 35 material properties variables
- 2 atmospheric conditions
- 2 inlet conditions
- 1 heat transfer coefficient

[1] http://www.northropgrumman.com/MediaResources/Pages/MediaGallery.aspx?ProductId=UC-10028

Aero-thermo-structural analysis of a jet engine nozzle

Computational setup

A multiphysics problem (forward coupling)

- An **Engine simulator** provides the inlet conditions of the nozzle
- The **SU2** CFD solver computes the temperature and pressure profile along the walls
- The Finite Element solver **AERO-S** computes (several metrics for) mechanical and thermal stresses in the structure

Quantities of Interest (QoIs)

- **Mass** as a surrogate for the cost of the device
- **Thrust** for the aerodynamics performance
- A temperature failure criterion in the inner load layer (**Thermal stresses**)
- A strain failure criterion in the thermal layer (**Mechanical stresses**)

NOTE: this problem naturally leads to a multifidelity setup

- Several CFD choices ranging from 1D ideal solver up to 3D RANS
- Geometrical approximations (Axisymmetric assumption)
- Several spatial resolutions for both the CFD and FEM meshes
- etc.

Preliminary results for the Sequoia problem

Computational setup

- We demonstrated that all the recursive schemes (MLMC, MFMC, MLMF, MIMC etc.) are bounded by the correlation of the first low-fidelity model
- We want to verify that for the Sequoia problem a more efficient estimator can be built, *i.e.* $R^2_{OCV} > R^2_{OCV-1}$

CFD	FEM (Thermal/Structural)	Cost
1D	COARSE	2.63e-04
Euler 2D COARSE	COARSE (axisymmetric)	9.69e-04
Euler 2D MEDIUM	MEDIUM (axisymmetric)	3.18e-03
Euler 2D FINE	FINE (axisymmetric)	9.05e-03
Euler 3D COARSE	COARSE	1.16e-02
Euler 3D MEDIUM	MEDIUM	3.58e-02
RANS 3D COARSE	COARSE	1.00

Table: Relative computational cost for several model fidelities for the nozzle problem. All the cost are normalized with respect to the 3D RANS solver.

Preliminary results for the Sequoia problem

Comparison between OCV and OCV-1

	Variance reduction		
QoI	**OCV**	**OCV-1**	**Ratio OCV/OCV-1**
Thrust	0.020595	0.050432	0.41
Thermal stresses	0.0043612	0.0075662	0.58
Mechanical stresses	6.2981e-04	0.011720	0.05

Table: Performance of OCV and OCV-1 for the nozzle problem and three different QoIs.

- A separation between OCV and OCV-1 exists for all QoIs
- OCV-1 attains more than one order of magnitude reduction over MC
- For Thrust and Thermal stresses an additional 60% and 40% reduction can be gained with OCV
- For the Mechanical stresses the additional benefit is larger than 90%

The next step is to include the cost to understand how effectively we can exploit this gap with the estimators we proposes

Leveraging Active Directions for Multifidelity UQ

Can we enhance correlation between models?

Multifidelity UQ on the reduced (shared) space

Core Question

Q: Can we identify a shared space between models (possibly with independent/non-shared parameterization) where the correlation is higher?

A: Active Subspace method seems well suited for this (but this idea is not limited to it)

Pivotal idea and its main features

- For each model one can search for **Active Directions** independently
- If the **input variables** of a models are **standard Gaussian variables** then the Active Variables are also standard Gaussian variables
- Therefore, for each model the QoI can be represented on a (possibly reduced) space characterized by a join standard Gaussian distribution
- We can sample along these shared Active Directions and **'map back'** to the original coordinates of **each model separately**

Some Questions:

- How do we treat the inactive variables?
- What if the model input are not Gaussian variables?
- What does it happen if the Active Directions are different between models? We expect this to happen often in practice
- Why is this even supposed to work from a physical standpoint?

Active Subspaces in a Nutshell

(Almost) everything you need to know to use it with Multifidelity – see Constantine (2015) for more

We consider a black-box approach, *i.e.* the QoI Q is obtained through a computational model f given a vector of input parameters $\mathbf{x}$

$$\mathbf{x} \rightarrow \boxed{f(\mathbf{x})} \rightarrow Q$$

- Vector of Input parameters: $\mathbf{x} \in \mathbb{R}^m$ with joint distribution $\rho(\mathbf{x})$
- Let's introduce the $m \times m$ matrix $\mathbf{C}$

$$\mathbf{C} = \int \left(\vec{\nabla} f\right) \left(\vec{\nabla} f\right)^{\mathrm{T}} \rho(\mathbf{x}) \mathrm{d}\,\mathbf{x}$$

- Since $\mathbf{C}$ is I) Positive semidefinite and II) Symmetric, it exists a real eigenvalue decomposition

$$\mathbf{C} = \mathbf{W}\boldsymbol{\Lambda}\mathbf{W}^{\mathrm{T}}, \text{where}$$

- $\mathbf{W}$ is the $m \times m$ orthogonal matrix whose columns are the normalized eigenvectors
- $\boldsymbol{\Lambda} = \mathrm{diag}\left\{\lambda_1, \ldots, \lambda_m\right\}$ and $\lambda_1 \geq \cdots \geq \lambda_m \geq 0$

Let's define two sets of variables

$$\begin{cases} \mathbf{y} = \mathbf{W}_A^{\mathrm{T}}\mathbf{x} \in \mathbb{R}^n & \text{(Active)} \\ \mathbf{z} = \mathbf{W}_I^{\mathrm{T}}\mathbf{x} \in \mathbb{R}^{(m-n)} & \text{(Inactive)} \end{cases} \implies \mathbf{x} = \mathbf{W}_A\mathbf{y} + \mathbf{W}_I\mathbf{z} \approx \mathbf{W}_A\mathbf{y}$$

Linearity: $\boxed{\mathbf{x} \sim \mathcal{N}(\mathbf{0}, \mathbb{I})}$ $\left(\mathcal{X} = \mathbb{R}^m\right)$ then $\mathcal{Y} = \left\{\mathbf{y} \in \mathbb{R}^n, \mathbf{y} = \mathbf{W}_A^{\mathrm{T}}\mathbf{x}, \mathbf{x} \in \mathbb{R}^m\right\}$ and $\boxed{\mathbf{y} \sim \mathcal{N}(\mathbf{0}, \mathbb{I})}$

This is true for each model, i.e. there will always be a shared space between different models (even if they have a different parameterization)

A Quick Demonstration – Gaussian Input

Low-correlated models (Correlation squared 0.05)

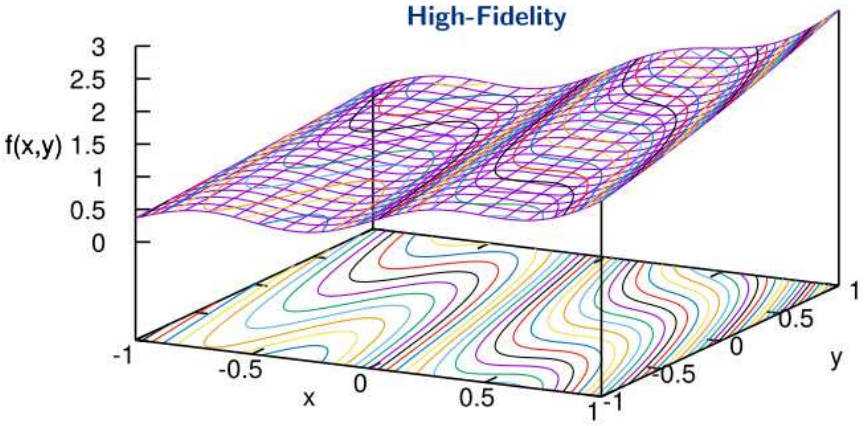

$$f(x,y) = \exp(0.7x + 0.3y) + 0.15\,(2\pi x)$$

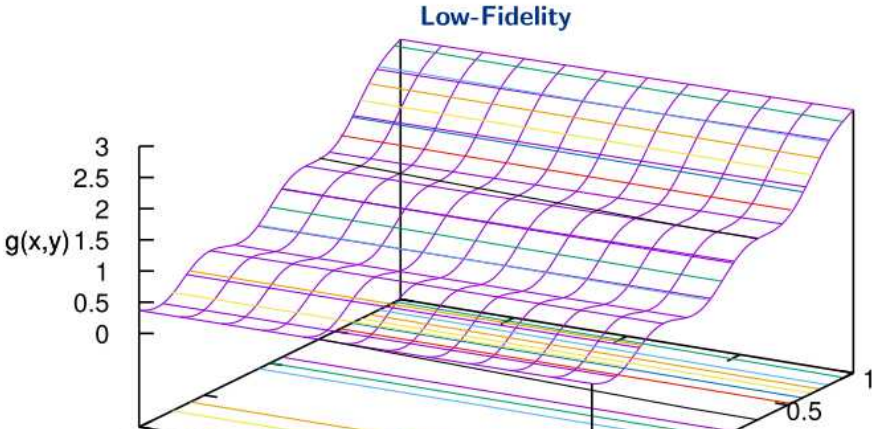

$$g(x,y) = \exp(0.01x + 0.99y) + 0.15\,(3\pi y)$$

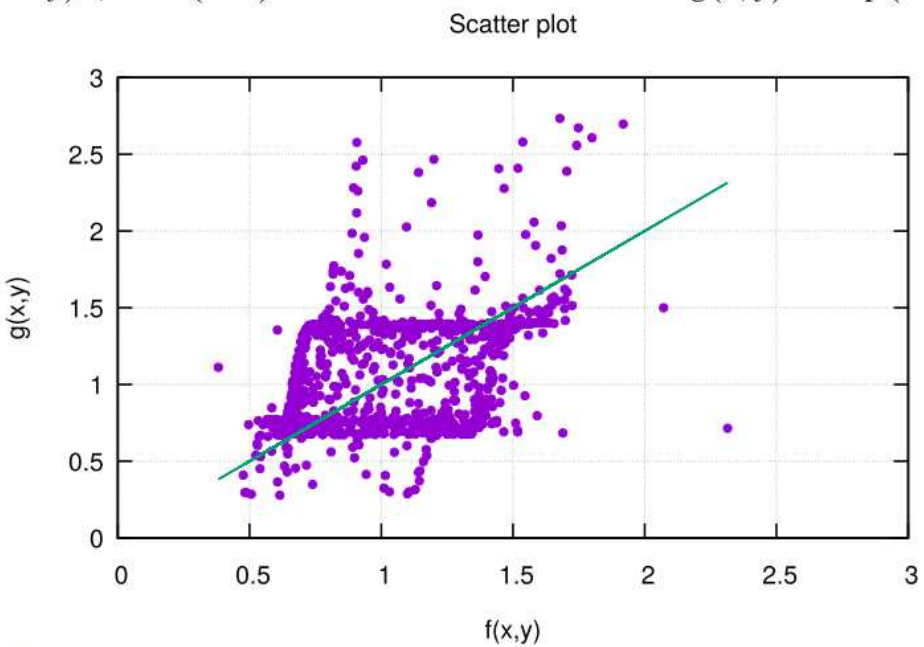

A Quick Demonstration – Gaussian Input

Important Directions in Actions (Correlation Squared from 0.05 to 0.9)

Independent Important Directions

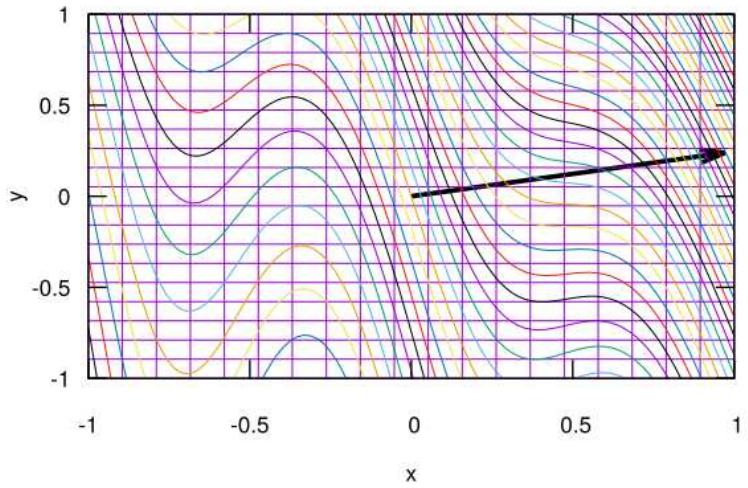

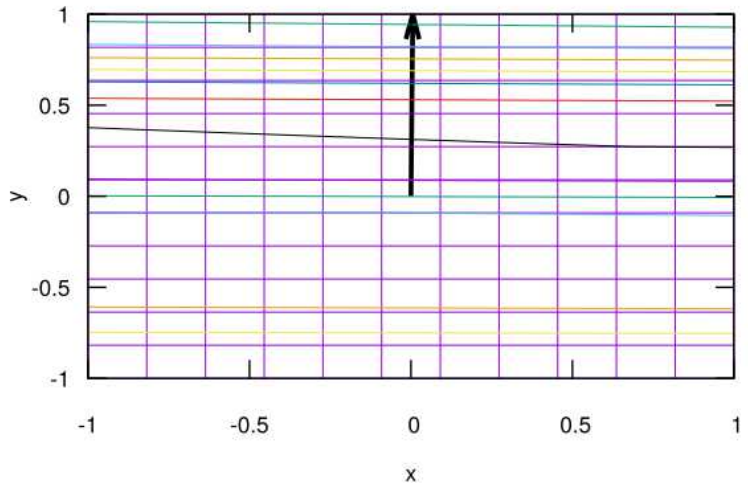

Responses and Correlation along the AS

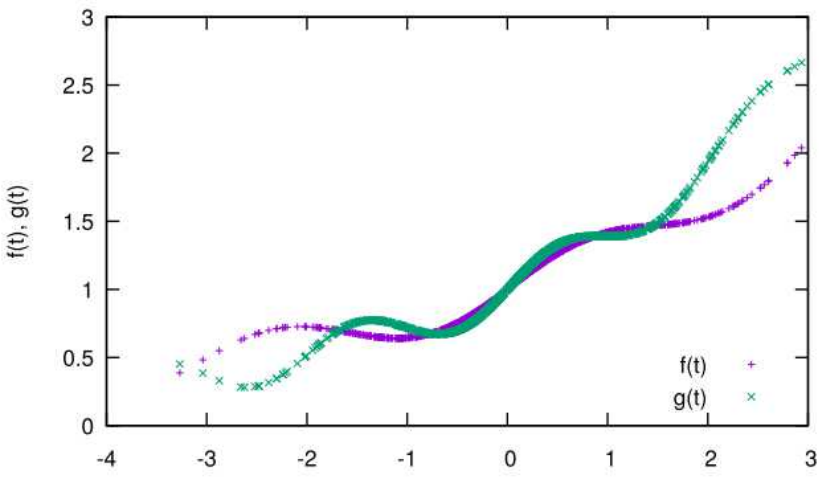

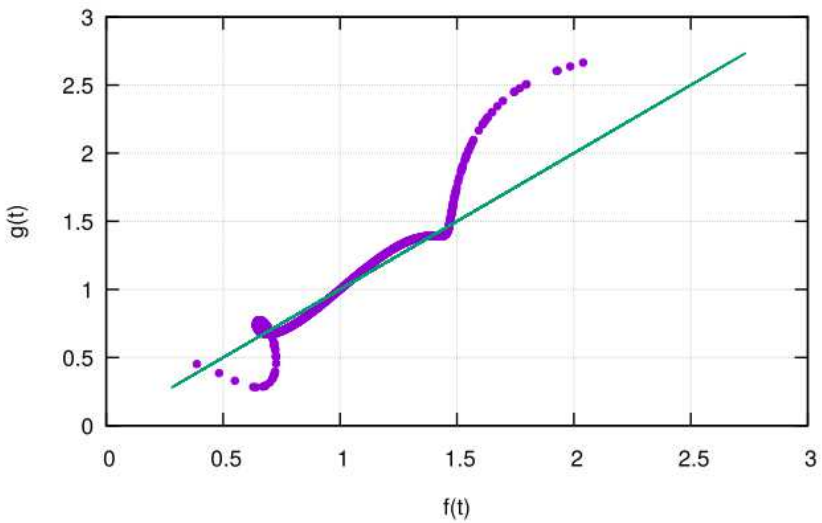

A Quick Demonstration – Gaussian Input

Numerical Experiment Setup

We performed the following numerical experiment:

- We **fix a computational budget** (300 HF runs)
- We compute **1000 realizations for each estimator**
- For MF estimator the cost of the total set of HF+LF runs is considered
- We report the pdf of the estimated Expected Value

NOTE 1: For this problem the expected value is known
NOTE 2: In this example the AS are searched for each estimator realization during the pilot sample phase (this cost is not included, but they can be reused if needed...)

A Quick Demonstration

Monte Carlo Versus Control Variate

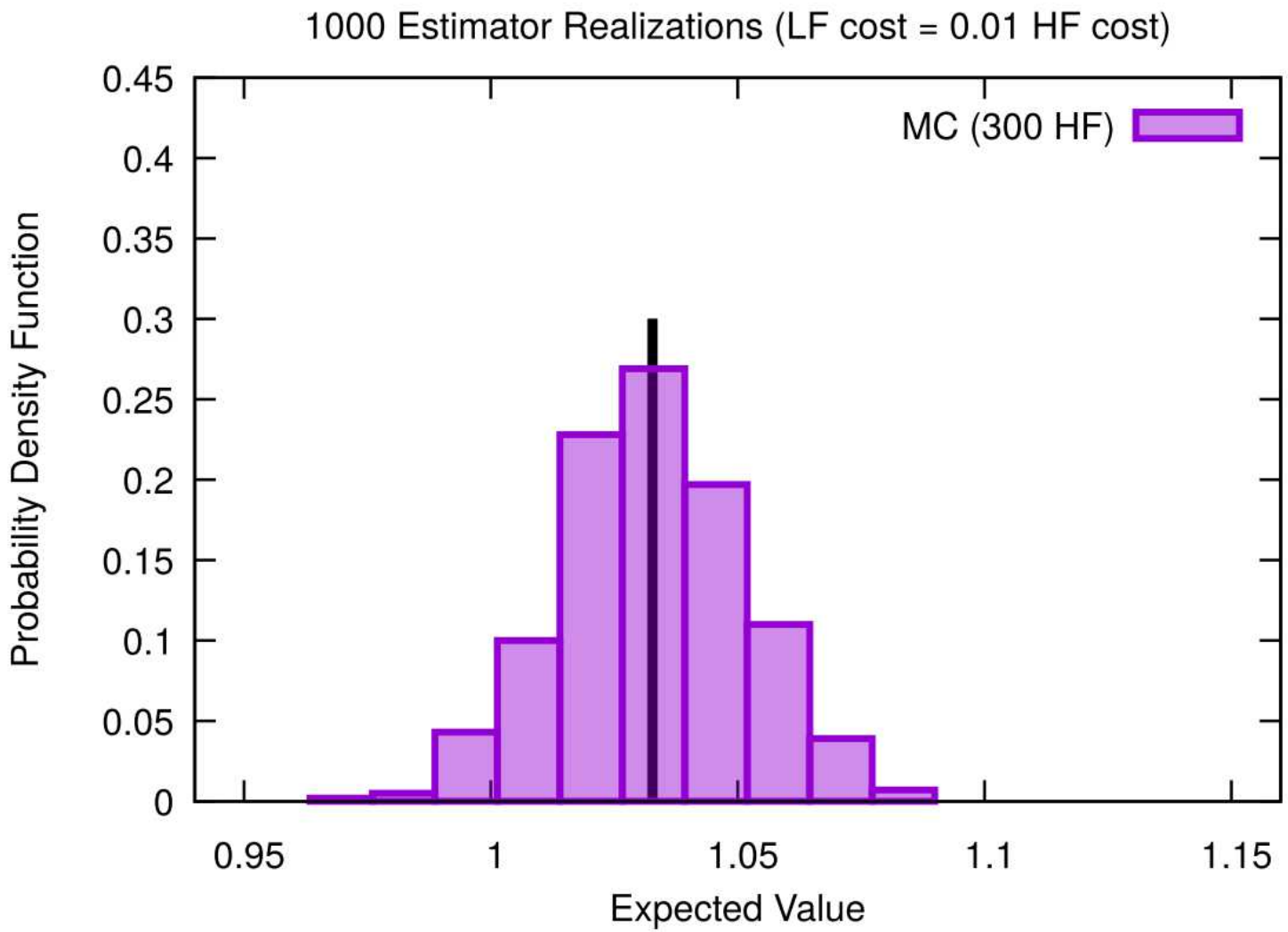

A Quick Demonstration

Monte Carlo Versus Control Variate

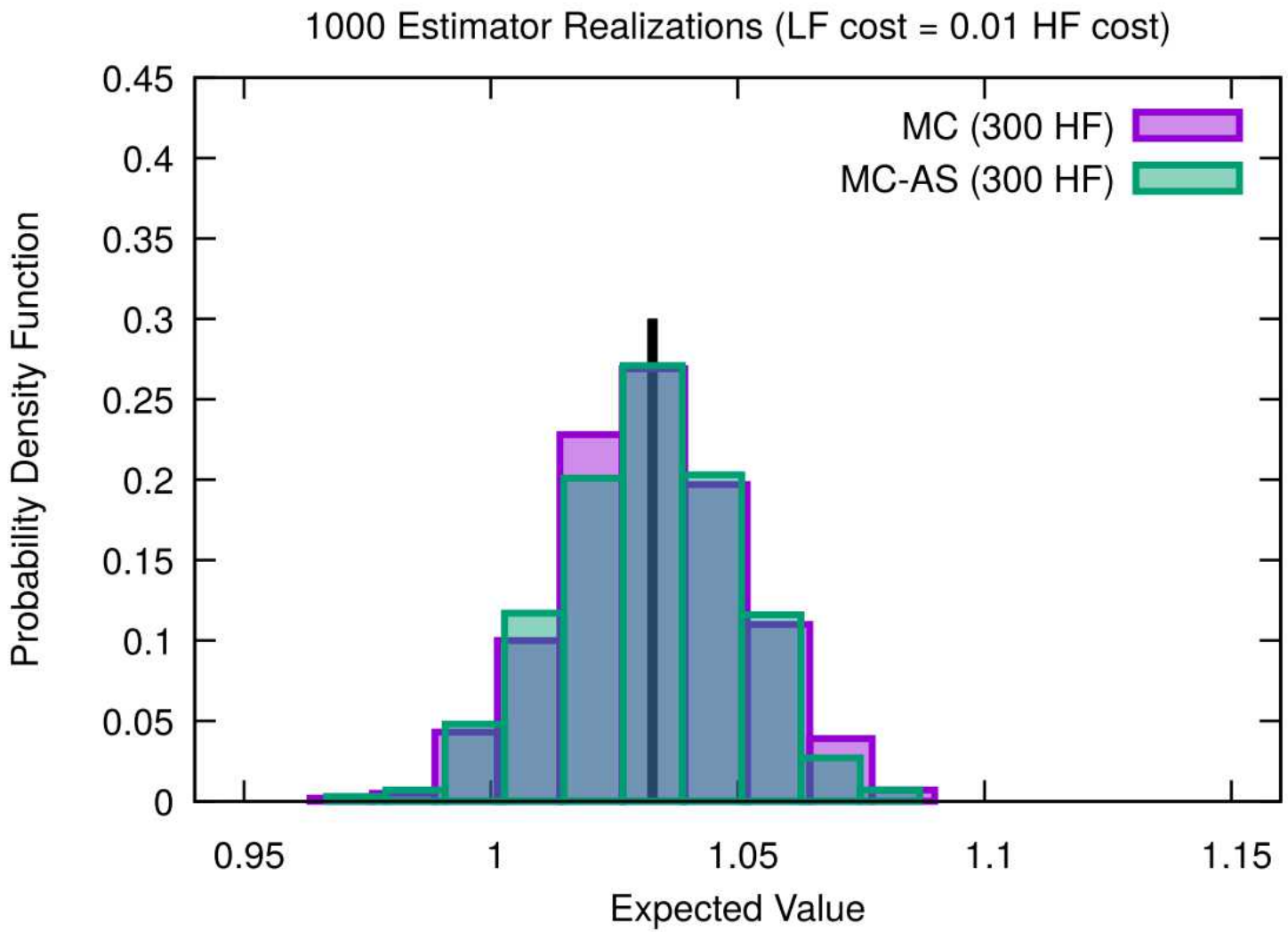

A Quick Demonstration

Monte Carlo Versus Control Variate

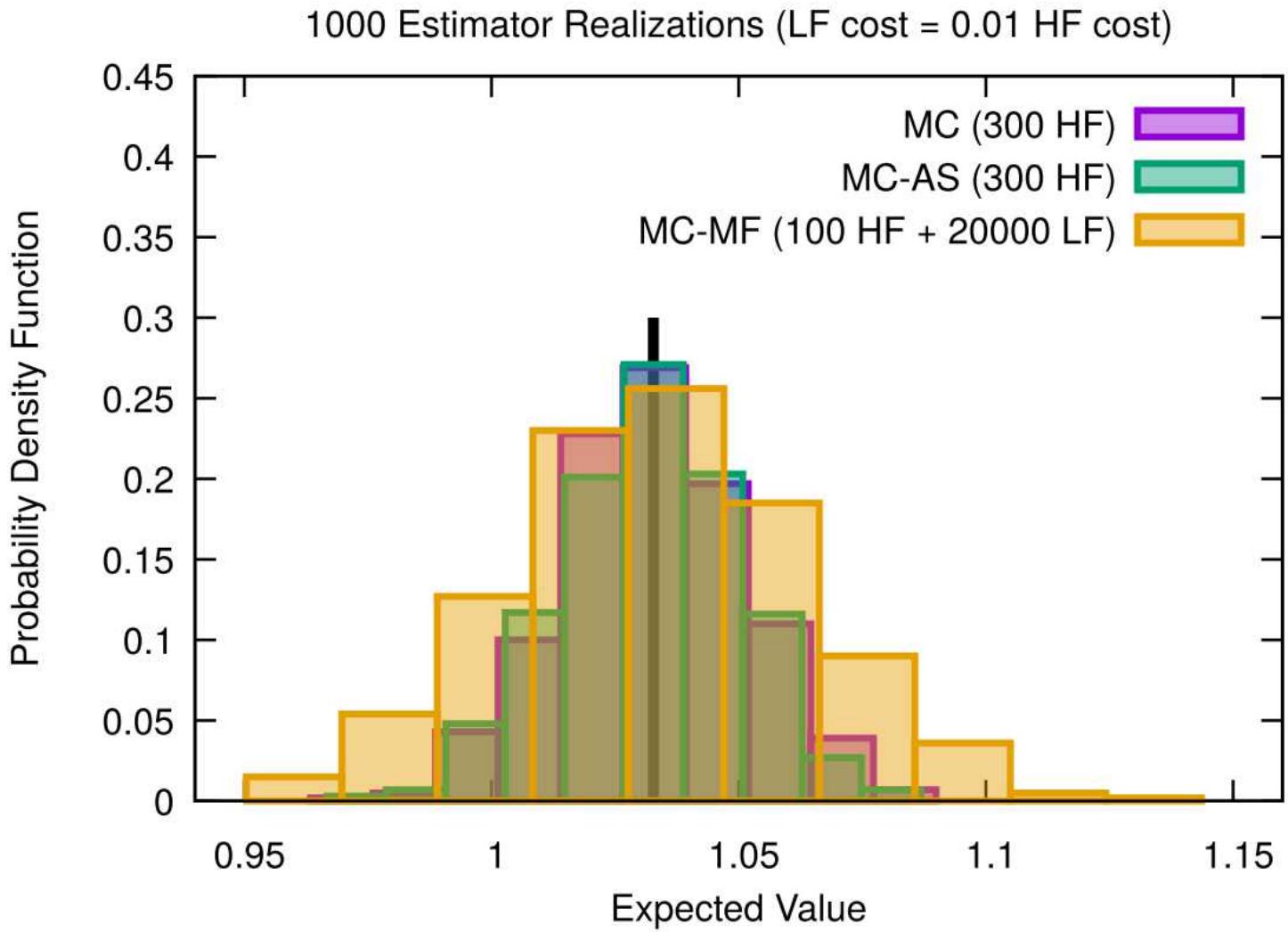

A Quick Demonstration

Monte Carlo Versus Control Variate

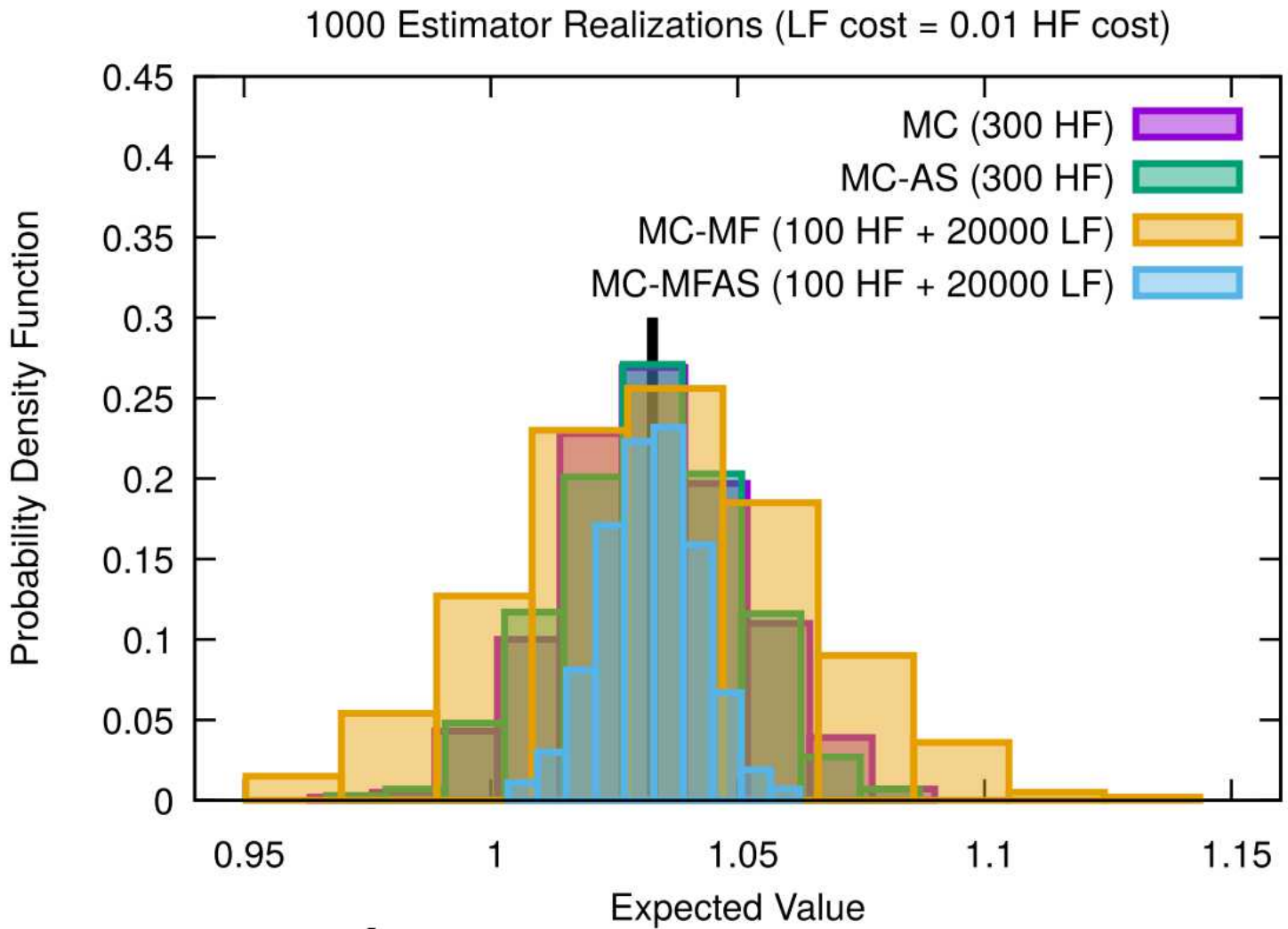

Same computational cost for all the estimators!

What about the inactive variables?

How do you treat the inactive variables?

$$\mathbf{x} = \mathbf{W_A}\mathbf{y} + \mathbf{W_{NA}}\mathbf{z}$$

- Given a sample along the Active Variable $\mathbf{y}$, we need to recover $\mathbf{x}$
- This mapping is ill-posed (infinitely many $\mathbf{x}$ exist)
- One possible regularization: conditional expected value of f given $\mathbf{y}$

$$f_{AS}(\mathbf{y}) = \int f(\mathbf{W_A}\mathbf{y} + \mathbf{W_{NA}}\mathbf{z})\, \rho_{\mathbf{z}|\mathbf{y}}\, \mathrm{d}\,\mathbf{z} \approx f(\mathbf{W_A}\mathbf{y} + \mathbf{W_I}\mathbb{E}[\mathbf{z}]) \int \rho_{\mathbf{z}|\mathbf{y}}\, \mathrm{d}\,\mathbf{z} = f(\mathbf{W_A}\mathbf{y})$$

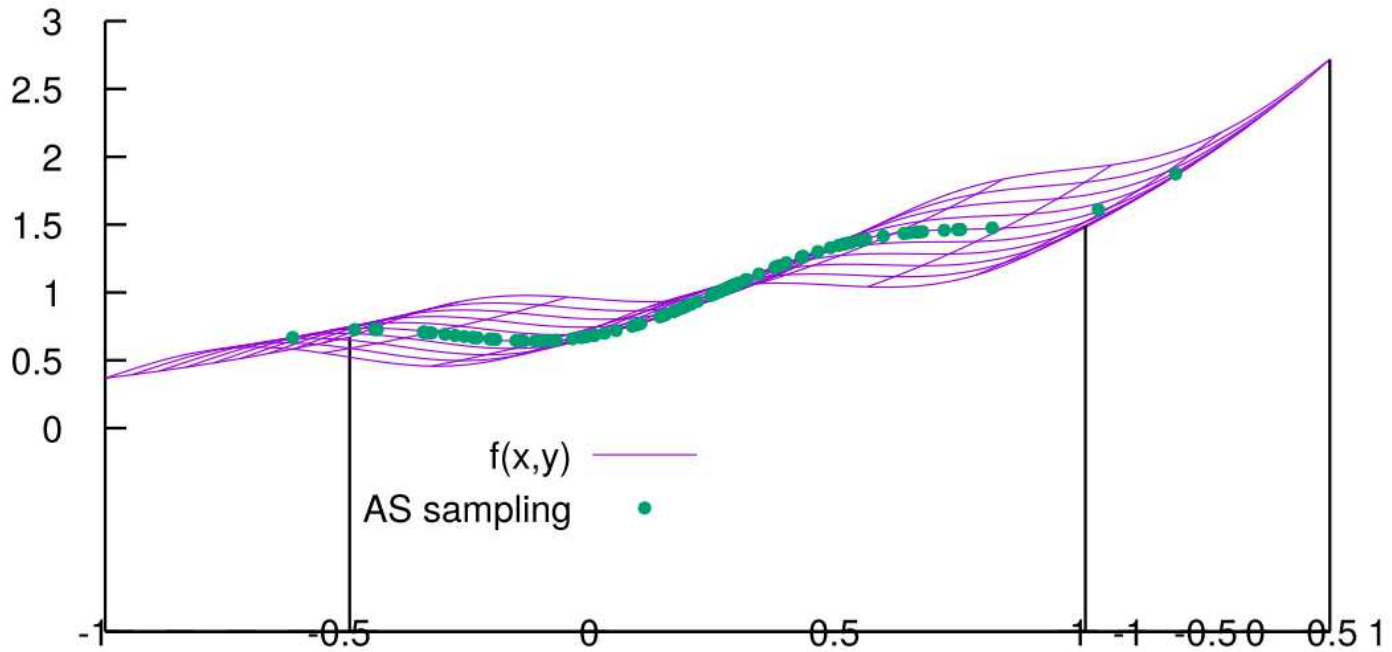

Joint Normality: Is this required?

Non linear transformation embedded in the black-box approach

Q: Is the assumption of **joint-normality** on the input space of the model required?
A: No, a normal distribution is used only for the AS mapping in order to obtain a shared space between models

Let's assume, for example $x_i \sim \mathcal{U}(-1, 1)$ and $\boldsymbol{\omega}_i \sim \mathcal{N}(0, 1)$, we can define (*i.e.* Rosenblatt, Nataf, *etc.*) a non linear function $\mathbf{x} = h(\boldsymbol{\omega})$ such that

$$\boldsymbol{\omega} \rightarrow \boxed{h(\omega)} \rightarrow \mathbf{x} \rightarrow \boxed{f(\mathbf{x})} \rightarrow Q, \quad \text{where} \quad x_i = h(\omega_i) = \operatorname{erf}\left(\frac{\omega_i}{\sqrt{2}}\right)$$

From an AS perspective, only $\boldsymbol{\omega}$ exists (however, for each $\boldsymbol{\omega}$ we can obtain $\mathbf{x}$)

$$\boldsymbol{\omega} = \mathbf{W_A}\mathbf{y} + \mathbf{W_{NA}}\mathbf{z} \approx \mathbf{W_A}\mathbf{t}$$

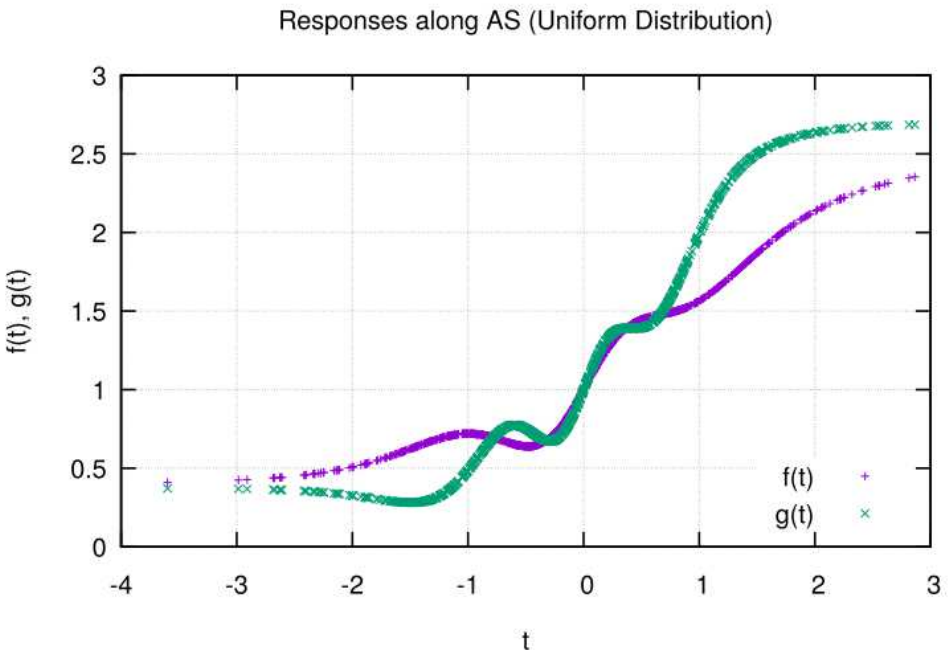

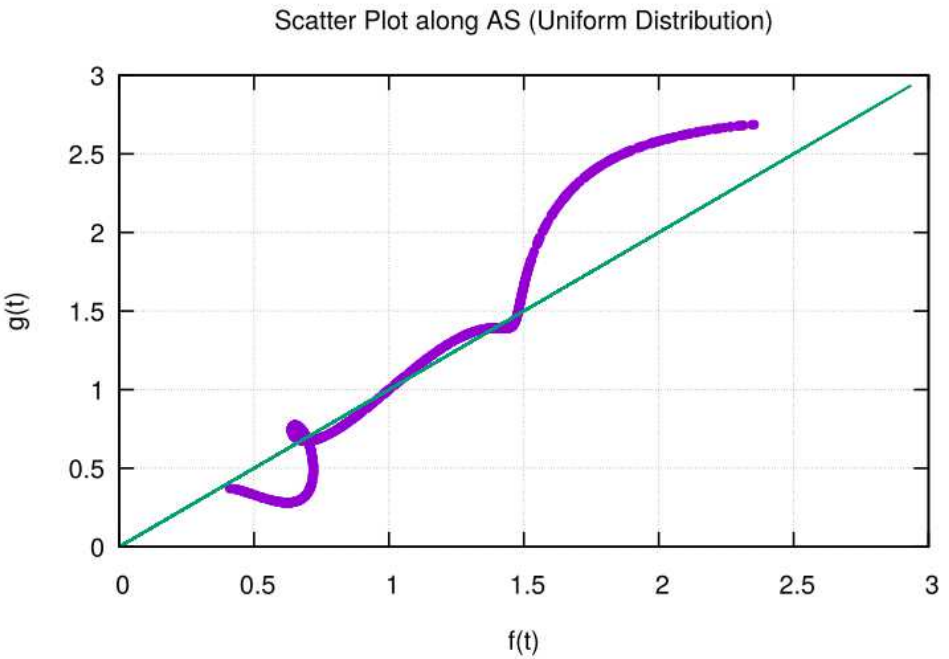

Joint Normality: Is this required?

Non linear transformation embedded in the black-box approach

Q: Is the assumption of joint-normality on the input space **of the model** required?
A: No, a normal distribution is used only for the AS mapping in order to obtain a shared space between models

Let's assume, for example $x_i \sim \mathcal{U}(-1, 1)$ and $\boldsymbol{\omega}_i \sim \mathcal{N}(0, 1)$, we can define (*i.e.* Rosenblatt, Nataf, *etc.*) a non linear function $\mathbf{x} = h(\boldsymbol{\omega})$ such that

$$\boldsymbol{\omega} \rightarrow \boxed{h(\omega)} \rightarrow \mathbf{x} \rightarrow \boxed{f(\mathbf{x})} \rightarrow Q, \quad \text{where} \quad x_i = h(\omega_i) = \operatorname{erf}\left(\frac{\omega_i}{\sqrt{2}}\right)$$

From an AS perspective, only $\boldsymbol{\omega}$ exists (however, for each $\boldsymbol{\omega}$ we can obtain $\mathbf{x}$)

$$\boldsymbol{\omega} = \mathbf{W_A}\mathbf{y} + \mathbf{W_{NA}}\mathbf{z} \approx \mathbf{W_A}\mathbf{t}$$

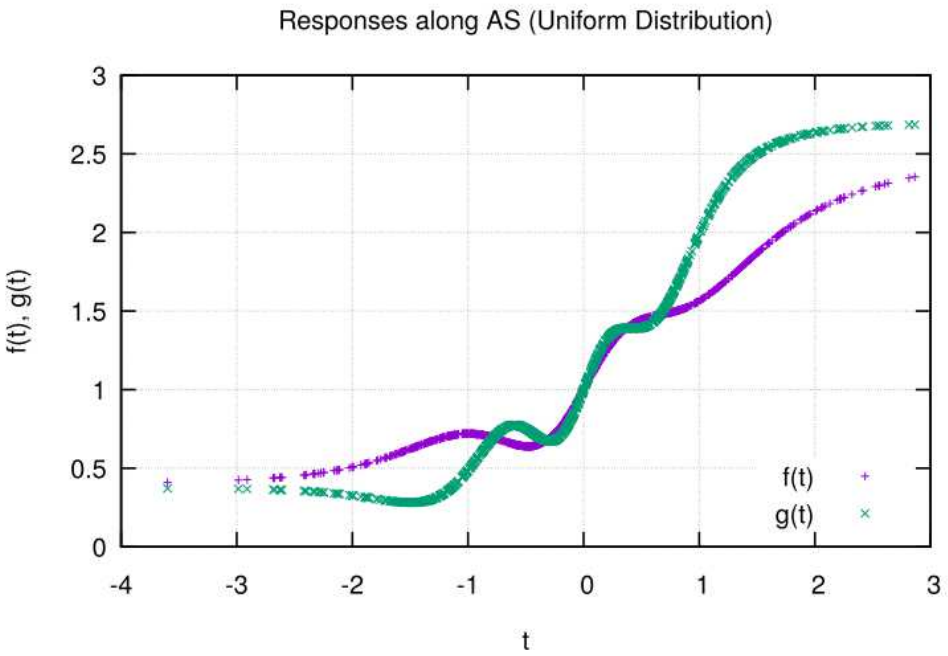

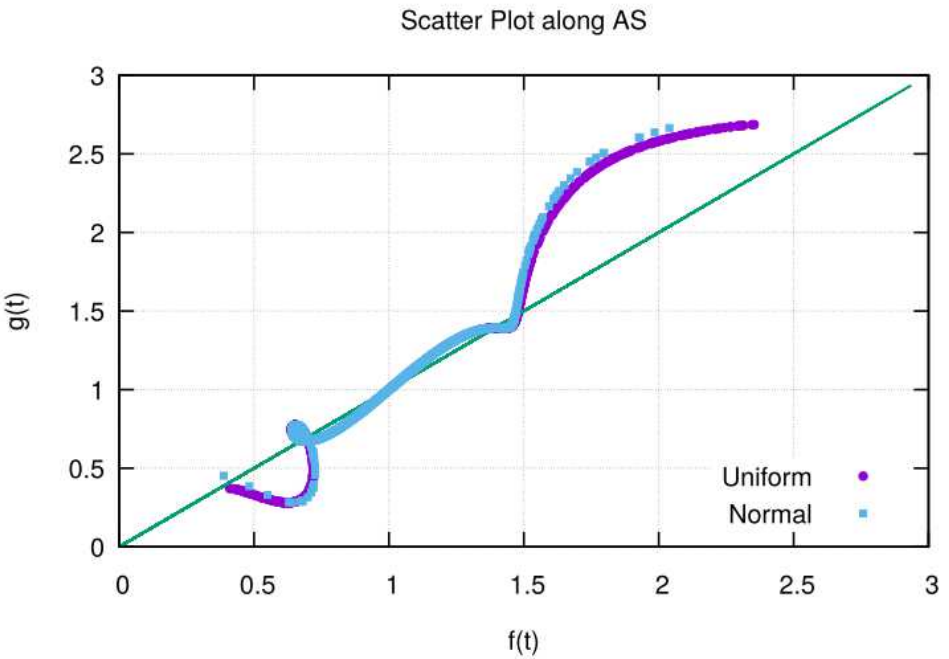

Dissimilar parameterization

Additional input variable for the high-fidelity model

$$f(x,y,z) = \exp(0.7x + 0.3y) + 0.15\sin(2\pi x) + \mathbf{0.75z^3}, \quad \text{where} \quad z \sim \mathcal{N}(0, 1/3)$$

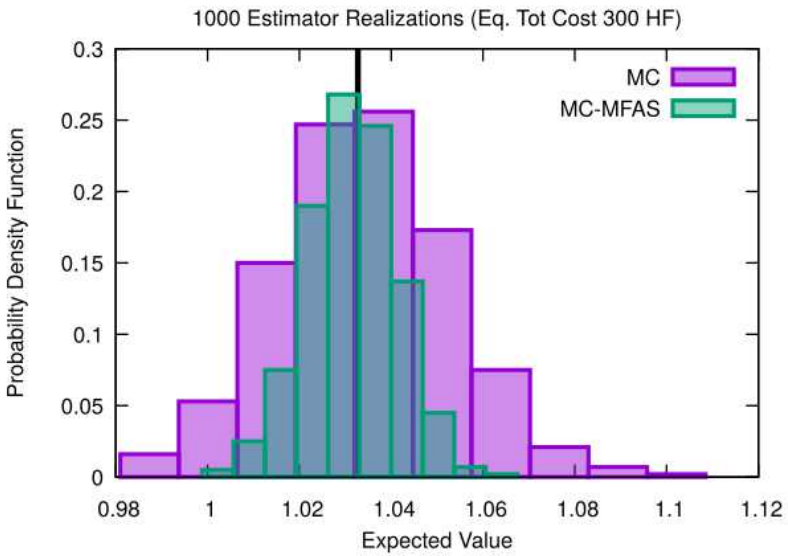

FIGURE: Normalized histograms for 1000 realizations in the case of dissimilar parametrization.

In this case we used 2 active directions for the HF and 1 for the LF

WHY IS THIS SUPPOSED TO WORK FROM A PHYSICAL POINT-OF-VIEW?

ACTIVE DIRECTIONS LET EMERGE THE UNDERLYING PHYSICS

As an example, let consider the **supersonic isoentropic flow** in a diverging nozzle (sonic throat)

$$P_e = P_0 \left(1 + \frac{\gamma - 1}{2} M_e^2\right)^{-\frac{\gamma}{\gamma - 1}}, \quad \text{where}$$

$$\underset{M_e}{\operatorname{argmin}}\, \mathcal{L} = f(M_e) - \frac{A_e}{A^\star} \quad \text{with} \quad f(M_e) = \frac{1}{M_e}\left[\frac{2}{\gamma+1}\left(1 + \frac{\gamma-1}{2}M_e^2\right)\right]^{\frac{\gamma+1}{2(\gamma-1)}}$$

- Given the shape of the nozzle (and its exit radius h_e), we can imagine 2 possible choices: 3D axisymmetric and 2D planar
- The area ratio $(A_e/A^\star)$ is linear in the 2D case (h_e/h_t) and quadratic in the 3D case (h_e^2/h_t^2)
- Given the same longitudinal shape, the 3D nozzle lets the fluid expands more than the 2D nozzle

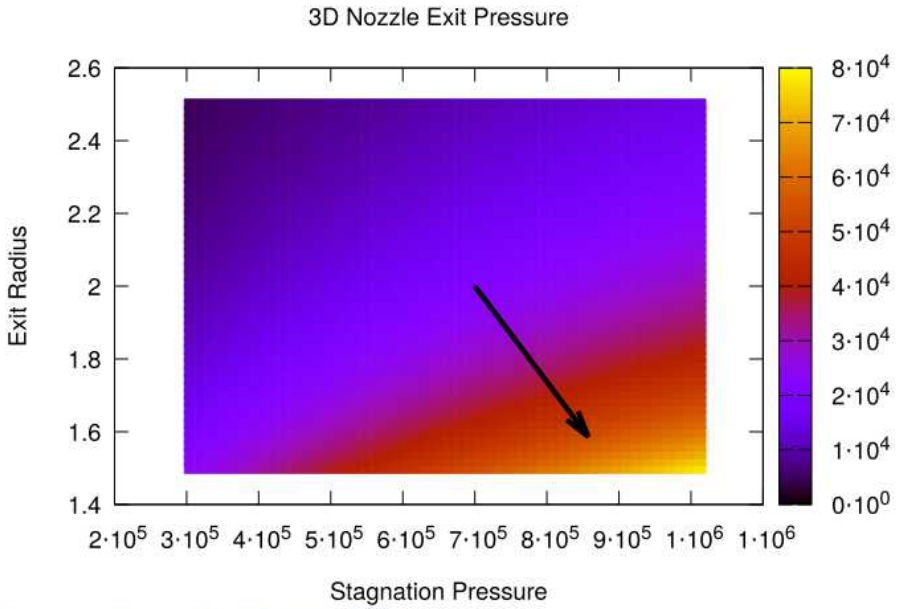

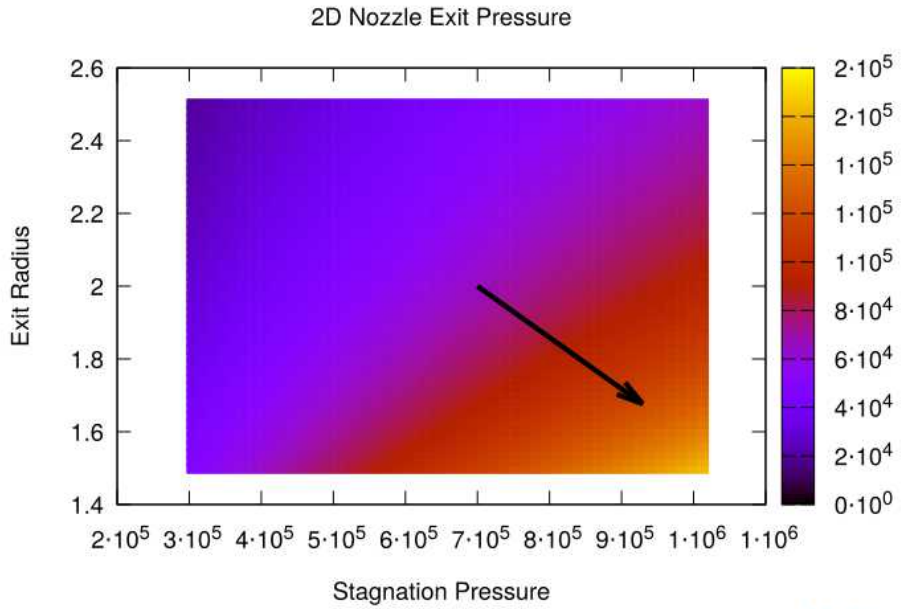

WHY IS THIS SUPPOSED TO WORK FROM A PHYSICAL POINT-OF-VIEW?

ACTIVE DIRECTIONS LET EMERGE THE UNDERLYING PHYSICS ($\rho^2 = 0.9 \rightarrow 0.99$)

As an example, let consider the **supersonic isoentropic flow** in a diverging nozzle (sonic throat)

$$P_e = P_0 \left(1 + \frac{\gamma - 1}{2} M_e^2\right)^{-\frac{\gamma}{\gamma - 1}}, \quad \text{where}$$

$$\underset{M_e}{\operatorname{argmin}} \mathcal{L} = f(M_e) - \frac{A_e}{A^\star} \quad \text{with} \quad f(M_e) = \frac{1}{M_e} \left[\frac{2}{\gamma + 1} \left(1 + \frac{\gamma - 1}{2} M_e^2\right)\right]^{\frac{\gamma + 1}{2(\gamma - 1)}}$$

- Given the shape of the nozzle (and its exit radius h_e), we can imagine 2 possible choices: 3D axisymmetric and 2D planar
- The area ratio ($A_e/A^\star$) is linear in the 2D case (h_e/h_t) and quadratic in the 3D case (h_e^2/h_t^2)
- Given the same longitudinal shape, the 3D nozzle lets the fluid expands more than the 2D nozzle

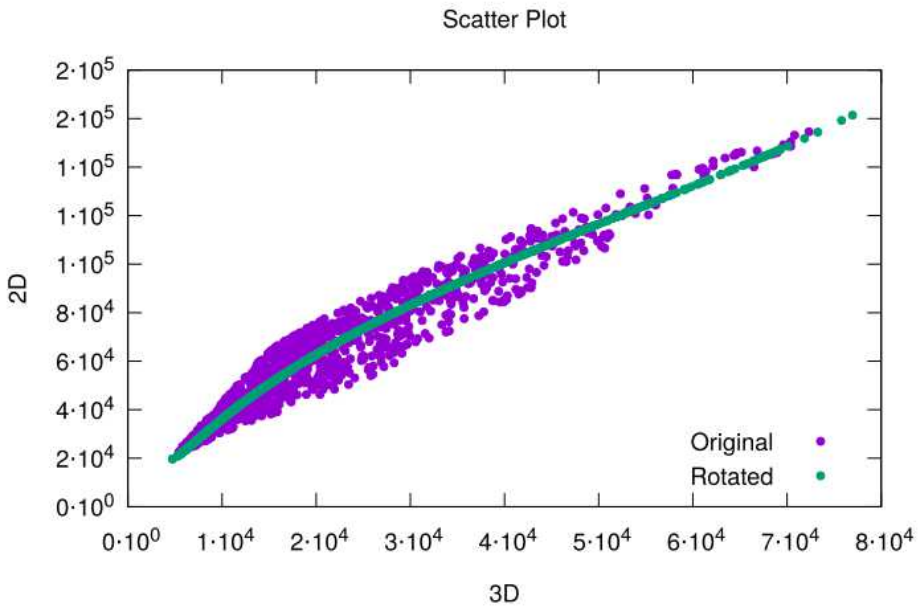

Non-linear elastic waves propagation – Hyperbolic CLAWs 1D

Non-linear elasticity problem

Can we enhance the correlation for this problem as well?

Let's consider an 'extreme' scenario (within the previous test problem)

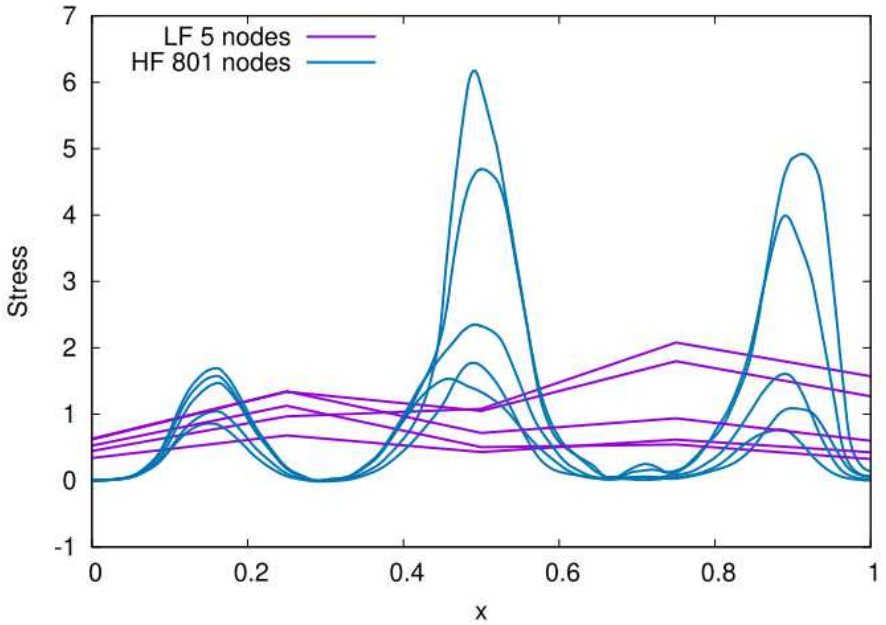

	N_x	N_t	Δ_t
Low-fidelity	5	50	36×10^{-4}
High-fidelity	801	600	30×10^{-5}

Table: HF to LF Cost ratio ~ 2800

- We compute the AS without the gradient (we use a linear regression)
- We use 40 HF samples for our estimator
- We perform 250 repetitions

Non-linear elasticity problem

Can we enhance the correlation for this problem as well?

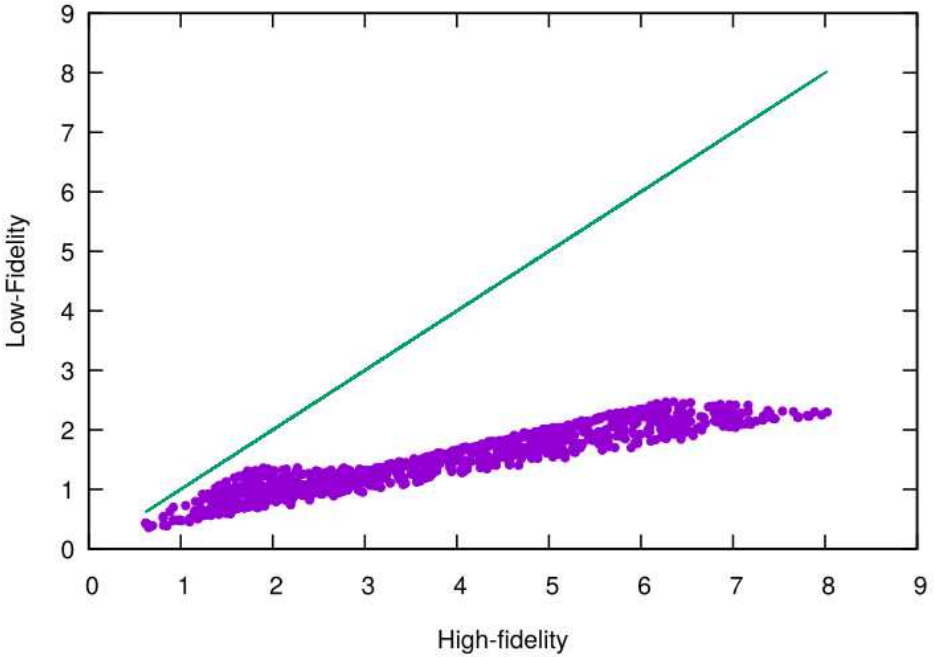

Active Direction Agnostic sampling: $\rho^2 = 0.89$

Non-linear elasticity problem

Can we enhance the correlation for this problem as well?

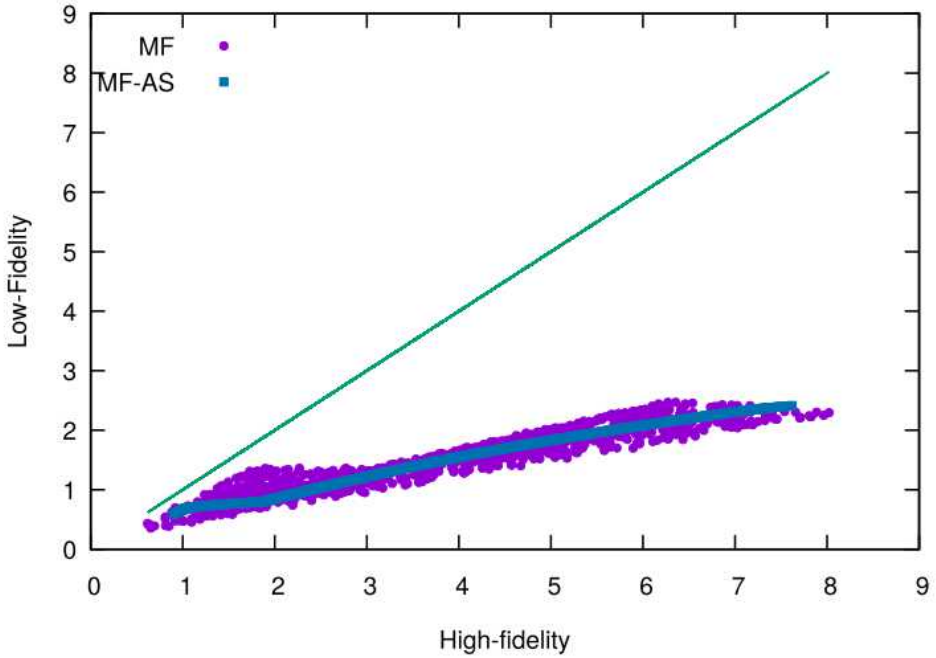

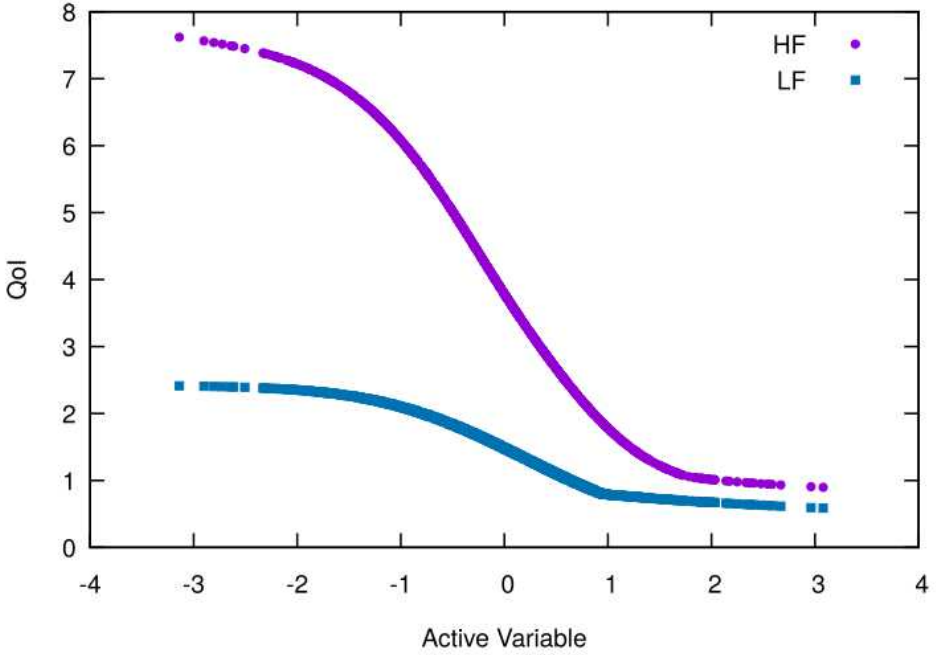

Active Direction Agnostic sampling: $\rho^2 = 0.89$

Active Direction Aware sampling:
$\rho^2 = 0.99$

Lid- and Buoyancy-driven cavity flow – A CFD example

Lid- and Buoyancy-driven Cavity Flow

Test case generalities

Physical test case

- **Combination** of the Lid- and Buoyancy-driven test cases
- **Navier-Stokes** equations for a fluid with density ρ and kinematic viscosity ν enclosed in a square cavity of size L
- **Top wall sliding** with velocity U_L
- Top and bottom walls held at **different temperature** $\rightarrow$ **net body force** (buoyancy term via Boussinesq approx.)
- Adiabatic side walls
- Cavity immersed in a gravity field with components g_h and g_v
- Nominal conditions: $Re = 1000$ and $Ra = 100000$ for air $Pr = 0.71$ (constant)

Non-dimensional parameters

$$Re = \frac{U_L L}{\nu}$$

$$Gr = |g| \frac{\beta (T_h - T_c) L^3}{\nu^2}$$

$$Pr = \frac{\nu}{\alpha}$$

$$Ra = Pr\, Gr$$

Numerical approach

- Implicit FV code on structured mesh with pressure-based SIMPLE discretization and dual-time stepping
- BC imposed via ghost cells

Lid- and Buoyancy-driven Cavity Flow

Flow field for the nominal conditions

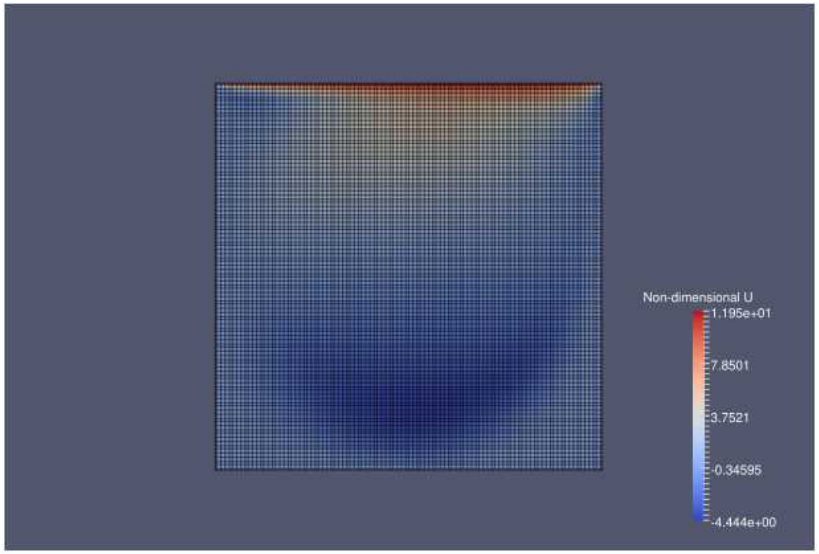

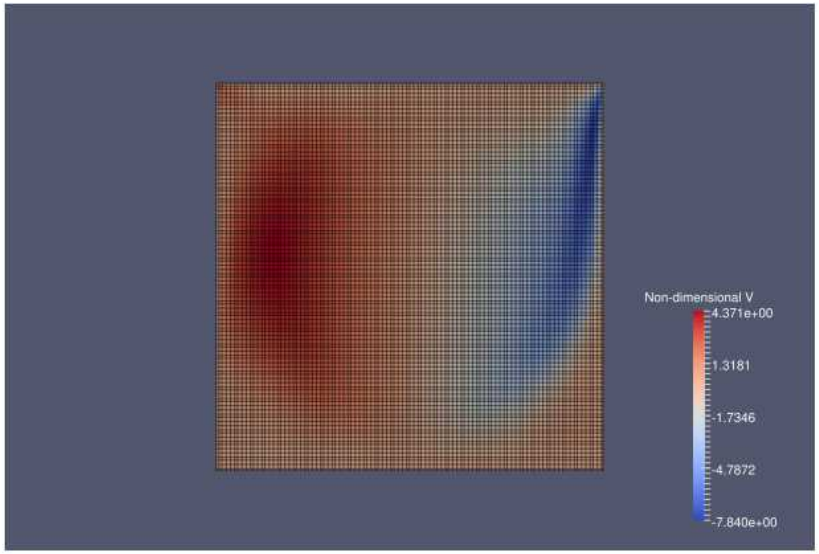

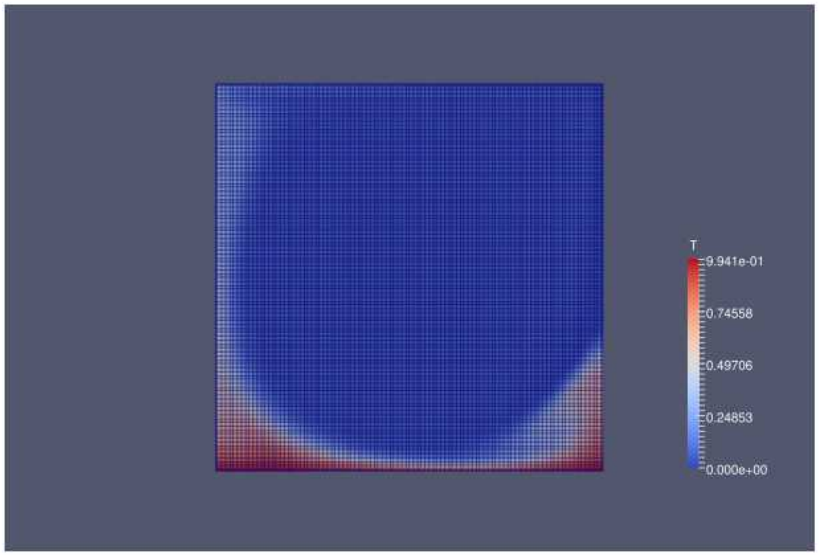

Lid- and Buoyancy-driven Cavity Flow

Multifidelity UQ case

- **HF:** 101×101 spatial cells, $T = 80$ and $Dt = 0.25 \rightarrow \mathcal{C}^{\mathrm{HF}} = 1$
- **LF:** 21×21 spatial cells, $T = 15$ and $Dt = 0.5 \rightarrow \mathcal{C}^{\mathrm{LF}} = 0.00107$

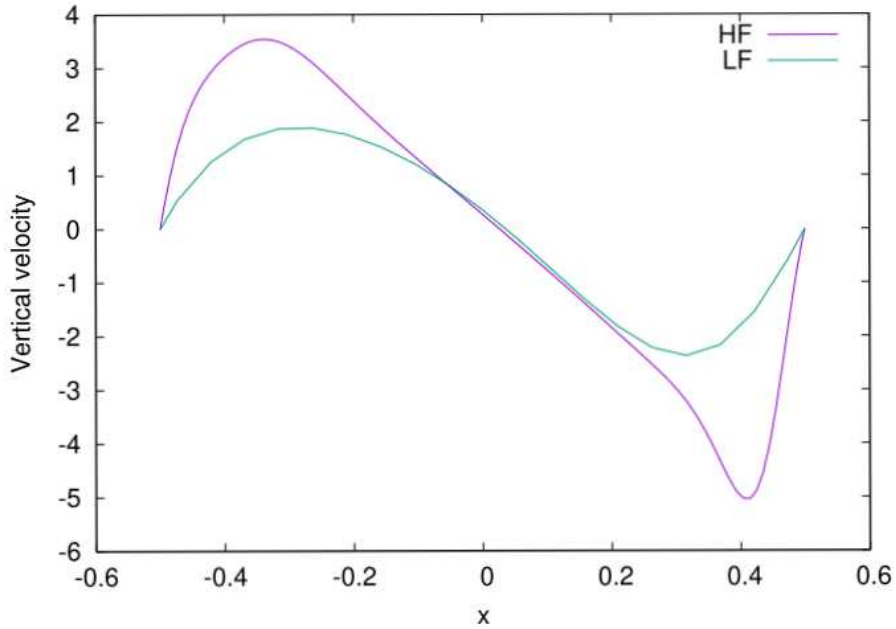

FIGURE: Vertical velocity profile at the horizontal mid-plane of the cavity for the reference condition for both HF and LF models.

Lid- and Buoyancy-driven Cavity Flow

Multifidelity parametrization

Parameter	Min	Max	Mean
ν	**0.009**	**0.011**	**0.01**
ΔT	**9**	**11**	**10**
g_v	8.1	9.9	9
g_h	3.6	4.4	4
U_L	9	11	10

Table: Ranges for the uniform variables of the cavity problem.

Let's have a look at the non-dimensional numbers (Pr is constant and $Gr = Gr(Ra, Re)$ for this case)

$$Re = Re(\nu, U_L)$$
$$Ra = Ra(g_v, g_h, \Delta T, \nu)$$

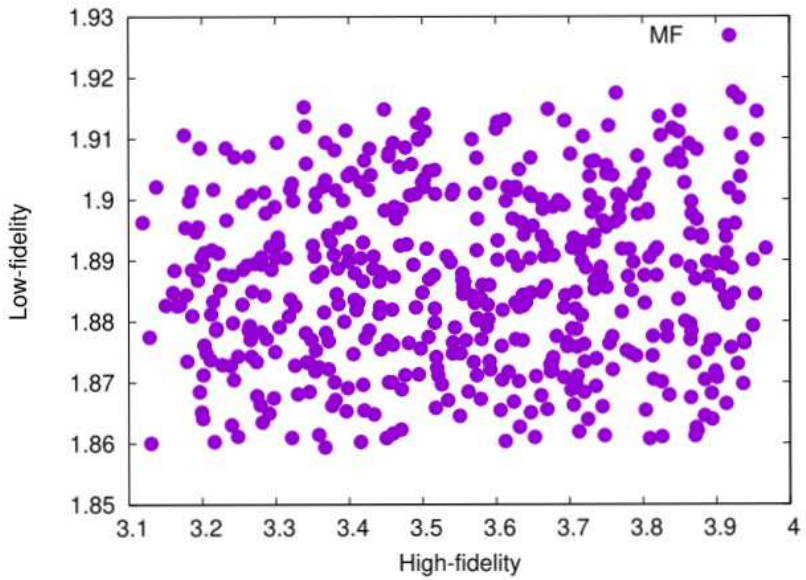

Lid- and Buoyancy-driven Cavity Flow

Multifidelity parametrization

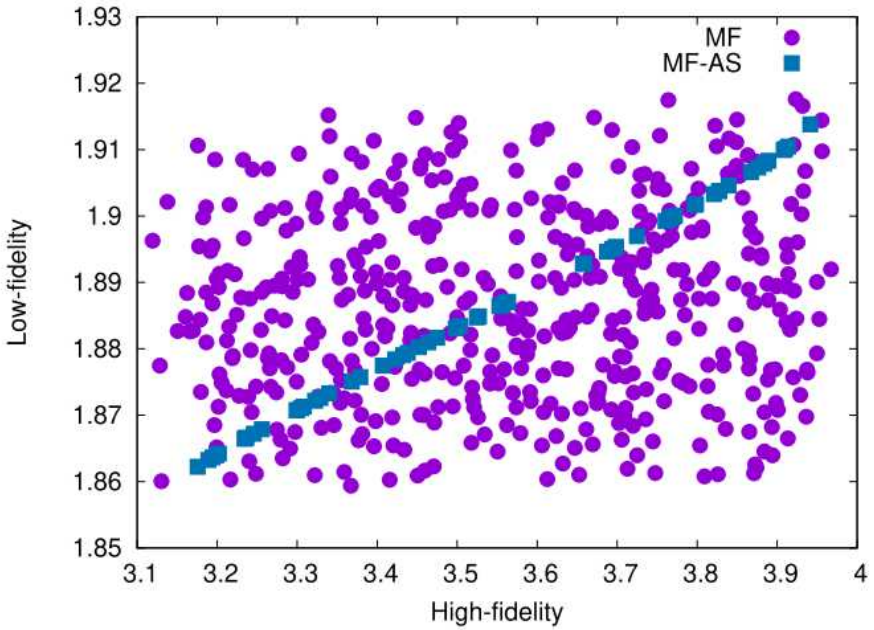

FIGURE: Scatter plot corresponding to 500 realizations of the HF and LF model with samples drawn in the physical space and 60 samples drawn along the common active direction.

Variable	Model	
	HF	LF
ν	-0.0860585	-0.31282
ΔT	-0.0036777	0.94981
g_v	-0.0057946	-
g_h	-0.0144436	-
U_l	0.9961617	-

TABLE: Dominant eigenvectors for the cavity problem.

Lid- and Buoyancy-driven Cavity Flow

Numerical test for Multifidelity

1. Fixed number of pilot samples equal to 30 samples (in the **physical space**)
2. AS evaluated (first order regression, no derivatives) from the pilot samples and **this sample set is discarded**
3. Initialization of the MF algorithm with 30 samples in the Active variables to estimate the correlation
4. Optimal oversampling ratio for the LF and perform the mean estimation

- Items (1-4) are **repeated 300 times** and the estimated mean are reported
- In mean we used an equivalent cost of **34 HF samples per estimator realization** (this number is used **for MC**, 300 repetitions)
- Variance of the mean estimator reduced by one order of magnitude

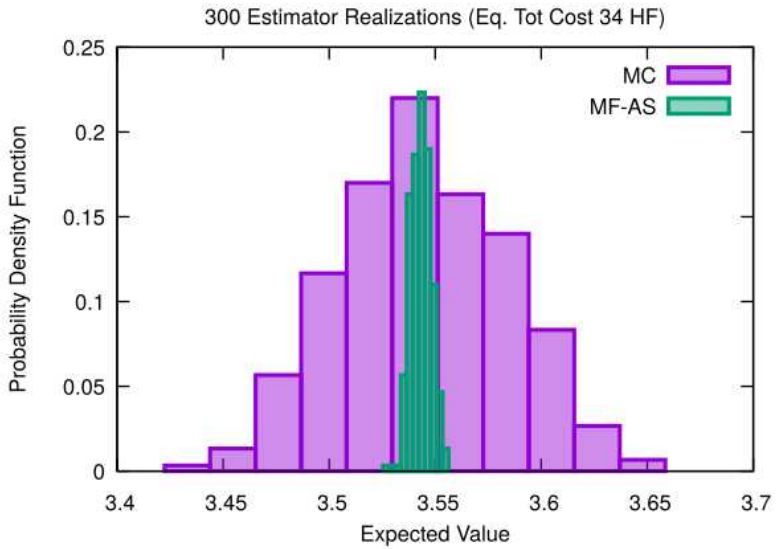

FIGURE: Probability density function for the estimators computed with 300 independent realizations.

Lid- and Buoyancy-driven Cavity Flow

Alleviating the cost of AS estimation

- The cost of the pilot samples accounted to $30 \times 1 + 30 \times 0.001 = 30.03$ HF (coming from HF mainly in this case)
- Can we re-use the HF samples without discarding them?

1. Pilot samples are generated in the physical space (30 as done before)
2. The LF samples are discarded
3. The HF pilot samples are projected onto the active direction
4. LF samples are generated at the Active Variables locations of the HF
5. Correlation is estimated and the oversampling is computed (always on the active variables)
6. The MF estimator is evaluated

- Items (1-6) are **repeated 300 times** and the estimated mean are reported

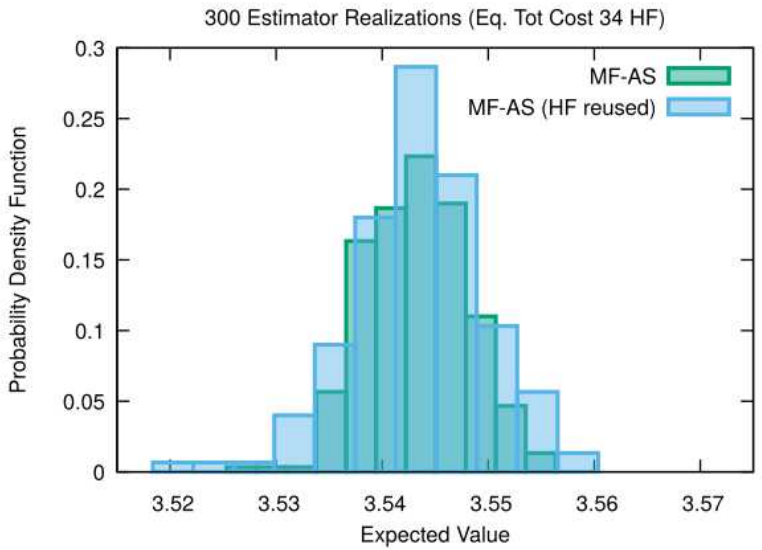

FIGURE: Probability density function for the estimators MF-AS computed with 300 independent realizations with and without reusing the HF samples.

Lid- and Buoyancy-driven Cavity Flow

Projecting onto the Active Variables from the pilot realizations

- By reusing the HF samples, we need to handle samples that have not been generated along the active variables
- Due to the nature of the mapping (inactive variables) this projection will exhibit a noisy behavior
- A very simple approach to improve this step is to perform a regression over the active variables

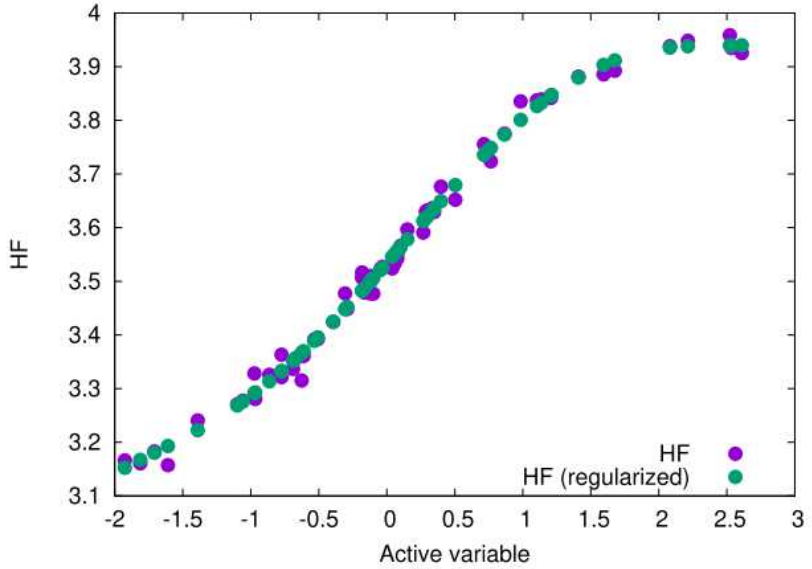

Figure: High-fidelity realizations for 40 pilot samples projected on to the active variable space with and without regularization.

Lid- and Buoyancy-driven Cavity Flow

Projecting onto the Active Variables from the pilot realizations

- By reusing the HF samples, we need to handle samples that have not been generated along the active variables
- Due to the nature of the mapping (inactive variables) this projection will exhibit a noisy behavior
- A very simple approach to improve this step is to perform a regression over the active variables

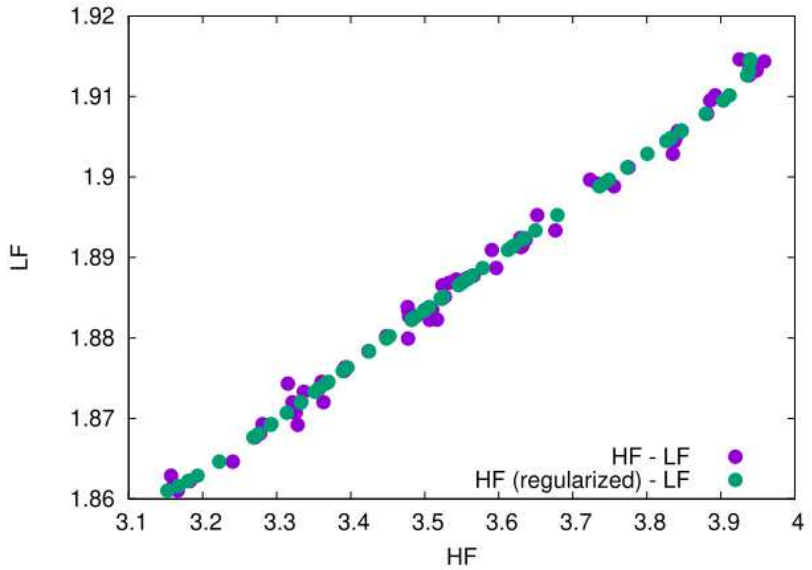

Figure: High-fidelity realizations for 40 pilot samples projected on to the active variable space with and without regularization.

Lid- and Buoyancy-driven Cavity Flow

Can I re-use also the LF pilot samples?

- We can conceptually apply the same strategy for the LF samples, however there is an additional **challenge**...
- ...we **do not have a common sample set to estimate the correlation** along the active variables
- In order to compute the correlation before evaluating the additional LF samples we use the PC expansion (analytical expression)
- Once the correlation is evaluated and the LF oversampling is defined the initial LF set might be fully re-used
- We can now perform MF-AS (re)starting from legacy dataset

1. 30 pilot samples extracted from a dataset of 500 evaluations (LF and HF are consistent)
2. 300 repetitions of the estimator with full re-use of both HF and LF

- **NOTE:** there is a non-zero probability of using the same evaluation multiple time (for different estimator realizations)

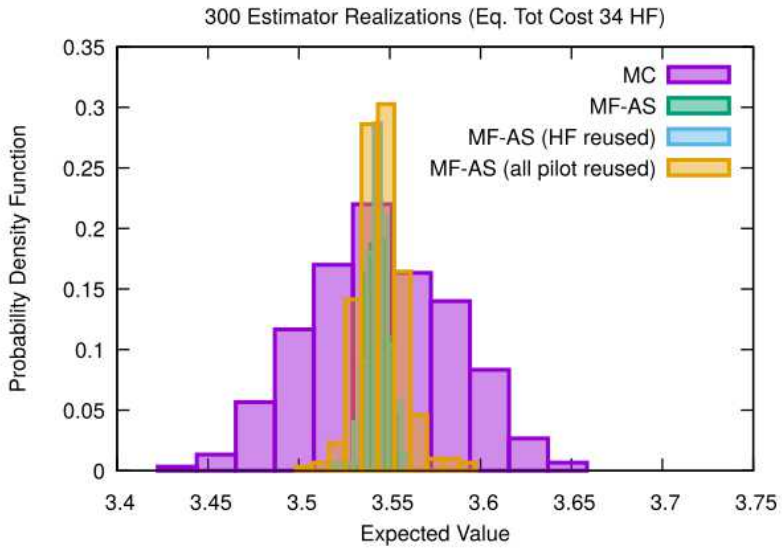

FIGURE: Probability density function for the estimators MF-AS computed with 300 independent realizations with and without reusing the pilot samples.

Aero-thermo-structural analysis – A more realistic engineering example

Preliminary results for the Sequoia problem

Problem setup

- We only consider the ACV-1 estimator here, but the extension to ACV is straightforward
- The high-fidelity model is 3D Euler with a COARSE mesh
- The low-fidelity model is 2D Euler with either a consistent or inconsistent parametrization, *i.e.* the area of the duct is forced to correspond to the one of 3D geometry

CFD	FEM (Thermal/Structural)	Parameterization	Cost
3D Euler COARSE	COARSE		1.00
2D Euler COARSE	COARSE (axisymmetric)	Consistent	0.201
2D Euler COARSE	COARSE (axisymmetric)	Inconstistent	0.135

Table: Relative computational cost for the models used for the Active Subspace tests for the nozzle problem. All the costs are normalized with respect to the 3D Euler COARSE solver.

We considered three scenarios

1. High- and low-fidelity model with **inconsistent parametrization** evaluated for the **same set of samples** (40 UQ parameterss);
2. High- and low-fidelity model with **consistent parametrization** evaluated at an **independent set of samples** (40 UQ parameters);
3. High- and low-fidelity model with **inconsistent parametrization** evaluated for the same set of nominal samples **(96 + 40 UQ parameters)**.

We use linear regression for all cases to compute AS...

Preliminary results for the Sequoia problem

Scenario 1 – inconsistent parameterization and same sample set

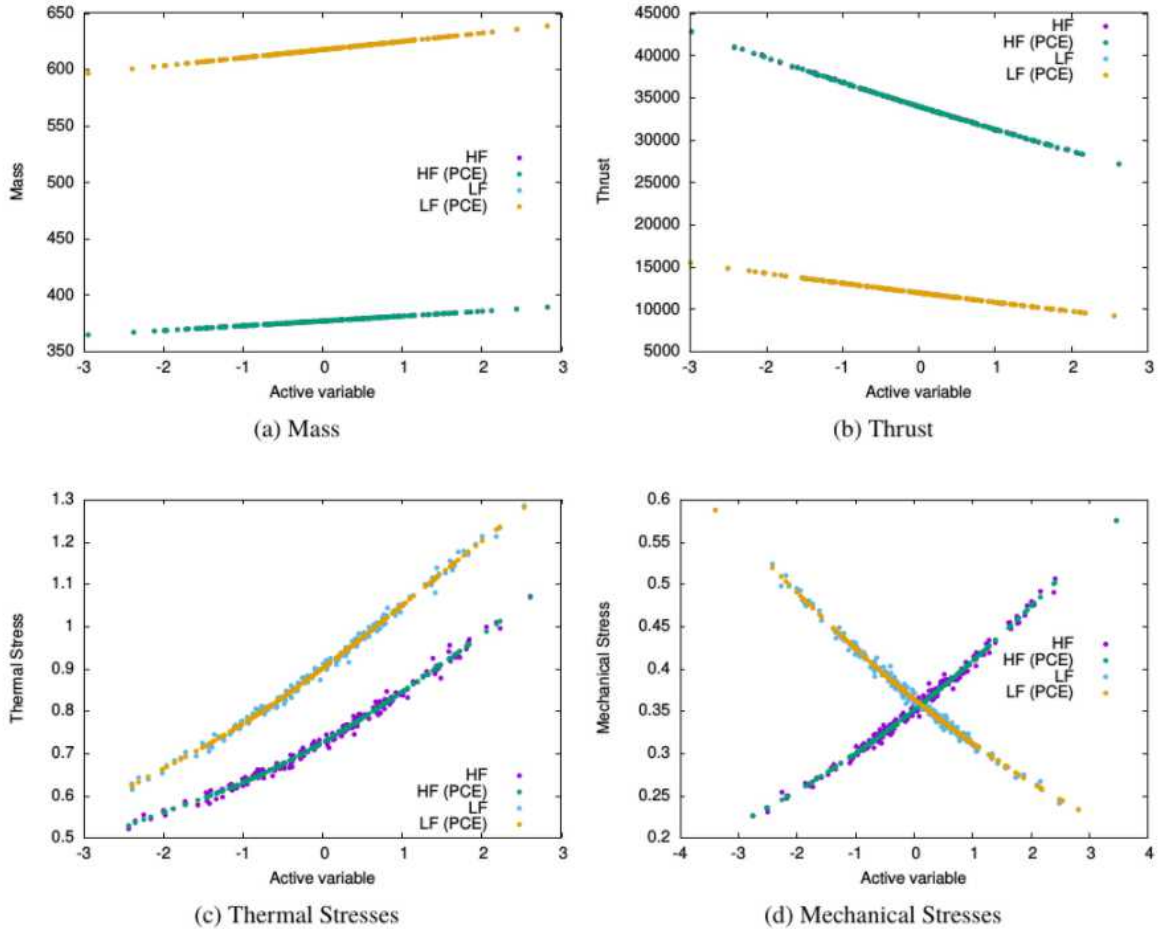

(a) Mass (b) Thrust

(c) Thermal Stresses (d) Mechanical Stresses

Figure: QoIs w.r.t. the active variable for the nozzle problem in the case of inconsistent parameterization for both the original data and the PCE regression with respect to the active variable (Scenario 1).

Preliminary results for the Sequoia problem

Scenario 2 – consistent parameterization and independent same sample set

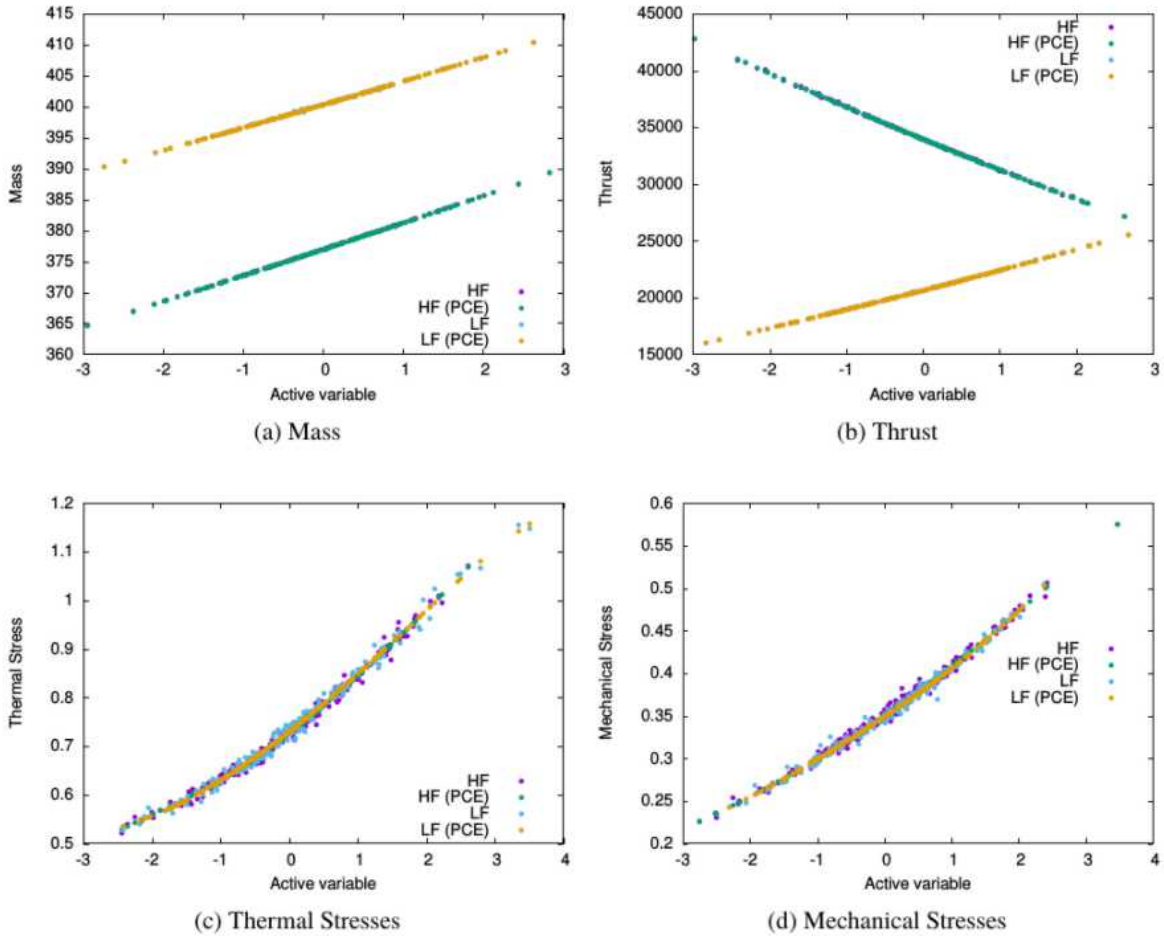

(a) Mass (b) Thrust

(c) Thermal Stresses (d) Mechanical Stresses

Figure: QoIs w.r.t. the active variable for the nozzle problem in the case of inconsistent parameterization for both the original data and the PCE regression with respect to the active variable (Scenario 2).

Preliminary results for the Sequoia problem

Scenario 3 – inconsistent dimensionality 136 vs 40

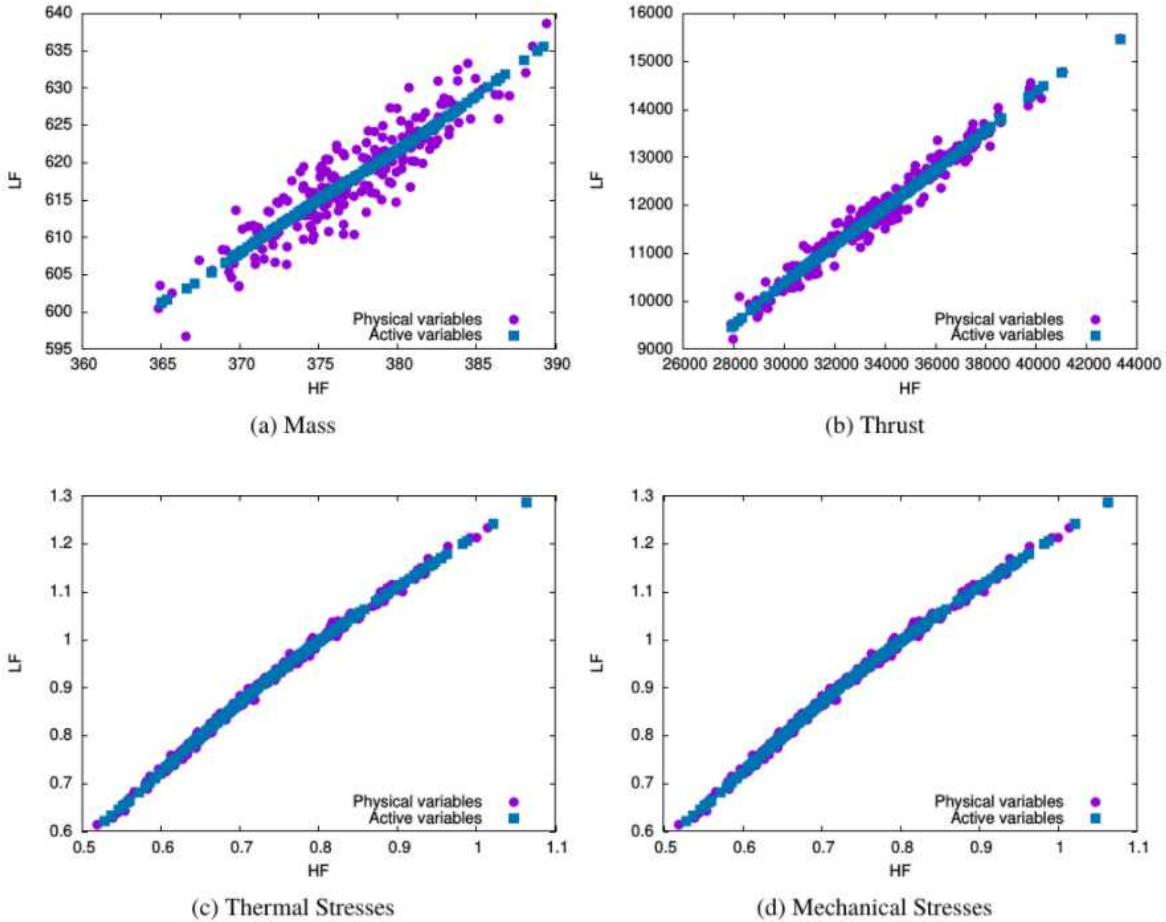

(a) Mass (b) Thrust

(c) Thermal Stresses (d) Mechanical Stresses

Figure: QoIs w.r.t. the active variable for the nozzle problem in the case of inconsistent parameterization for both the original data and the PCE regression with respect to the active variable (Scenario 3).

Preliminary results for the Sequoia problem

Scenario 3 – inconsistent dimensionality 136 vs 40

Qols	ρ^2	ρ^2_{AS}	Estimator St.Dev		
			MC	OCV-1	OCV-1 (AS)
Mass	0.822	0.999	1	0.178	0.001
Thrust	0.956	0.998	1	0.044	0.002
Thermal Stress	0.982	0.998	1	0.018	0.002
Mechanical Stress	0.985	0.986	1	0.015	0.014

Table: (Estimated) Standard Deviation for OCV-1 and OCV-1 (AS) (normalized w.r.t. MC) for the Sequoia application problem in the case of inconsistent parameterization and uncertain design input in HF (Scenario 3).

These results are estimated through the PCE along the active directions. We need to confirm the results by running the model

Scramjet engines

A little bit of context: Opportunities and Challenges

Supersonic combustion ramjet (Scramjet) engines

- are propulsion systems for **hypersonic flight**
- aim at directly utilize atmospheric air for **stable combustion while maintaining supersonic airflow**
- obviates the need to carry **on-board oxidizer**
- overcome the losses from **slowing flows** to subsonic speeds (no rotating element)

Several challenges

- characterizing and predicting **combustion properties** for multiscale and multiphysical turbulent flows (under extreme environments)
- **low throughput time** vs need for mixture and self-ignition
- **stable combustion** for constant thrust

Designing an optimal engine requires

- Maximization of the combustion efficiency
- Minimization of the pressure losses, thermal loading
- Reducing the risk of unstart and flame blow-out
- Accomplishing these tasks under uncertain operational conditions (robustness and reliability)

From Jurzay (2018): *The challenge of enterprising supersonic combustion in scramjet is [...] as difficult as lighting a match in a hurricane.*

[1] Urzay, J., Supersonic Combustion in Air-Breathing Propulsion Systems for Hypersonic Flight, Annual Review of Fluid Mechanics, Vol. 50, No. 1, 2018, pp. 593627. doi:10.1146/annurev-fluid-122316-045217.

[2] Leyva, I., The relentless pursuit of hypersonic flight, Physics Today, Vol. 70, No. 11, 2017, pp. 3036. doi:10.1063/PT.3.3762.

Hypersonic International Flight Research and Experimentation (HIFiRE)

Problem description

- The HIFiRE project studied a cavity-based hydrocarbon-fueled dual-mode scramjet configuration
- Ground test rig, HIFiRE Direct Connect Rig (HDCR), built to replicated the isolator/combustion section

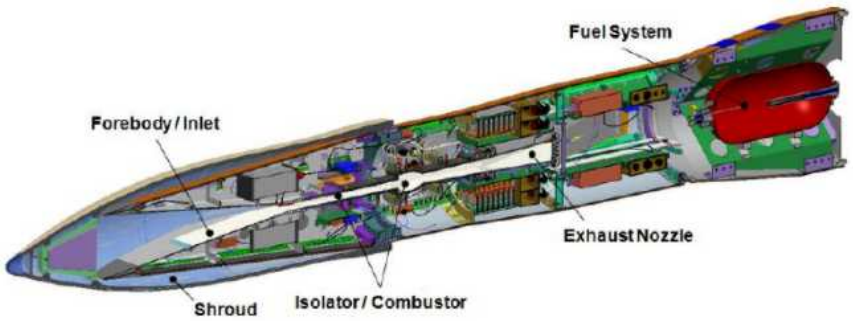

(a) HIFiRE Flight 2 payload

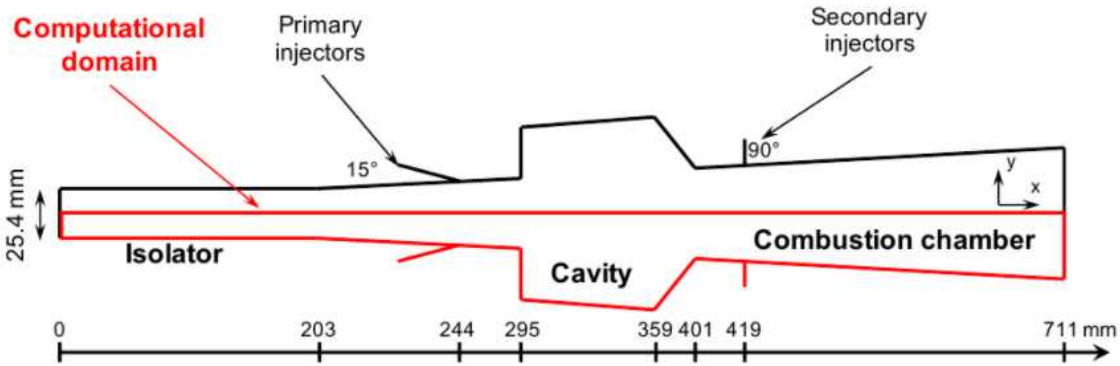

(b) HDCR computational domain

Figure: Top: HIFiRE Flight 2 payload [1]. Bottom: HDCR schematic.

[1] Jackson, K. R., Gruber, M. R., and Buccellato, S., HIFiRE Flight 2 Overview and Status Uptate 2011, 17th AIAA International Space Planes and Hypersonic Systems and Technologies Conference, AIAA Paper 2011–2202, San Francisco, CA, 2011. doi:10.2514/6.2011-2202.

HIFiRE Direct Connect Rig

Device Features and Computational Setup

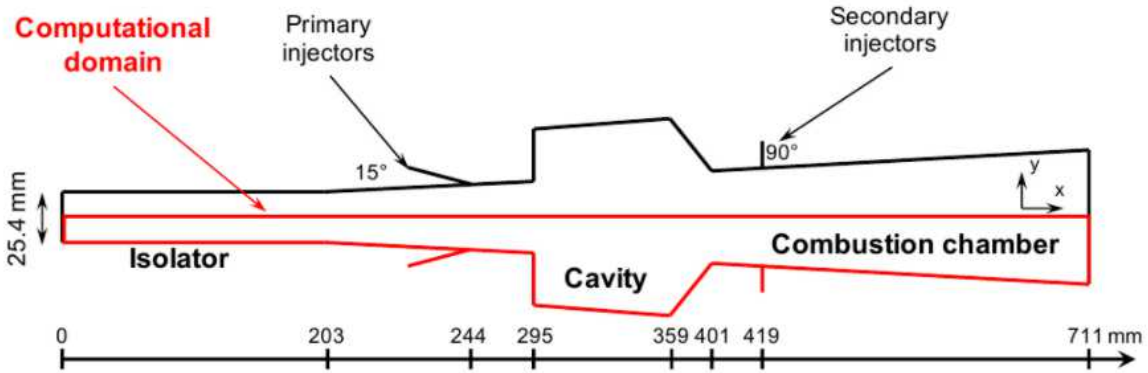

(b) HDCR computational domain

Given the **publicly available data for HDCR** we used this device as reference in our ScrajetUQ project

- Constant area isolator attached to a combustion chamber
- Primary injector are mounted upstream of flame stabilization cavities (top and bottom walls)
- Secondary injectors are mounted similarly downstream of the cavities
- Geometry symmetric about the centerline in the y direction (we model only half rig)
- The fuel supplied is a gaseous mixture containing 36% methane and 64% ethylene by volume (similar to the JP-7 fuel)

Computational setup

- A reduced three-step mechanism to characterize the combustion process
- Arrhenius formulations of the kinetic reaction rates (parameters are fixed at values that retain robust and stable combustion)
- Large Eddy Simulations carried out by using RAPTOR code (Oefelein)

RAPTOR CODE
COMPUTATIONAL FEATURES

RAPTOR

- Fully coupled conservation equations of mass, momentum, total-energy, and species for a chemically reacting flow
- can handles high Reynolds numbers
- real gas effects
- robust over wide range of Mach numbers
- non-dissipative, discretely conservative, staggered finite-volume schemes

Numerical settings

- 2D simulations
- 3 grid resolutions where cell sizes are $1/8$, $1/16$, and $1/32$ of the injector diameter $d = 3.175$ mm (denoted as $d/8$, $d/16$, and $d/32$)
- $63K$, $250K$ and $1M$ grid points, respectively
- adaptive time steps with approximately equal simulation physical time
- warm start from a quasi-steady state nominal condition run
- 1.7×10^3, 1.1×10^4, and 7.3×10^4 CPU hours per run, respectively
- Roughly a cost factor equal to 8 between resolution levels

RAPTOR CODE

EXAMPLE OF FLOW FIELDS

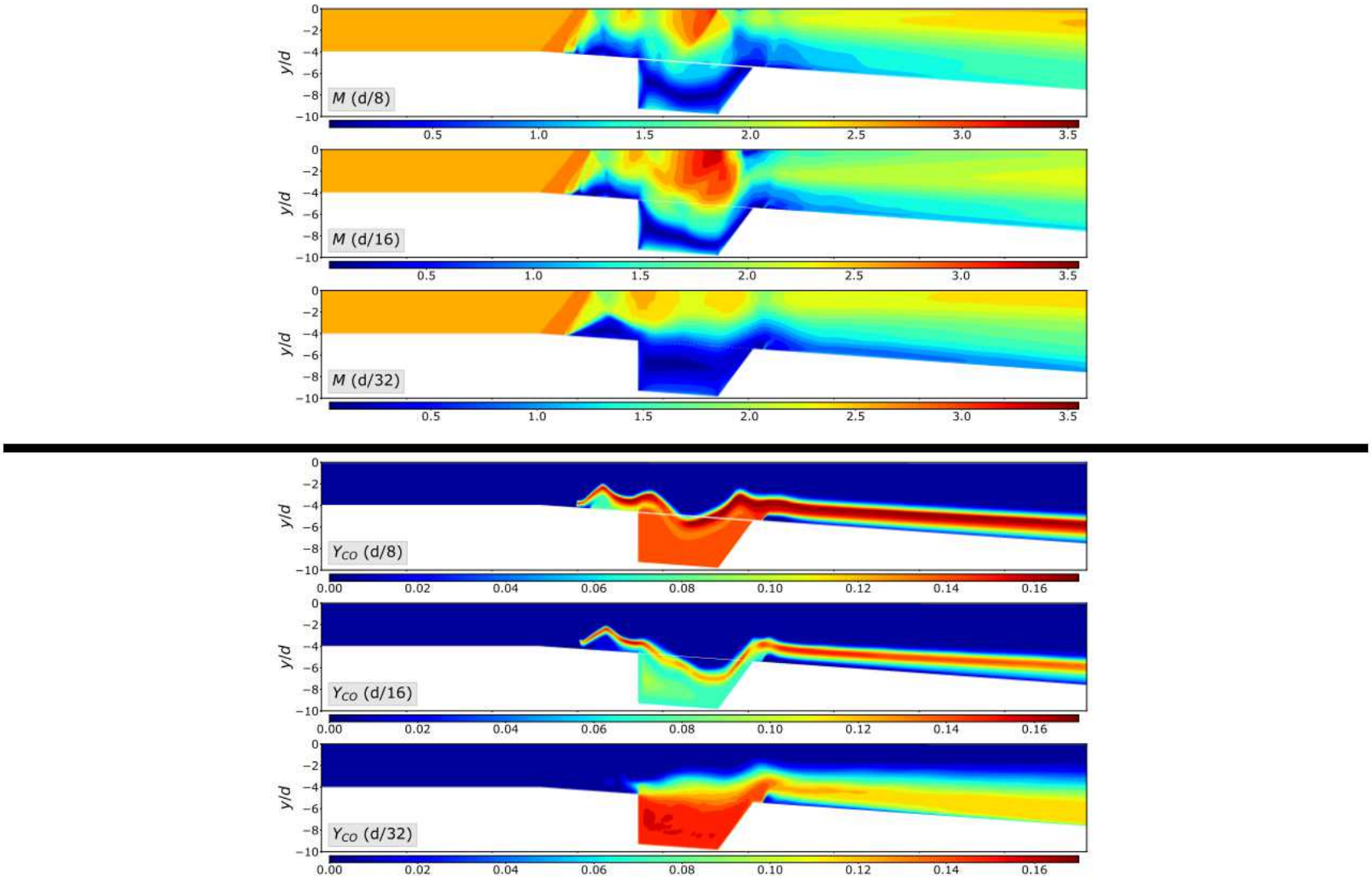

FIGURE: Solution fields of Mach number M (top three) and carbon monoxide mass fraction Y_{CO} (bottom three) simulated at a randomly sampled input settings using the three different grids.

SCRAMJET

Quantities of Interest (5)

- **Combustion efficiency (η_{comb})**, defined based on static enthalpy quantities

$$\eta_{\text{comb}} = \frac{H(T_{\text{ref}}, Y_{\text{e}}) - H(T_{\text{ref}}, Y_{\text{ref}})}{H(T_{\text{ref}}, Y_{\text{e,ideal}}) - H(T_{\text{ref}}, Y_{\text{ref}})}.$$

- **Burned equivalence ratio (ϕ_{burn})** is defined to be equal to $\phi_{\text{burn}} \equiv \phi_G \eta_{\text{comb}}$.
- **Stagnation pressure loss ratio (P_{stagloss})** is defined as

$$P_{\text{stagloss}} = 1 - \frac{P_{s,e}}{P_{s,i}}.$$

- **Maximum and average root-mean-square (RMS) pressures (max P_{rms} and ave P_{rms})** are, respectively, the maximum RMS pressure across the entire spatial domain, and the RMS pressure averaged across the spatial domain between two injectors:

$$\max P_{\text{rms}} = \max_{x,y} \sqrt{\overline{P(x,y)^2} - \left[\overline{P(x,y)}\right]^2},$$

$$\text{ave}\, P_{\text{rms}} = \frac{1}{\mathcal{V}} \int_{x,y} \sqrt{\overline{P(x,y)^2} - \left[\overline{P(x,y)}\right]^2}\, dx\, dy.$$

- **Initial shock location (x_{shock})** is the most upstream shock location.

SCRAMJET

Uncertain parameters (11)

Parameter	Range	Description
Inlet boundary conditions:		
p_0	$[1.406, 1.554] \times 10^6$ Pa	Stagnation pressure
T_0	$[1472.5, 1627.5]$ K	Stagnation temperature
M_0	$[2.259, 2.761]$	Mach number
I_i	$[0, 0.05]$	Turbulence intensity horizontal component
R_i	$[0.8, 1.2]$	Ratio of turbulence intensity vertical to horizontal components
L_i	$[0, 8] \times 10^{-3}$ m	Turbulence length scale
Fuel inflow boundary conditions:		
I_f	$[0, 0.05]$	Turbulence intensity magnitude
L_f	$[0, 1] \times 10^{-3}$ m	Turbulence length scale
Turbulence model parameters:		
C_R	$[0.01, 0.06]$	Modified Smagorinsky constant
Pr_t	$[0.5, 1.7]$	Turbulent Prandtl number
Sc_t	$[0.5, 1.7]$	Turbulent Schmidt number

Table: Uncertain model input parameters. The uncertain distributions are assumed uniform across the ranges shown.

SCRAMJET DATASET

MULTIFIDELITY APPROACH FROM DATASET

- 2 spatial resolutions
- 16 random variables
- Dataset with 200 realizations (consistent parameterization)

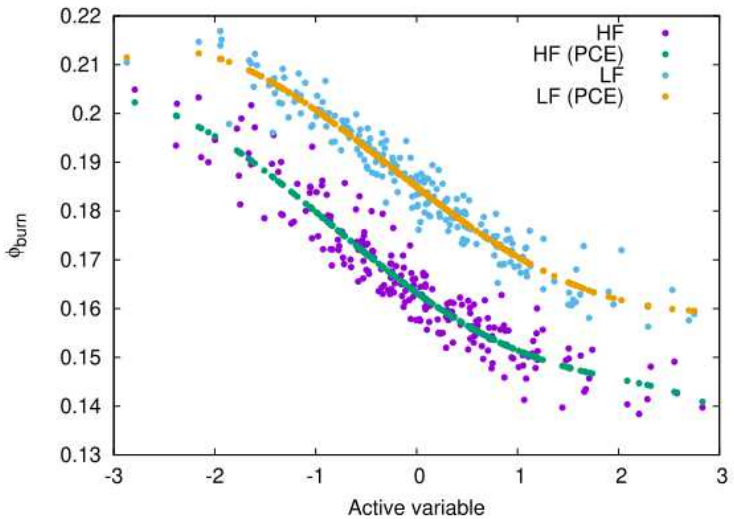

(a) ϕ_{burn}

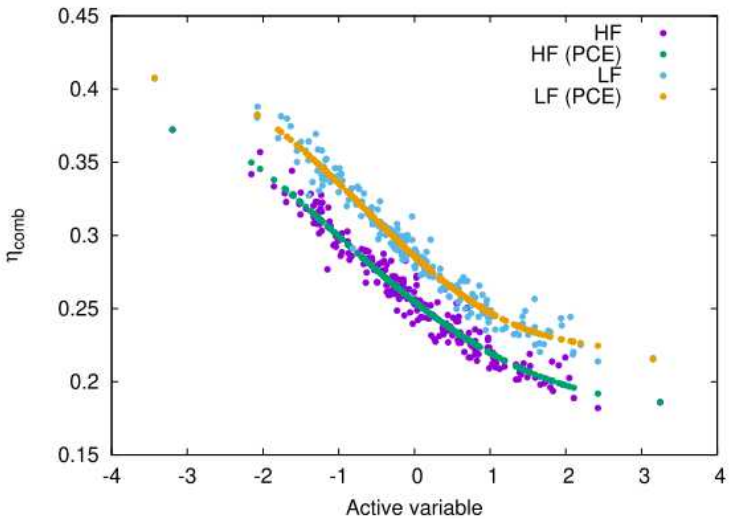

(b) η_{comb}

FIGURE: Qols w.r.t. the active variables for the scramjet application problem.

SCRAMJET DATASET

MULTIFIDELITY APPROACH FROM DATASET

- 2 spatial resolutions
- 16 random variables
- Dataset with 200 realizations (consistent parameterization)

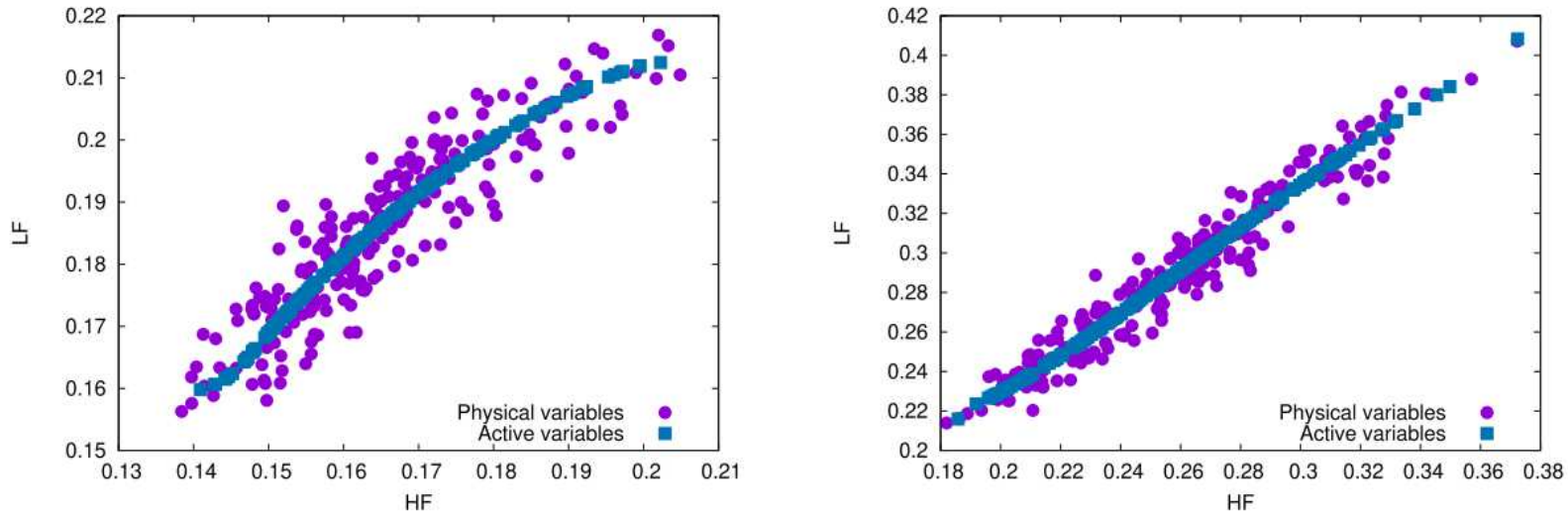

(a) ϕ_{burn} (b) η_{comb}

FIGURE: Scatter plot for the active variables for the scramjet application problem.

SCRAMJET DATASET

MULTIFIDELITY APPROACH FROM DATASET

- 2 spatial resolutions
- 16 random variables
- Dataset with 200 realizations (consistent parameterization)

Qols	ρ^2	ρ^2_{AS}	Estimator St.Dev		
			MC	OCV-1	OCV-1 (AS)
ϕ_{burn}	0.802	0.967	1	0.198	0.033
η_{comb}	0.933	0.986	1	0.067	0.014

TABLE: (Estimated) Standard Deviation for MF and MF-AS (normalized w.r.t. MC) for the scramjet application problem.

Conclusions

Concluding Remark

Still an active research area

Summary:

- Multifidelity strategies are appealing techniques for UQ
- Recursive estimators are limited by the correlation of the first low-fidelity model
- We proposed a new framework to overcome this issue
- Enhancing the correlation seems also possible by resorting to Active Directions (which also provide greater flexibility)

Work in progress:

- Fusion between ACV and AS
- Optimal selection/sub-selection of models in order to increase the cost effectiveness ($(r-1)/r\rho^2$)
- Beyond samples allocation: samples placement and OED
- Treatment of inactive variables
- Beyond Active Subspaces (Ridge regression)

Advancements in the surrogate-based area (not discussed here):

- Greedy multilevel/multifidelity adaptation
- Adaptive multi index collocation
- Additionally, Multiple information sources can be leveraged by learning a structure among latent variables

The Approximate Control Variate work is based on the paper:

1 A.A. Gorodetsky, G. Geraci, M.S. Eldred & J.D. Jakeman, A Generalized Framework for Approximate Control Variates. *arXiv preprint arXiv:1811.04988v2* [stat.CO]. Submitted, 2018.

2 G. Geraci, M.S. Eldred, Leveraging Intrinsic Principal Directions for Multifidelity Uncertainty Quantification. *Sandia Report SAND2018-10817*, 2018.

THANKS!

Acknowledgements

- DARPA Equips Program
- Gianluca Iaccarino, Juan Alonso, Rick Fenrich and Victorien Menier – Stanford University
- Paul Constantine and Jeff Hokanson – University of Colorado at Boulder
- Daniel Turner – Sandia National Labs (NM)
- Laboratory Directed Research & Development Funds @ Sandia
- DOE EERE through the A2e program

Sandia National Laboratories is a multimission laboratory managed and operated by National Technology and Engineering Solutions of Sandia, LLC., a wholly owned subsidiary of Honeywell International, Inc., for the U.S. Department of Energys National Nuclear Security Administration under contract DE-NA-0003525.